To the Graduate Council:

I am submitting herewith a thesis written by Stephen Paul Anderson entitled "A Study of the Hydrolysis of Uranium Hexafluoride by Fourier Transform Infrared Spectroscopy." I have examined the final copy of this thesis for form and content and recommend that it be accepted in partial fulfillment of the requirements for the degree of Master of Science, with a major in Chemistry.

Geo. K. Schweitzer
George K. Schweitzer, Major Professor

We have read this thesis
and recommend its acceptance:

James F. Adcock

Glenn Mauldin

Accepted for the Council:

L. Evans Bell
Vice Chancellor
Graduate Studies and Research

C

A STUDY OF THE HYDROLYSIS OF URANIUM HEXAFLUORIDE BY FOURIER TRANSFORM INFRARED SPECTROSCOPY

A Thesis

Presented for the

Master of Science

Degree

The University of Tennessee, Knoxville

Stephen Paul Anderson

August 1982

3062954

DEDICATION

The author wishes to dedicate this work to the memory of Joseph Anderson whose support and encouragement were always gratefully appreciated.

ACKNOWLEDGEMENT

The author wishes to express his sincere gratitude to Dr. George K. Schweitzer for his advice, guidance, and trust during the course of this work.

Appreciation is also extended to Dr. William H. McCulla and his co-workers at K-25 and to the Union Carbide Nuclear Division, Oak Ridge Gaseous Diffusion Plant (K-25) whose financial support made this work possible. Thanks is also extended to Dr. Gleb Mamantov for making some of his instrumentation available which allowed this study to be conducted.

The author also wishes to express his gratitude to Dr. Arlene Garrison and Dr. Richard Crocombe for their help and guidance during the course of this work. Thanks is also extended to Myron L. Cherry for his help during the Summer of 1981.

Appreciation is also extended to Dr. Schweitzer and Dr. Garrison for editing this manuscript and to Rene Hensley for typing it.

ABSTRACT

The reaction of uranium hexafluride with water has been studied by using Fourier transform infrared (FT-IR) spectroscopy. Several different methods for accomplishing this task have been carried out. In addition, interpretations of the results have been made. These interpretations have been based on literature values for the reactants and for compounds analogous to possible products.

It was shown that classical matrix-isolation techniques proved to be unsatisfactory for studying this reaction. Other methods were developed in order to obtain results. They were: (1) the co-deposition of pure UF_6 and H_2O on a cold window at 16°K, (2) the co-deposition of argon matrix to sample ratios of 10:1 to 2:1 of UF_6 and H_2O at 16°K, and (3) the annealing of the samples produced by (1) and (2) while they were being scanned with FT-IR.

Other methods which were tried and found to be non-productive are also presented. Also, an experiment in which an attempt to volatilize UOF_4 in vacuo is presented. This volatilization was attempted in a cryostat at 16°K with the hope of isolating UOF_4 in a matrix on a cold window.

FT-IR spectra obtained in these experiments are presented and discussed. The results obtained are: (1) UF_6 and H_2O show no propensity to react at cryogenic temperatures because of thermodynamic factors, (2) they do react at temperatures above 150°K, (3) there is a concentration factor that influences their reaction, (4) their reaction seems to be relatively complex and the reaction

pathway involves several comparatively stable species, (5) these species are evidenced by possible U-F, UO_2, U-O and other IR bands, and (6) the attempted volatilization of UOF_4 supports prior indications that the molecule undergoes disproportionation into UF_6 and other products when heated. Finally, possibilities of extending these experiments are discussed.

TABLE OF CONTENTS

CHAPTER		PAGE
I.	INTRODUCTION	1
	A. Properties of UF_6, UOF_4, UO_2F_2, and UO_3	1
	1. UF_6	
	2. UOF_4	
	3. UO_2F_2	
	4. UO_3	
	B. Properties of Analogous MF_6, MOF_4, MO_2F_2, and MO_3 Compounds	10
	1. NpF_6 and PuF_6	
	2. WF_6 and MoF_6	
	3. $NpOF_4$ and $PuOF_4$	
	4. WOF_4 and $MoOF_4$	
	5. NpO_2F_2 and PuO_2F_2	
	6. WO_2F_2 and MoO_2F_2	
	7. MoO_3 and WO_3	
	C. Matrix Isolation	23
	D. Proposed Studies	24
II.	INSTRUMENTATION	26
	A. Design Considerations	26
	B. Description	33
III.	EXPERIMENTAL PROCEDURE	46
	A. Gas Phase Experiment	46
	B. Matrix-Isolated Water in Argon	47
	C. Matrix-Isolated UF_6 in Argon	49
	D. Matrix-Isolated UF_6 and Water in Argon	50
	E. Matrix-Isolated Water in Nitrogen	51
	F. Matrix-Isolated UF_6 in Nitrogen	52
	G. Matrix-Isolated UF_6 and Water in Nitrogen	52
	H. Matrix-Isolated UF_6 and Water in Xenon	53

CHAPTER PAGE

I. Pure UF_6 and Water 53

J. Merging Streams of UF_6 and Water 55

K. Low-Ratio Deposition Studies 56

L. Low-Ratio Mixing Nozzle Experiments 57

M. UOF_4 Volatility Study 58

IV. RESULTS AND DISCUSSION 59

A. Results 59
1. Preliminary UF_6 Vapor Experiments
2. UF_6-Ar Matrix-Isolation Studies
3. Matrix-Isolated H_2O in Argon
4. UF_6 and H_2O Co-deposited in Argon
5. Matrix-Isolated UF_6 in Nitrogen
6. UF_6 and H_2O Matrix-Isolated in Nitrogen
7. Co-deposition of UF_6 and H_2O Sans Matrix
8. Matrix-Isolated UF_6 and H_2O in Xenon
9. UF_6 and H_2O Merging Streams Co-deposition Experiment
10. Low-Ratio UF_6 and H_2O Experiment
11. Low-Ratio Nozzle Studies
12. UOF_4 Volatility Studies

B. Discussion 158

LIST OF REFERENCES 166

VITA 172

LIST OF TABLES

TABLE		PAGE
I.	Heat and entropy of fusion of UF_6, NpF_6, PuF_6	11
II.	Fundamental vibrational frequencies (cm^{-1}) and metal-fluorine bond distances (Å) for UF_6, NpF_6, and PuF_6	12
III.	Fundamental vibrational frequencies (cm^{-1}) of MoF_6 and WF_6	14
IV.	Physical and thermochemical constants of WF_6, MoF_6, and ReF_6	16
V.	Thermochemical constants for $MoOF_4$, and WOF_4	18
VI.	Fundamental frequencies (cm^{-1}) of monomeric WOF_4 and $MoOF_4$	20
VII.	IR absorptions (cm^{-1}) of important species found in previous investigations and UF_6 hydrolysis study	161

LIST OF FIGURES

FIGURE		PAGE
1.	Local environment of uranium atom in solid UOF_4 . . .	4
2.	(a) Infrared spectrum of UOF_4 in KBr disc (b) Raman spectrum of polycrystalline sample of UOF_4	6
3.	Cross section of layer structure of UO_2F_2	8
4.	Top view of lower level of dual gas manifold cart . .	29
5.	Side view of lower level of cart	30
6.	Top view of upper level of dual gas manifold	31
7.	Side view of water manifold	34
8.	Side view of UF_6 manifold	36
9.	Front and side views of CsI sample window holder	40
10.	Side and top views of refrigeration unit cover and deposition port	41
11.	Arrangement used to merge and mix UF_6 and H_2O sample streams	42
12.	Post-deposition port mixing nozzle	44
13.	Deposition port and sample holder for UOF_4 vapor studies	45
14.	FT-IR spectrum of initial sample of UF_6 gas at 10-torr placed in sample cell	60
15.	FT-IR spectrum after several admissions of small amounts of air	62
16.	FT-IR spectrum after several large pulses of air	63
17.	FT-IR spectrum after cell was pressurized to atmosphere	64
18.	FT-IR spectrum of initial sample of UF_6 gas at 50-torr placed in sample cell	66

FIGURE PAGE

19. FT-IR spectrum of sample after only small pulses of air were admitted 67

20. FT-IR spectrum of sample which was recorded after the sample cell was exposed to air for approximately one minute 69

21. Matrix-isolated FT-IR spectrum of $Ar:UF_6$ at 500:1 71

22. Enlargement of UF_6 absorption 72

23. Enlargement of impurity region 73

24. Matrix-isolated FT-IR spectrum of $Ar:UF_6$ at 100:1 74

25. (a) Enlargement of UF_6 absorption, before annealing. (b) Enlargement of UF_6 absorption after annealing to 25°K 76

26. Matrix-isolated FT-IR spectrum of a 1000:1 sample of $Ar:H_2O$ 77

27. Enlargement of 3800-3500 wavenumber region 79

28. Enlargement of the 1650-1550 wavenumber region, $Ar:H_2O$ = 1000:1 80

29. Enlargement of 3800-3500 wavenumber region after annealing to 32°K 81

30. Enlargement of 1650-1550 wavenumber region after annealing to 32°K 82

31. Matrix-isolated FT-IR spectrum of a 100:1 sample of $Ar:H_2O$ 83

32. Enlargement of 3800-3400 wavenumber region 84

33. Enlargement of 1650-1550 wavenumber region, $Ar:H_2O$ = 100:1 85

34. Enlargement of 3800-3400 wavenumber region after annealing to 30°K 86

35. Enlargement of 1650-1550 wavenumber region after annealing to 30°K 87

FIGURE PAGE

36. Matrix-isolated FT-IR spectrum of 20:1 sample of Ar:H_2O 89

37. Enlargement of 3800-3000 wavenumber region 90

38. Enlargement of 1700-1550 wavenumber region 91

39. Matrix-isolated FT-IR spectrum of Ar:UF_6 (500:1) and Ar:H_2O (100:1) held at 16°K 93

40. Enlargement of the 1800-500 wavenumber region at 16°K 94

41. Enlargement of 1800-500 wavenumber region after annealing to 26°K 95

42. Enlargement of the 1800-500 wavenumber region after annealing to 34°K 96

43. Enlargement of the 1800-500 wavenumber region after annealing to 37°K 97

44. Matrix-isolated FT-IR spectrum of 700-500 wavenumber region of 100:1 sample of N_2:UF_6 99

45. Same region after sample was annealed to 24°K 101

46. Spectrum of same sample after it was annealed to 28°K 102

47. Matrix-isolated FT-IR spectrum of UF_6:N_2 (1:100) and H_2O:N_2 (1:500) at 16°K 103

48. Enlargement of H_2O absorptions 105

49. Enlargement of 1700-1500 wavenumber region after sample was annealed to 30°K 106

50. FT-IR spectrum of neat deposited sample of UF_6 and H_2O prior to any annealing 108

51. Enlargement of the 1000-400 wavenumber region prior to annealing 109

52. Enlargement of 1000-400 wavenumber region after sample had been annealed to 150°K 110

53. Enlargement of 1000-400 wavenumber region after sample had been annealed to about 165°K 111

FIGURE PAGE

54. Enlargement of 1000-400 wavenumber region after sample had been annealed to about 180°K 112

55. Enlargement of 1000-400 wavenumber region after sample had been annealed to about 195°K 114

56. Enlargement of 1000-400 wavenumber region after sample had been annealed past 220°K 115

57. (a) Matrix-isolated FT-IR spectrum of Xe:UF_6 and Xe:H_2O held at 16°K.
(b) Spectrum taken after sample was annealed past 150°K 118

58. (a) Spectrum of same region after annealing further.
(b) Spectrum of same region after annealing past 200°K 119

59. Matrix-isolated FT-IR spectrum of sample of UF_6:H_2O:Ar (1:1:100) that was mixed in-line prior to deposition 121

60. Matrix-isolated FT-IR spectrum of identical sample that was mixed in-line prior to deposition 122

61. Matrix-isolated FT-IR spectrum of similar sample in which the UF_6 and H_2O were deposited sequentially 123

62. FT-IR spectrum that was recorded after only pure Ar was passed through the H_2O side and deposited 124

63. Matrix-isolated FT-IR spectrum of 100:1 Ar:UF_6 and 1000:1 Ar:H_2O samples were mixed and deposited at 16°K 126

64. Matrix-isolated FT-IR spectrum of Ar:UF_6:H_2O (100:1:1) sample in which the samples were mixed in a 100-cm tube prior to deposition 127

65. Spectrum recorded after sample had been annealed somewhat 128

FIGURE PAGE

66. Matrix-isolated FT-IR spectrum of sample similar to the sample recorded in Figure 64 129

67. Spectrum recorded after sample annealed somewhat . . . 130

68. Spectrum recorded after sample had been annealed to about 35°K 131

69. Enlargement of 950-600 wavenumber region of 1000:1:1 of Ar:UF_6:H_2O sample that was mixed in 100-cm tube prior to deposition 132

70. FT-IR spectrum of 100:1 Ar:UF_6 and pure water samples that were mixed in a heated 30-cm tube prior to deposition 134

71. Spectrum of sample similar to the one recorded in Figure 70 135

72. Spectrum of same sample after it was annealed somewhat 136

73. FT-IR spectrum of 5:1 Ar:UF_6 and a 2:1 Ar:H_2O sample that was co-deposited at 16°K 138

74. FT-IR spectrum of sample under same experimental conditions as in Figure 73 139

75. FT-IR spectrum of UF_6:H_2O:Ar (1:1:2) sample recorded at 16°K 141

76. FT-IR spectrum of sample under same experimental conditions as in Figure 75 142

77. FT-IR spectrum of sample under same experimental conditions as in Figure 76 143

78. FT-IR spectrum of 3:1 Ar:UF_6 and 2:1 Ar:H_2O samples which were co-deposited at 16°K 144

79. FT-IR spectrum of the sample after it had been warmed to approximately 130°K 145

80. Spectrum recorded after sample had been warmed to about 180°K 147

81. Spectrum recorded after sample had been warmed further 148

FIGURE PAGE

82. Spectrum recorded after sample had been warmed to about 200°K 149

83. Spectrum recorded after sample had been warmed past 220°K 150

84. Infrared spectrum of $K^+UF_5O^-$ and $NF_4^+UF_5O^-$ samples recorded by Wilson and associates 156

85. FT-IR spectrum of 2:1 Ar:UF_6 and 2:1 Ar:H_2O sample that was co-deposited through nozzle at 16°K 157

86. FT-IR spectrum of volatilized UOF_4 sample at 20°K 159

CHAPTER I

INTRODUCTION

A. Properties of UF_6, UOF_4, UO_2F_2 and UO_3

Uranium hexafluoride and its hydrolysis products have received considerable interest recently due to the escalating production in uranium-enrichment facilities around the world. If an accidental leakage of uranium hexafluoride gas into the atmosphere occurred, it would be important to know something about its thermodynamic and kinetic stability as well as the stabilities of its reaction products. It is believed that UF_6 would have the greatest propensity to react with water giving a possible reaction pathway perhaps describable as:

$$UF_6 + H_2O \rightarrow UOF_4 + 2HF$$

$$UOF_4 + H_2O \rightarrow UO_2F_2 + 2HF$$

$$UO_2F_2 + H_2O \rightarrow UO_3 + 2HF$$

1. $\underline{UF_6}$

Uranium hexafluoride is a colorless solid that melts at approximately 64.5°-64.8°C[1] and sublimes at 56.54°C at one atmosphere pressure.[2] The densities of the solid and liquid are 5.060 and 3.595 g/cm^3, respectively;[3] the vapor pressure is reported to be 17.65 torr at 0°C and 111.9 torr at 25°C.[2]

The molecules appear to be slightly distorted octahedrons in the solid state,[4] but they probably possess a regular octahedral geometry in both the liquid and gaseous states.[5]

Fundamental vibrational frequencies of gaseous UF_6 correspond to Raman shifts at 66.71 (ν_1, A_{1g}), 532.5 (ν_2, E_g) and 202 (ν_5, F_{2g}) cm^{-1}, and IR bands at 624(ν_3, F_{1u}) and 186.2 (ν_4, F_{1u}) cm^{-1}.[6] The ^{19}F-NMR spectrum of UF_6 has been reported by Seppelt and Bartlett;[7] both $^{238}UF_6$ and $^{235}UF_6$ in a $CFCl_3$ solvent produced singlets at -764.0±5ppm; however, the line widths of $^{238}UF_6$ and $^{235}UF_6$ were reported to be 12 and 550 ppm, respectively.

The most recent matrix-isolation studies of UF_6 were performed by Paine[8] and associates at the Los Alamos Scientific Laboratory. Their investigations were performed in dilute Ar matrices at 14°K. They believe that their IR spectra support the formation of aggregates of UF_6 molecules in matrix samples and also reveal that strong perturbations exist for different hosts, and that stretching frequencies are more susceptible to matrix shifts than bending frequencies. They report vibrations at 66.6 (ν_1, A_{1g}), 530 (ν_2, E_g), 619 (ν_3, F_{1u}), 183.5 (ν_4, F_{1u}), 200 (ν_5, F_{2g}) and 143.2 (ν_6, F_{2u}) cm^{-1}.

It has long been known that UF_6 hydrolyzes in the presence of excess water to form uranyl fluoride, but whether it reacts further to uranium trioxide is somewhat nebulous. Difficulties often arise in storing UF_6 in glass because of the cyclic process:

$$SiO_2 + 4HF \rightarrow SiF_4 + 2H_2O$$

$$UF_6 + 2H_2O \rightarrow UO_2F_2 + 4HF.$$

This problem can be solved by storing UF_6 over KF or NaF which absorbs HF and halts the hydrolysis cycle. Recently, as a result of the work done by P.W. Wilson,[9] UF_6 has been hydrolyzed to uranium

oxide tetrafluoride (UOF_4) and its structure has been verified by Paine and associates.[10] P.W. Wilson prepared UOF_4 by the hydrolysis of UF_6 suspended in an HF slurry.

There are no known adducts of UF_6 with H_2O or HF; however, the congruently melting compound $UF_6 \cdot XeF_2$ has been reported.[11]

A report which was submitted by Okamato and Keyose[12] evaluated the release of UF_6 vapor into the atmosphere in postulated accidents under a wide variety of different conditions. These postulated accidents dealt with the rupture of a UF_6 gas line connected to a hot UF_6 cylinder. The amount of gaseous UO_2F_2 and HF released to the environment was estimated.

2. UOF_4

As previously described, uranium oxide tetrafluoride has been synthesized by the hydrolysis of UF_6 in the condensed phase. It is an incongruently melting solid that is only slightly soluble in anhydrous HF. Analysis of the thermal gravimetric analysis (TGA) trace supports a two-step thermal decomposition, but a three-step decomposition has also been proposed.[9] The products of the decomposition are UF_6 and UO_2F_2. Unlike other transition metal oxide tetrafluorides, UOF_4 is reported to be non-volatile, and gas-phase or matrix spectra have not been obtained.[9]

The structure (Figure 1) of the solid compound synthesized by Wilson has been determined by X-ray diffraction by Paine, Ryan, and Asprey[10] and verified by neutron diffraction by Levy, Taylor, and Wilson.[13] They proposed a pentagonal bipyramid of light atoms surrounding the uranium atom - the atoms in the axial positions are

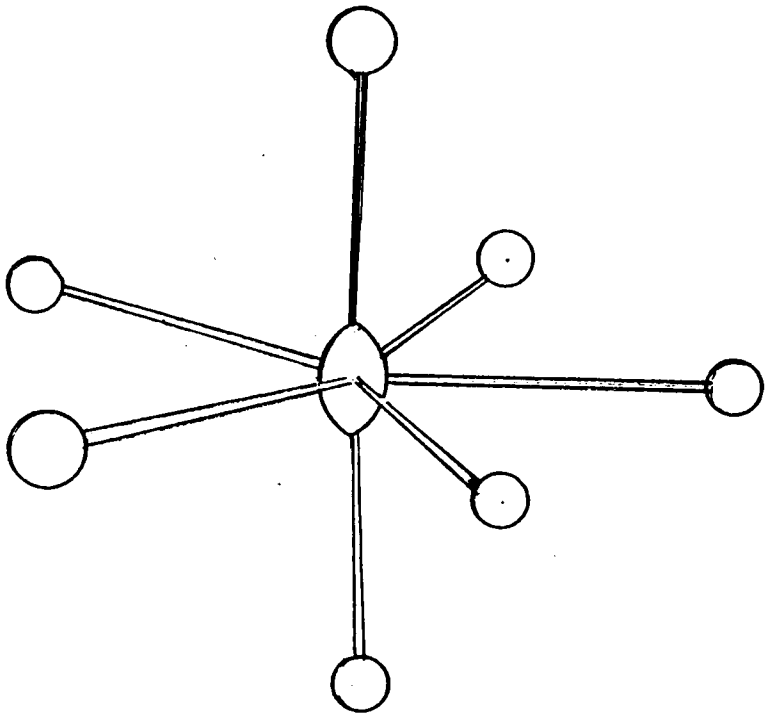


Figure 1. Local environment of uranium atom in solid UOF_4. Uranium atom (center) surrounded by pentagonal bipyramid of light atoms; the oxygen atoms lie in the axial positions and the fluorine atoms rest in the equatorial plane.[10]

1.870Å and 1.884Å from the uranium atom; in the pentagonal plane one terminal atom exists 2.05Å from uranium and four bridging atoms occur at approximately 2.271±0.001Å. They proposed that the oxygen atom is in a terminal axial position, and also concluded that the oxygen atoms alternated between the up and down positions. They concluded that four of the equatorial fluorine atoms were bridging and one was non-bridging. This structure was labelled alpha (α-UOF_4). A second polymorph has been synthesized and characterized via X-ray diffraction by Taylor and Wilson and designated beta (β-UOF_4).[14] This form was prepared by slow growth of crystals of α-UOF_4 partially dissolved in anhydrous HF; these crystals are yellow and very hygroscopic. This molecule was determined to be tetragonal and isostructural with β-UF_5; it was also proposed to be pentagonal bipyramidal but two non-bridging fluorines occupy the axial position and a non-bridging oxygen occupies an equatorial position along with four bridging fluorines. The non-bridging axial fluorines showed a bond distance of 1.92 Å; the oxygen bond distance was reported to be 1.87Å and the equatorial fluorine bond distances were reported at 2.18Å.

Both the IR and Raman spectra (Figure 2) of α-UOF_4 have been determined by Paine[10] and associates; the IR spectrum of α-$U^{18}OF_4$ has also been reported by Jacob and Polligkeit.[15] The IR spectrum of a powder sample at 25°C is characterized by bands at 893, 667, 558, 478, and 375 cm^{-1}. Jacob and Polligkeit assign the band at 891 cm^{-1} (893) as a terminal U-O stretch on the basis of isotopic shifts. The two bands at 667 and 558 cm^{-1} were assigned to the

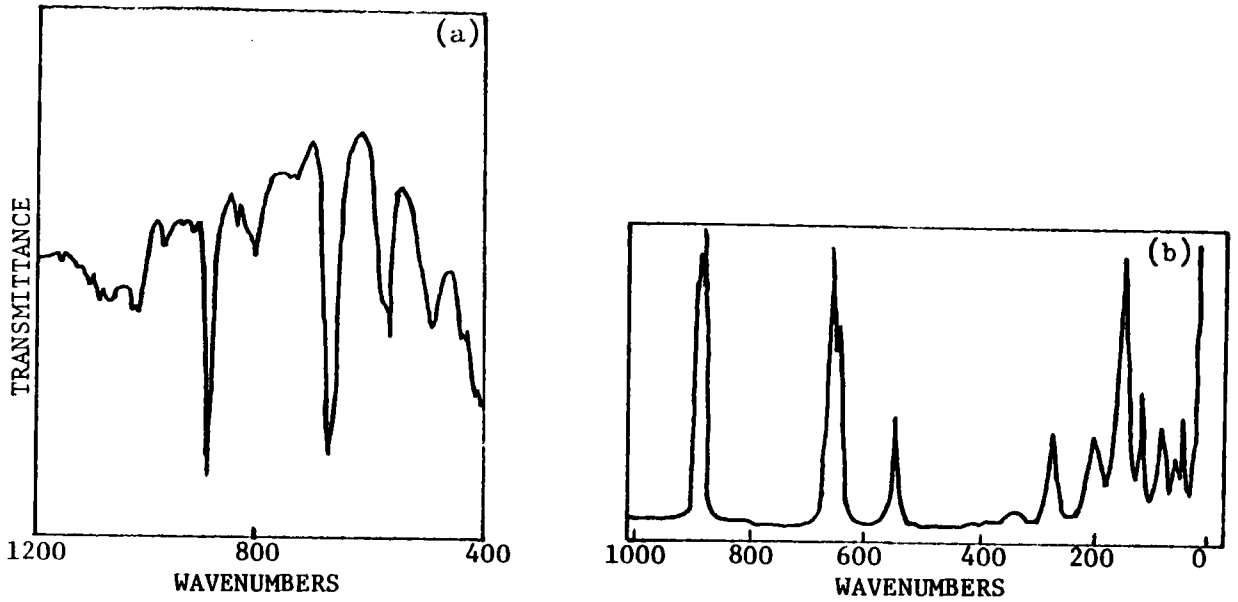


Figure 2. (a) Infrared spectrum of UOF_4 in KBr disc. (b) Raman spectrum of polycrystalline sample of UOF_4.[10]

terminal U-F stretch and broad bands at 472 and 375 cm^{-1} were assigned to U-F-U bridge modes. The Raman spectrum of a polycrystalline sample showed shifts at 552, 660, and 389 cm^{-1}. No known matrix studies have been reported on UOF_4. Also, Paine et al.[8] stated that lowering the sample temperature to -196°C produced some additional sharpening in their spectra.

Since UOF_4 is a very hygroscopic compound, upon standing for several minutes in moist air it will react to produce hydrated uranyl fluoride ($UO_2F_2 \cdot nH_2O$). Therefore, it is difficult to achieve a clean IR spectrum with KBr, polyethylene, or polytetrafluoroethylene discs which usually show a uranyl band at 940 cm^{-1} that is due to hydrolysis.[10] More careful handling and use of mulling agents might lead to better results.

3. UO_2F_2

The hydrolysis reaction of UF_6 to uranyl fluoride is exothermic and releases about 50 kcal/mole of heat at 25°C.[16] Uranyl fluoride is a pale yellow non-melting solid that undergoes thermal decomposition at high temperatures.[17]

Uranyl fluoride was reported to have rhombohedral symmetry;[18] the molecular structure (Figure 3) consists of a semi-distorted hexagonal bipyramid; the uranyl group is perpendicular to the bisecting plane of fluorine atoms arranged around the uranium atom in a puckered hexagon that resembles the chair configuration in cyclohexane. The fluorine atoms purportedly alternate above and below the bisecting plane around the uranium atom, but a following study by Taylor[19] contradicted this arrangement. He concluded via

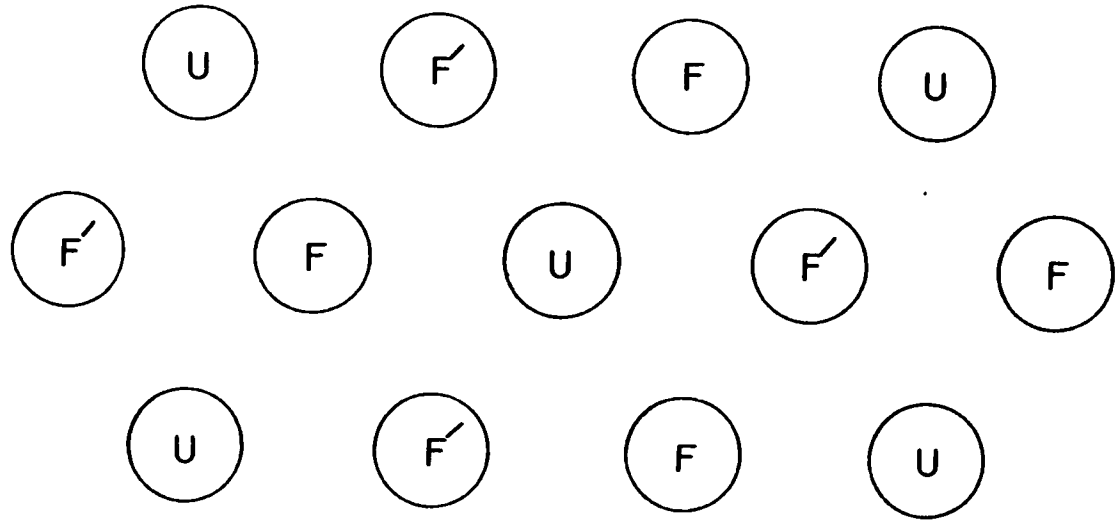


Figure 3. Cross section of layer structure of UO_2F_2. The uranium atoms (U) rest in the same plane (page). The oxygen atoms (not pictured) lie directly above and below the uranium atoms. The fluorine atoms alternately lie 0.61 angstroms above (F) and below (F′) the plane of uranium atoms.[20]

neutron diffraction that the arrangement of fluorine atoms is not puckered but that they are co-planar with the uranium atoms.

Several investigations have reported the IR spectrum of UO_2F_2, and the most characteristic peak is the one assigned to the uranyl stretch at 990 cm^{-1}.[20] Ohwada[21] described the far-IR spectrum of UO_2F_2 as having three bands located at 260, 234, and 146 cm^{-1}. Ohwada assigned the band at 260 cm^{-1} to the U-F stretching vibration (E_u, ν_7), and the 234 and 146 cm^{-1} peaks were assigned to the O-U-O (E_u, ν_8) and F-U-F (A_{2u}, ν_4) bending vibrations, respectively.

UO_2F_2 is soluble in water and its solubility increases with temperature.[22] Hydrated complexes of the form $UO_2F_2 \cdot nH_2O$ (n=2,3) have been prepared by dissolving uranium trioxide (UO_3) in aqueous HF.[23] UO_2F_2 also forms a combined adduct with HF and H_2O ($UO_2F_2 \cdot 2HF \cdot 4H_2O$).[24] UO_2F_2 will hydrolyze in the presence of steam heated above 450°C to form uranium trioxide and HF.[25]

4. UO_3

Uranium trioxide, possibly the final product in the hydrolysis of UF_6, exists in at least six crystal forms (α-UO_3 to ε-UO_3 and high pressure ξ-UO_3) and an amorphous form.[26] It is difficult to produce the compound in pure form due to its phase instability - it must be produced at moderate temperatures (400 - 700°C).[23] The most stable form γ-UO_3 is a yellow powder, β-UO_3 is an orange-red powder, and α-UO_3 is a tan powder. It is difficult to obtain an accurate density measurement due to its phase impurity; however, it

is approximately 7.29g cm^{-3} at 15°C[25] for what appears to be α -UO_3. The vapor pressure of UO_3 at 1600°K is 10^{-4} atm.[25]

Matrix-isolation studies of UO_3 have been performed by Gabelnick and associates[27-29] and confirmed by others.[30] The following assignments were made by Gabelnick and associates: $\nu_1(A_1)$= 843.5, $\nu_2(A_1)$=745.6, $\nu_4(B_1)$=852.6, $\nu_3(A_1)$=186.2, $\nu_5(B_1)$=211.6, and $\nu_6(B_2)$=151.5 cm^{-1}. Gabelnick and associates[28] determined UO_3 to be T-shaped in the matrix. The two oxygens in line with the uranium are equivalent and have a shorter U-O bond length than the oxygen which rests at a right angle to them.

B. Properties of Analogous MF_6, MOF_4, MO_2F_2, and MO_3 Compounds

1. NpF_6 and PuF_6

Both neptunium and plutonium hexafluoride are very similar to uranium hexafluoride in many ways. Some of their thermodynamic properties are compared in Table I.[31] Notice that the melting points of the three compounds decrease in the order UF_6>NpF_6>PuF_6. This can be attributed to the increase in covalent character due to a lanthanide-type contraction observed in these elements.[31] An anomaly is observed for the vapor pressure of NpF_6 because it is not intermediate between UF_6 and PuF_6 but is greater than either of them. This quirk has not been explained.

IR and Raman data for the three gaseous actinide hexafluorides are listed in Table II along with metal-fluorine bond distances derived from electron diffraction studies.[6] The Raman spectra of liquid and gaseous NpF_6 were observed by Gasner and Frlec.[32] Malm,

TABLE I

HEAT AND ENTROPY OF FUSION OF UF_6, NpF_6 AND PuF_6[31]

	Temperature °C	Vapor Pressure torr (25°C)	ΔH cal mol^{-1}	ΔS cal mol^{-1} deg^{-1}
UF_6	64.0	111.9	4555	13.51
NpF_6	54.0	126.8	4112	12.53
PuF_6	50.8	104.9	4456	13.72

TABLE II

FUNDAMENTAL VIBRATIONAL FREQUENCIES (cm^{-1}) AND METAL-FLUORINE BOND DISTANCES (Å) FOR UF_6, NpF_6 AND PuF_6[6]

Compound	ν_1 (R)	ν_2 (R)	ν_3 (IR)	ν_4 (IR)	ν_5 (R)	ν_6 (inactive)	M-F (Å)
UF_6	667.1	532.5	624	186.2	202	(142)	1.996
NpF_6	654	535	624	198.6	208	(164)	1.981
PuF_6	(628)	(523)	616	206.0	(211)	(173)	1.971

Weinstock, and Claassen[33] have studied the IR spectra of gaseous NpF_6 and PuF_6. They used a nickel absorption cell fitted with AgCl windows. Their attempt to obtain the Raman spectrum of PuF_6 failed because the compound absorbs in the visible region and undergoes photochemical decomposition. Their report compared their results to previous UF_6 spectra, and because of the similarities, they concluded that both NpF_6 and PuF_6 have regular octahedral symmetry.

NpF_6 and PuF_6 hydrolyze in the presence of water, and like UF_6 must be stored in dry quartz or Pyrex over anhydrous NaF or KF to prevent the cyclic process described earlier. Usually they hydrolyze according to the reaction:

$$MF_6 + 2H_2O \rightarrow MO_2F_2 + 4HF \ (M=Np, Pu).^{34}$$

Recently, investigators[35,36] have produced compounds with the formula MOF_4 according to the reaction:

$$MF_6 + H_2O \xrightarrow{HF} MOF_4 + 2HF.$$

This process is identical to the one used for production of UOF_4 in which an HF slurry is employed to suppress further hydrolysis.

2. $\underline{WF_6}$ and $\underline{MoF_6}$

Tungsten hexafluoride (WF_6, M.W.=297.92 g/mol) is a white solid that melts at 2.0±0.3°C and boils at 17.06±0.05°C.[47] According to Barber and Cady[37] the vapor pressure is 1029.2 torr at 25.24°C.

The vapor phase IR and Raman spectra of WF_6 have been reported by several investigators (see Table III).[38] Recently, Bernstein and Meredith[39] have obtained Raman spectra of WF_6 (also UF_6 and MoF_6) in the solid phase at 77°K, and at this temperature they determined UF_6 and WF_6 to have D_{4h} and O_h geometries, respectively.

TABLE III

FUNDAMENTAL VIBRATIONAL FREQUENCIES (cm^{-1}) OF MoF_6 AND WF_6[38]

Compound	ν_1 (R)	ν_2 (R)	ν_3 (IR)	ν_4 (IR)	ν_5 (R)	ν_6 (inactive)
WF_6	769	760	712	256	322	261
MoF_6	736	641	742	269	319	240

In a study Selig and associates[40] concluded that hydrolysis of WF_6 in anhydrous HF produces the oxonium salt $H_3O^+WOF_5$, which undergoes thermal decomposition at 150°C probably to yield WO_2F_2. According to Canterford and Colton,[41] WF_6 in the presence of H_2O hydrolyzes to WO_2F_2:

$$WF_6 + 2H_2O \rightarrow WO_2F_2 + 4HF \quad K_{eq} = 6x10^2.$$

Therefore there is a direct analogy between the hydrolysis of UF_6 and WF_6.

Molybdenum hexafluoride is similar to WF_6 in many ways, and a number of its physical constants is compared to those of WF_6 in Table IV. Raman analysis of crystalline MoF_6 supports an O_h symmetry.[39] The thermochemical constants of MoF_6 are compared to those of WF_6 in Table IV.[41]

The characteristic peaks in the IR spectrum of MoF_6 resemble those of WF_6. There are bands at 742(ν_3), 269(ν_4), and 240(ν_6) cm^{-1}, whereas WF_6 shows peaks at 712(ν_3), 256(ν_4) and 261(ν_6) cm^{-1}. A comparison of the values in Table IV reveals that the M-F bond lengths of the transition metal hexafluorides increase upon descending the group; however, one must be cautious about predicting the relative reactivities of the three hexafluorides from this, because the bond length factor is offset by the increased stability of the higher oxidation state as one descends a group in the transition-metal block. Therefore the reactivity decreases in the order $MoF_6 < WF_6 < UF_6$. Vibrational spectra are compared in Table III.

Unlike WF_6, MoF_6 hydrolyzes in the absence of HF to yield $MoOF_4$, and then hydrolyzes further to MoO_2F_2.[41]

TABLE IV

PHYSICAL AND THERMOCHEMICAL CONSTANTS OF WF_6, MoF_6 AND ReF_6[41]

Molecule	M-F distance Å	M.P. °C	V.P. torr (20°C)	ΔH kcal/mole	ΔS cal/deg/mole
MoF_6	1.820	17.5	446	6.360	20.6
WF_6	1.833	2.3		6.250	21.5
ReF_6	1.832	19.0	269	6.366	19.8

3. $NpOF_4$ and $PuOF_4$

The oxide tetrafluorides of plutonium and neptunium have been prepared by the slow hydrolysis of their respective hexafluorides in an anhydrous HF slurry.[36,42] According to Burns and O'Donnell,[36] $PuOF_4$ is a chocolate-brown solid with a very low vapor pressure at room temperature. Peacock and Edelstein[42] reported that $NpOF_4$ is a brownish-purple solid that when allowed to stand in moist air leads to discoloration and the appearance of a new crystalline phase.

X-ray powder studies revealed that both oxide tetrafluorides are isostructural with the trigonal form of uranium oxide tetrafluoride (α-UOF_4).

All three oxide tetrafluorides (MOF_4, M=Np, Pu, U) hydrolyze in moist air; however, only $PuOF_4$ is unstable in the presence of anhydrous HF at room temperature. It reacts in the following manner:

$$2PuOF_4 \xrightarrow{HF} PuF_6 + PuO_2F_2.^{36}$$

UOF_4 has the greatest thermal stability of the three, $NpOF_4$ being intermediate in stability.

4. WOF_4 and $MoOF_4$

Molybdenum and tungsten oxide tetrafluoride are white crystalline solids that can be prepared by the controlled hydrolysis of their respective hexafluorides.[43] Their thermodynamic constants are very similar (see Table V).[44]

Alexander and associates[45] have proposed with support from vibrational analysis that molecular $MoOF_4$ and WOF_4 have C_{4v} symmetry in the vapor phase and most probably in the solid phase. Paine and

TABLE V

THERMOCHEMICAL CONSTANTS FOR $MoOF_4$ AND WOF_4[44]

Molecule	B.P.	ΔH fus	ΔH vap	ΔH sub	ΔS fus	ΔS vap
$MoOF_4$	186.0	1.020	12.090	13.110	2.768	26.3
WOF_4	185.9	2.260	14.230	16.490	5.981	31.0

ΔH in kcal $mole^{-1}$
ΔS in cal deg^{-1} $mole^{-1}$
B.P. in °C

McDowell[46] have stated that the solid phase metal atom is octahedrally surrounded. Four equatorial fluorines rest at right angles to each other; one of the equatorial fluorines is bridging while an additional bridging fluorine occurs trans to an apical oxygen.

Studies by Robiette (WOF_4)[47] and Iijima ($MoOF_4$)[48], utilizing electron diffraction, verified C_{4v} symmetry and obtained precise geometrical data for both gaseous WOF_4 and gaseous $MoOF_4$. Iijima described $MoOF_4$ as square pyramidal in the gas phase but said it is distorted in the solid due to bridging via fluorine to another molecule. Alexander and associates[45] performed gas and solid-phase Raman and IR analysis together with matrix-isolated Raman and IR studies on $MoOF_4$ and WOF_4, and their results are shown in Table VI. In this study they revealed that the W-O stretching frequency is independent of phase and, therefore, since the gas phase is principally monomeric, concluded that neither the solid nor the melt is oxygen bridged.

The controlled hydrolysis of WOF_4 yields WO_2F_2.[49] This was accomplished by distilling stoichiometric quantities of H_2O in anhydrous HF onto WOF_4 at -196°C in FEP tubes. MoO_2F_2 has not been prepared in this manner. Reaction of the difluoro dioxo forms with XeF_2 yields $MOF_4 \cdot XeF_2$ (M=Mo, W) which have been characterized by Holloway and Atherton.[50]

5. $\underline{NpO_2F_2}$ and $\underline{PuO_2F_2}$

Very little is known about the chemical and physical properties of neptunyl or plutonyl fluoride. Pink NpO_2F_2 and white PuO_2F_2 possess rhombehedral symmetry.[51]

TABLE VI

FUNDAMENTAL FREQUENCIES (cm^{-1}) OF MONOMERIC WOF_4 AND $MoOF_4$[45]

Mode	Symmetry	WOF_4	$MoOF_4$
ν_1	a_1	1055	1048
ν_2	a_1	733	714
ν_3	a_1	248	264
ν_4	b_1	631	
ν_5	b_1	328	
ν_6	b_2	291	
ν_7	e	698	720
ν_8	e	298	294
ν_9	e	236	236

Both oxyfluorides are soluble in water. The phase diagrams of the compounds have been studied extensively. Plutonyl fluoride forms an adduct of the form $PuO_2F_2 \cdot H_2O$ and also a water-HF adduct of the form $PuO_2F_2 \cdot 2HF \cdot H_2O$.

6. MoO_2F_2 and WO_2F_2

Remarkably little investigation has been done on the dioxo fluorides of molybdenum(VI) and tungsten(VI) and the most recent study still leaves much to be desired.[49] Atherton and Holloway[49] performed NMR, IR, and mass spectrometry along with chemical analysis; however, the spectra were not included in their report because of poor results. They prepared MoO_2F_2 by reaction of MoO_2Cl_2 with anhydrous HF. The substance does not melt or sublime at temperatures up to 310°C in a vacuum.

The IR spectrum supports a solid state polymeric structure. They compared their spectra with those of MoO_2Cl_2 and MoO_2Br_2 and assigned a broad absorption at 835 cm^{-1} to a bridging Mo-O-Mo stretching vibration. The F-19 NMR spectrum of MoO_2F_2 in HF and SO_2ClF mixture reveals a broad singlet at -131.5 ppm versus $CFCl_3$. Their studies of WO_2F_2 revealed little about the compound. Vibrational spectra were poor and no ^{19}F-NMR analyses were performed.

7. MoO_3 and WO_3

Molybdenum trioxide is a white solid which turns yellow upon heating; its melting point is 795°C.[52] Tungsten trioxide is a pale lemon-yellow powder.[53] It melts at about 1470°C and boils at approximately 1427°C.[54] Both oxides are insoluble in pure water but

dissolve in alkaline solutions to give tungstates or molybdates.[53] The densities of WO_3 and MoO_3 are 6.47 and 4.69 g/cm^3, respectively.[55]

The MoO_3 crystal structure is described as rhombic with lattice constants: a=3.9, b=13.8, c=3.7Å. WO_3 is described as monoclinic below 700°C (lattice constants a=7.285, b=7.517, c=3.835Å) and tetragonal above 700°C (a=5.250, c=3.915Å).[56] Loopstra and Boldine,[57] who performed neutron diffraction studies, described WO_3 as a "deformed ReO_3 type structure... the W-O bonds form zigzag chains in three directions ... in the x direction the bonds are of equal length ... in the y and z directions they are alternately short and long." Both MoO_3 and WO_3 are polymeric in the vapor phase; they are of the form $(MO_3)_n$ where n=3, 4, 5.[58]

Mattes and Schroeder[59] performed vibrational analysis on solid WO_3 and MoO_3; their spectra can be compared with the Raman spectra of the vapors that were done by Krasser.[60]

Unlike UO_3, MoO_3 and WO_3 have only one and two known forms, respectively. The most stable structure of the UO_3 polymorphs is α-UO_3 and it is comparable to the high temperature form of WO_3; the β-UO_3 polymorph can be compared to the low temperature form of WO_3.

Weltner and McLeod[61] have performed IR studies on matrix-isolated samples of WO, WO_2, WO_3, W_2O_6, W_3O_8, W_3O_9 and W_4O_{12}. They concluded that there is insufficient evidence to assign any definite geometry to WO_3 in the matrix.

C. Matrix Isolation

Matrix isolation is the process of preparing a sample in which a molecule is isolated, immobilized and held in an inert rigid matrix usually at low temperatures. The molecule of interest to host ratio is typically very low and usually ranges anywhere from 1:50 to 1:10,000. Species which may otherwise exist for only a few fleeting moments may be preserved practically indefinitely, since bimolecular collisions are virtually nullified. Most conventional types of spectroscopy, namely, IR, Raman, UV-visible, and ESR may be used in association with matrix isolation. Modern matrix isolation was developed independently in 1954 by Norman and Porter[62] and by Whittle, Dows, and Pimentel.[63] Pimentel's group was responsible for developing most of the modern-day technique, and also for formulating criteria that must be met for isolation of species using noble gases or nitrogen as the host matrix. From their research came the first reported characterization by IR spectroscopy of a free radical (HCO) held in a rigid matrix at low temperatures.

The criteria for the host lattice in this study are rigidity, inertness, good thermal conductivity, appropriate volatility, and ability to accommodate guest species. Ideally the guest species should be isolated in a host matrix that is transparent to the spectroscopic measurement to be used. Several criteria have been advanced by Downs and Peake[64] for experimental conditions that must be met to achieve the best possible results: (1) The deposition rates must be slow (1-5 mmol of matrix gas per hour) for isolation of small molecules. (2) The deposition temperature must be low

enough so that the sample is condensed fast enough to restrict diffusion of molecules during condensation, and that it be cold enough to inhibit subsequent diffusion of trapped species. (3) The matrix ratio must be scrutinized because it has a profound effect on the degree of isolation.

The most significant effect that matrix-isolating the samples has upon IR spectra is the absence of rotational bands in all but the simplest of molecules. The resulting vibrational bands are very sharp and correspond to pure molecular vibrations. One area where IR spectroscopy has been useful with matrix isolation is in sample-warming or annealing experiments in which diffusion allows bimolecular reactions. An annealing experiment can allow one to slow a reaction to the point where one can detect a reaction intermediate that could not otherwise be detected.

D. Proposed Studies

(1) Matrix-isolated samples with ratios ranging anywhere from matrix to sample (M/S) equal to 10:1 to 1000:1 matrix gas with water and matrix gas with uranium hexafluoride will be deposited at 16°K and the Fourier transform infrared (FT-IR) spectrum recorded. Both argon and nitrogen will be used as the host matrix. Annealing experiments will then be performed with these samples. (2) Matrix-isolated samples with matrix to sample ratios ranging from 10:1 to 1000:1 of argon:water ($Ar:H_2O$) and argon: UF_6 ($Ar:UF_6$) will be deposited simultaneously at 16°K and then warmed in order to induce chemical reaction. Nitrogen will also be used as a

host matrix. (3) Pure water and UF_6 will be deposited simultaneously sans matrix and annealing experiments will be conducted. (4) Matrix-isolated samples of UF_6:Ar and H_2O:Ar will be merged into one stream just prior to deposition in order to allow more time for them to react. The amount of time that the streams will be allowed to mix will be varied by using various lengths of tubing. (5) Low ratio samples of UF_6:Ar and H_2O:Ar ranging from 2:1 to 10:1 will be co-deposited and annealing experiments will be performed. (6) A nozzle will be fitted over the deposition tubes inside the cryostat sample chamber to allow the streams to mix immediately before deposition. (7) An attempt will be made to volatilize a pure sample of uranium oxide tetrafluoride (UOF_4) inside the cryostat sample chamber in order to isolate individual or small aggregates of UOF_4 molecules.

CHAPTER II

INSTRUMENTATION

A. Design Considerations

The unit designed for the UF_6 hydrolysis matrix-isolation FT-IR spectroscopy experiments was a dual-gas manifold coupled with a cryostat-refrigeration unit for preparing and holding the sample. This was used in conjunction with an FT-IR spectrometer. Several aspects needed to be considered when designing and constructing the dual-gas manifold refrigeration unit for UF_6 hydrolysis studies. These considerations were: (1) that the system be as inert as possible towards the highly reactive UF_6 gas, (2) that the system be able to operate at low pressures (10^{-4} torr or lower) in order to ensure purity of samples, (3) that every precaution be taken to ensure safety for apparatus users, (4) that the unit be mobile in order to use it in conjunction with the FT-IR spectrometer, (5) that the unit be flexible as well as adaptable in order to be able to do a variety of experiments, (6) that the refrigeration unit be able to cool the sample container to a temperature of 15°K in a reasonable amount of time (2 hrs), and to also have moderate control over sample temperature during annealing experiments, and (7) that the unit be easy to use in order to provide the ability to reproduce the experiments rather easily.

If the UF_6 side of the gas manifold was to be as inert as possible to reaction with the UF_6 gas, it was important to choose

stainless steel valves since they are very resistant to UF_6 attack. It would also have been better to use stainless steel tubing and fittings but the budget would not allow this. Instead, copper tubing and brass fittings were used and were reasonably inert to the UF_6 because the manifold was passivated with pure fluorine gas for a 48 hour period prior to any UF_6 being introduced into the system. Also a stainless steel mixing tank was used, and no glass flow meter was employed since it would react with UF_6.

In order to obtain the low pressures needed for the experimental work, a dual pumping system was used. The primary pump was a rotary pump with a capability to lower the pressure to about one micron. The secondary pump was a diffusion pump with the ability to lower the pressure from one micron to approximately 10^{-5} torr under ideal conditions with the limiting factor being the vapor pressure of the pump oil which is 8×10^{-6} torr. The system was also designed so that the diffusion pump could be disengaged at higher pressures ($>50 \times 10^{-3}$ torr) and then re-engaged after the primary pump had lowered the pressure to about 50×10^{-3} torr.

A liquid nitrogen trap was installed to collect any gaseous material, primarily UF_6 or its hydrolysis products which might be toxic. Also, the trap helped to achieve the low pressures needed by cryo-pumping at liquid nitrogen temperatures to desorb gases from the vacuum manifold. Leak testing of the system was done by a variety of techniques. First, as the manifold was being constructed, small sections of the manifold were tested for leaks before they were incorporated into the whole. Second, after the

manifold was completely constructed, sections of the manifold were isolated and leak tested, and then later larger sections were tested. Two different brands of leak detectors were used. The first was a Veeco (MS-90) which has a good pumping capacity but poor sensitivity and was used to detect the larger leaks. Later, after the larger leaks were found, a Leybold-Heraeus was used because of its greater sensitivity. It must be noted here that after the manifold had been constructed, the major leaks found, and the pump engaged, it was important to allow the pump to evacuate the lines for about one week in order to remove species adsorbed on the inner surfaces of the gas manifold. This procedure often saves time because it keeps the operator from confusing pressure due to adsorbed species with leaks.

The manifold and refrigeration unit were mounted on a steel-framed cart since the spectrometer could not be solely dedicated to this study. The cart had two levels. The bottom level (Figures 4 and 5) was used to carry the compressor unit, the rotary and diffusion pumps, and the liquid nitrogen trap. One-half inch aluminum rods were used to construct a support for the gas manifold on the upper level (Figure 6). Also, on the upper level, a corrugated-steel mount which had been previously constructed, but had to undergo slight modification, was placed to support the cryostat.

Another desirable feature of the manifold-refrigeration unit was its flexibility. It was designed with a number of outlets so that it could be used for several different purposes simultaneously. It could be used to handle just about any gas, with relative safety

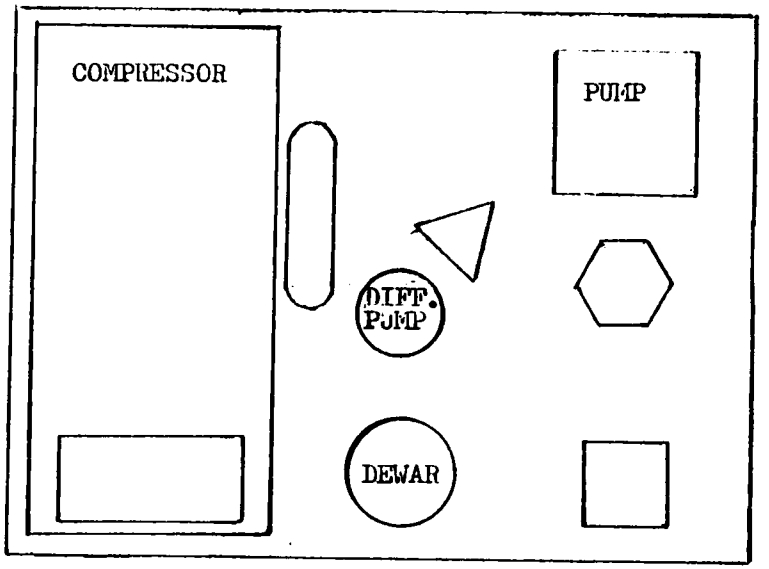


Figure 4. Top view of lower of dual gas manifold cart.

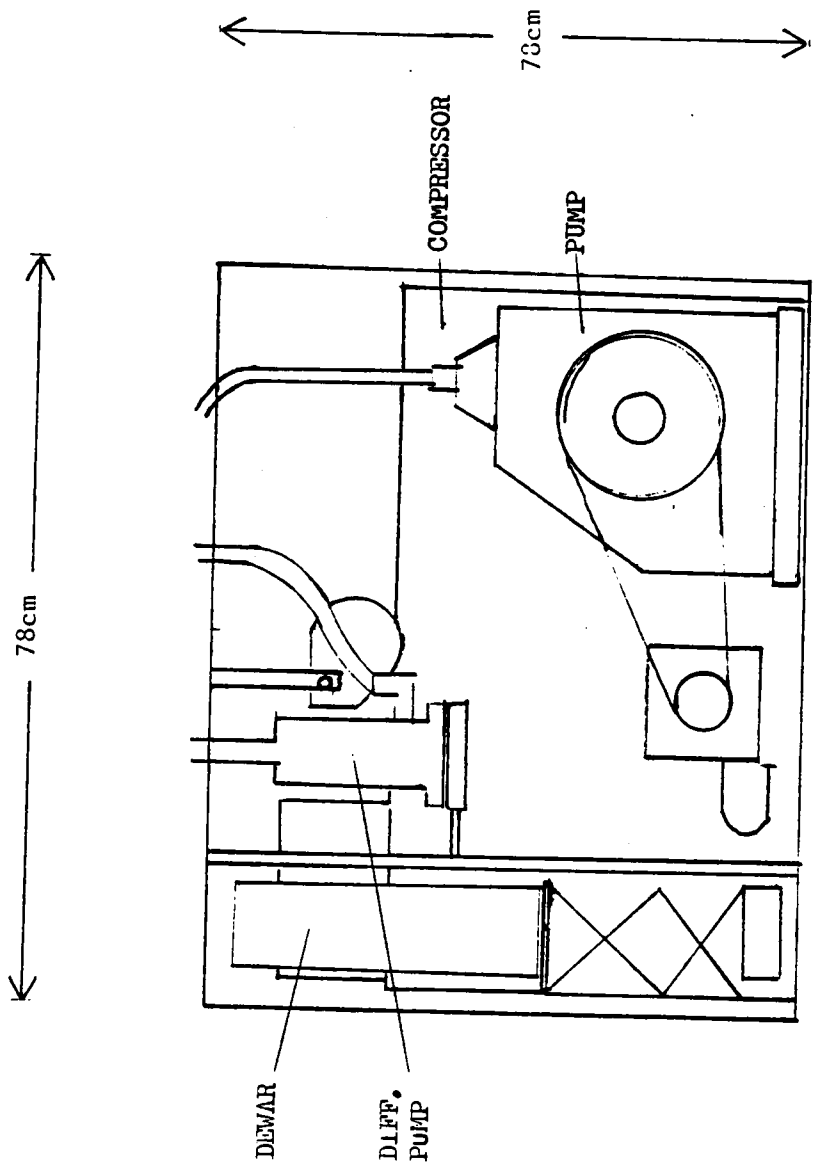


Figure 5. Side view of lower level of cart.

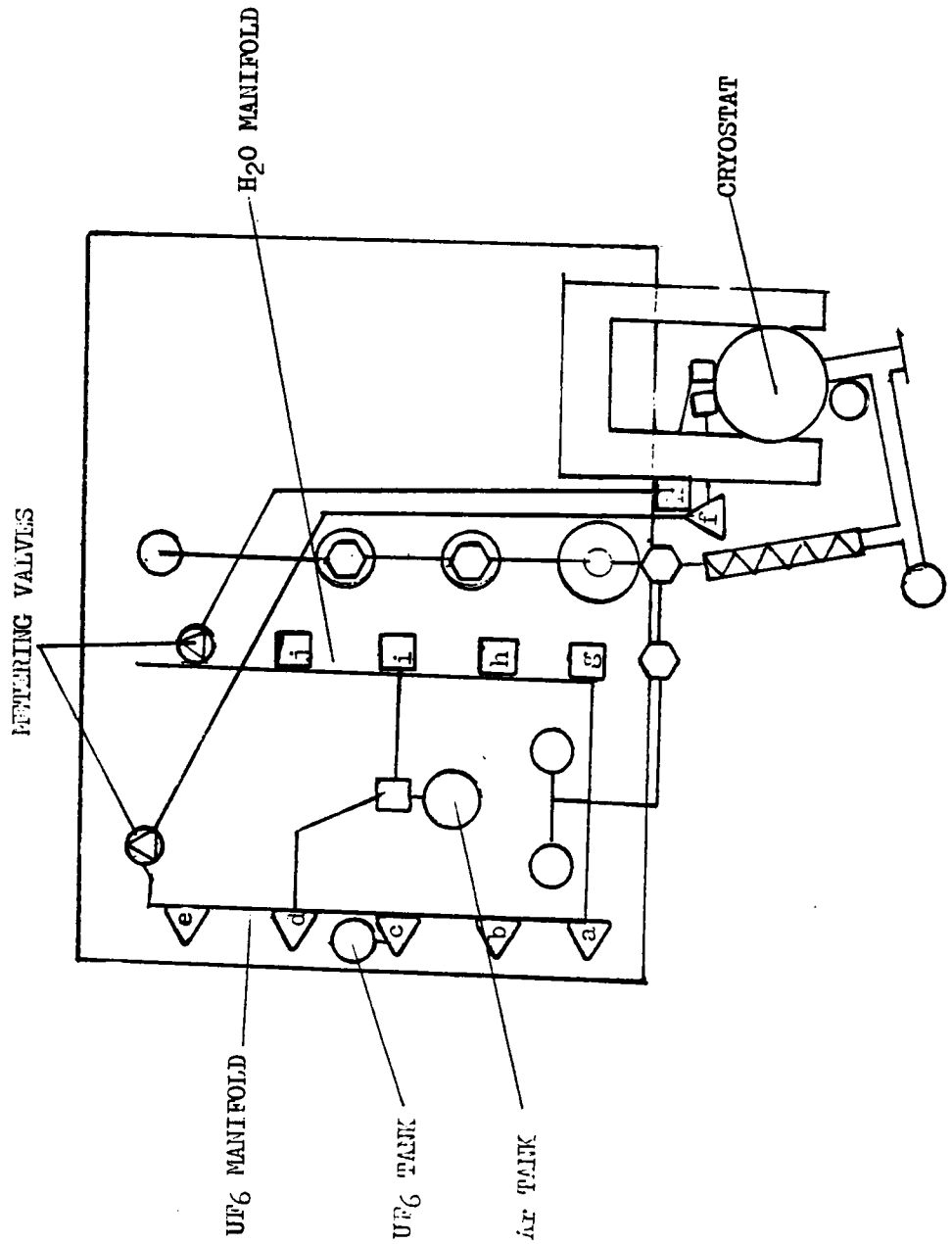


Figure 6. Top view of upper level of dual gas manifold.

and ease. Also, the fact that the unit was mobile added further to its flexibility, and since many of the joints on the manifold used Swagelok (Crawford Fitting Co., Solon, Ohio) and Cajon (Cajon Co., Macedonia, Ohio)-type fittings, the unit could be altered rather easily to fit other needs.

Another desirable feature of the unit was that the compressor-cryostat unit work efficiently so that the cooling be easy and rapid. It was also necessary that one be able to control the temperature as much as possible. Therefore, an Air Products (Air Products and Chemicals, Inc., Allentown, PA) temperature controller was employed.

One of the most important considerations when designing the system was that the unit be easy to use and that the experiments be easy to reproduce. This consideration was accomplished by several methods. First, all of the valves in the gas manifold were mounted above the upper level so they would be easy to reach which is especially convenient if the user has to perform several manual operations in rapid sequence. Also, the valves and tubing on the UF_6 and water sides were panel-mounted at eye level. Metering valves were used on both sides of the dual-gas manifold, and a glass-flow meter was mounted on the water side of the dual manifold unit. Three different types of pressure gauges were also used: (1) the first which was installed on both the UF_6 and water sides of the manifold was a Robertshaw (Robertshaw Co., Knoxville, Tenn.) Acragage which measures pressures from 760 torr to 1 torr, (2) the second was a Hastings (Teledyne Hastings-Raydist, Virginia) pressure gauge which

measures pressure from 100μm (10^{-1} torr) to 1μm (10^{-3} torr), and finally, (3) the third was a Penning (CVC, Inc., New York) type which was used to measure pressures from 10^{-3} torr to 10^{-6} torr. These gauges were necessary to reproduce the experiments.

B. Description

The type of FT-IR spectrometer that was employed was a Digilab FTS-20C/V (Digilab Inc., Cambridge, Mass.). It was equipped with a nichrome wire source and TGS pyroelectric bolometer detector. A KBr beam splitter was used, and interferograms were subjected to "boxcar" truncation before transformation. Spectra were recorded at either 1 cm^{-1} or 4 cm^{-1} resolution.

The primary pump chosen was a Sargent-Welch model 1402 rotary pump (see Figure 5); an accumulation of debris developed, which was probably uranyl fluoride, in the pump's oil case. This material adsorbed on the inner surface of the oil case, and successive oil changes failed to remove the material. After the manifold had been exposed to atmospheric pressure, it took several days for the pumps to evacuate the system to approximately 0.2 millitorr.

The secondary pump chosen was a V.I.C. DA-100 air-cooled two-inch oil diffusion pump (see Figure 5); it can accommodate a pumping speed of 150 liters/sec at 5×10^{-5} torr. The primary pump and diffusion pump were installed so that the diffusion pump could be by-passed (Figure 7) at higher pressures. This modification produced some difficulties. Because of the location of the diffusion pump a flexible rubber hose had to be used to connect the exhaust outlet of

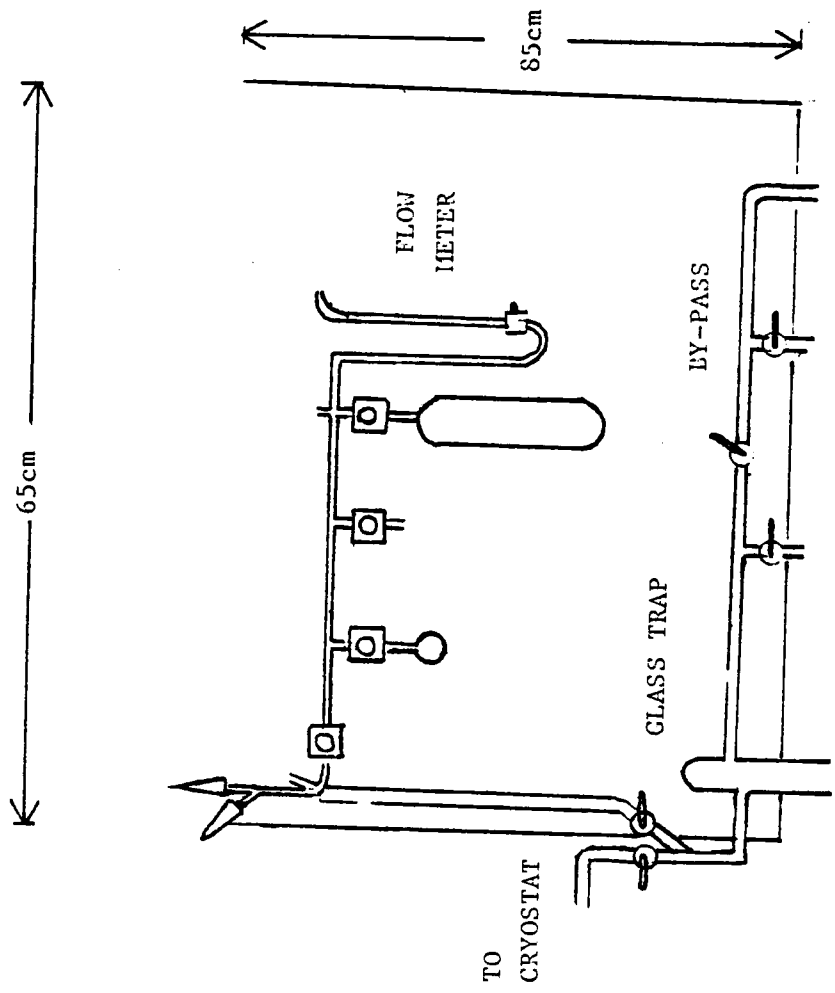


Figure 7. Side view of water manifold.

the diffusion pump to the copper tubing coupled to the forepump (see Figure 5). This rubber tubing was probably a factor in the inability of the pumping system to evacuate the manifold below 10^{-5} torr. Secondly, the trap which was located next to the diffusion pump imposed some strain on the pump as the trap reached its capacity. A small fan was used to cool the diffusion pump (Figure 5).

The liquid nitrogen trap which was located between the manifold-cryostat and the pumps was a conventional glass trap in design (Figure 5), and its outer jacket was 10.5 inches long and two inches in diameter. The primary purpose of the trap was to collect UF_6 or any other harmful materials. It was believed that the UF_6 would not react significantly with the glass trap or the silicone-based stopcock grease at liquid nitrogen temperature, but, since a relatively small amount of debris was found in the trap, it lends doubt about the ability to trap UF_6 in that fashion, especially at low concentrations.

The pump and trap section (see Figure 7) of the manifold was constructed of 1/2-inch copper tubing joined by brass Swagelok fittings and brass Circle Seal (Circle Seal, California) 9200 series plug shutoff valves.

The UF_6 manifold (Figure 8) included 1/4-inch copper tubing joined by brass Swagelok fittings and stainless-steel Autoclave Engineers (Autoclave Engineers Co., Erie, Pennsylvania) packed valves. A.E. valves are very durable and were chosen because of their resistance to attack from the UF_6 and ease of replacement of packing. Valve "a" (see Figure 6) was used as a cut-off between the

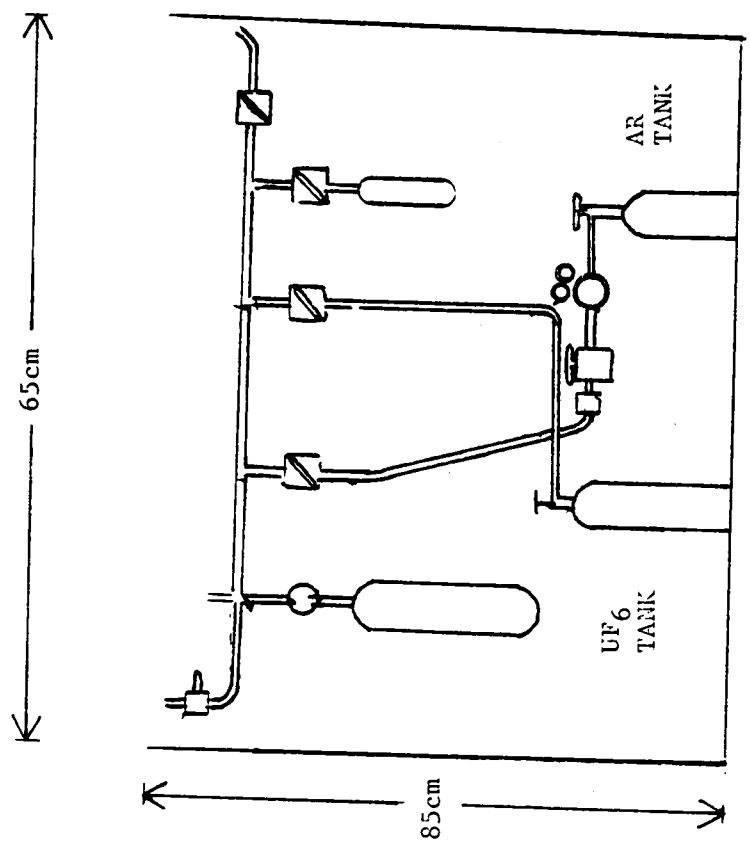


Figure 8. Side view of UF_6 manifold.

UF_6 side and the rest of the manifold. Valve "b" was connected to the auxilliary outlet. It was used to connect a gas tank containing fluorine. The fluorine was employed to passivate the UF_6 manifold, but the outlet was mainly designed as a multi-purpose outlet. Valve "c" was connected to the UF_6 gas tank outlet. There was a valve on the tank itself, but the stainless-steel A.E. valve was added as an extra precaution. The UF_6 flow could be regulated with either valve. Valve "d" was used to regulate the flow of matrix gas. Valve "e" was a Hoke (Hoke Inc., New Jersey) 3700 series packed valve that was used to regulate the flow from the mixing tank (The mixing tank was made of aluminum and had a volume of 500 ml). The metering valve was a brass Nupro MG series with a stainless steel stem. No glass flow meter was used because UF_6 will react with glass. A Robertshaw Acragage gauge was employed to monitor the UF_6 flow, and it was also used to determine or establish the matrix mixtures. Valve "f", also an A.E. valve, was used to isolate the UF_6 manifold from atmosphere when the deposition line was not connected to the cryostat sample compartment.

In between the UF_6 and water side of the manifold, vacuum gauge tubes from Penning and Hastings gauges were positioned on 1/4-inch copper tubing in order to be able to read pressures when evacuating either or both sides of the manifold.

The water side of the manifold (see Figure 7) consisted of a slightly different arrangement than the UF_6 side. It consisted of 1/4-inch copper tubing joined by brass Swagelok fittings and brass valves; the valves were Nupro (Nupro Co., Willoughby, Ohio) "H"

series bellows valves. Valve "g" was used to isolate the H_2O manifold from the rest. Valve "h" regulated the flow of water vapor into the manifold, and a 25-ml glass bulb container was used to hold the water and was joined to the manifold by a Cajon Ultra-Torr fitting. Valve "i" was used to regulate the matrix gas into the water side. The matrix gas tank was connected to both sides of the manifold through the same line (see Figure 6), and a Nupro valve was used to isolate the matrix gas when the gas was not in use. Also, a brass Nupro valve was used to regulate the flow from the mixing tank. The mixing tank was identical to the one used on the UF_6 side. A glass-flow meter was obtained from Lab Crest (catalogue no. 448-001); it had a maximum flow rate of 43.5 cm^3/min. of air at STP. The metering valve which just preceded the flow meter was identical to the one used on the UF_6 side. Valve "j" was used to regulate the H_2O-matrix mixture from the mixing tank. The final valve (k) on the water side was a brass Nupro valve which was used to isolate the water manifold when the deposition line was not in use.

Because the cryostat refrigeration unit had to be elevated and turned slightly when being placed in the spectrometer, a flexible stainless steel tube (see Figure 6) was used to connect the vacuum manifold to the cryostat. This tubing was a Cajon 321 stainless steel tube one-inch in diameter and 12 inches long.

The cryostat-refrigeration unit was a Cryodyne Helium Refrigerator Model 350 manufactured by Cryogenic Technology. It works on the principle of cooling as helium gas is expanded through

a nozzle. It could cool the sample window from room temperature to 16°K in approximately 90 minutes. The sample window holder (Figure 9) and refrigeration unit cover (Figure 10) were constructed in house. The cover was constructed of stainless steel, and the CsI window holder was made from oxygen free high conductivity (OFHC) copper. The stainless-steel cover included four portholes. Two of the portholes held CsI windows which were in line with the CsI sample window and IR beam. Another porthole contained a glass observation window, and the final porthole was used as the deposition port. The deposition port was covered by a brass plate with two 1/8-inch stainless-steel tubes passing through. The tubes were aligned so that the sample mixture could be deposited onto the sample window without interfering with the infrared beam path. Passage of the sample through the tubes could be regulated using stainless-steel Nupro "H" series valves.

In order to connect the deposition lines from the manifold to the deposition port, Cajon VCR vacuum couplings were used. The deposition lines were made from 1/4-inch copper tubing up to the brass Nupro valve on the water side and the stainless-steel A.E. valve on the UF_6 side. Following these valves, 1/8-inch stainless-steel tubing and stainless-steel fittings were used. Silver-plated nickel gaskets were employed in the VCR coupling.

In the in-line studies, the UF_6 and H_2O deposition lines were merged into one (see Figure 11); this was accomplished by using 1/8-inch stainless-steel tubing and stainless-steel fittings. Variable lengths of 1/8-inch stainless-steel tubing could be

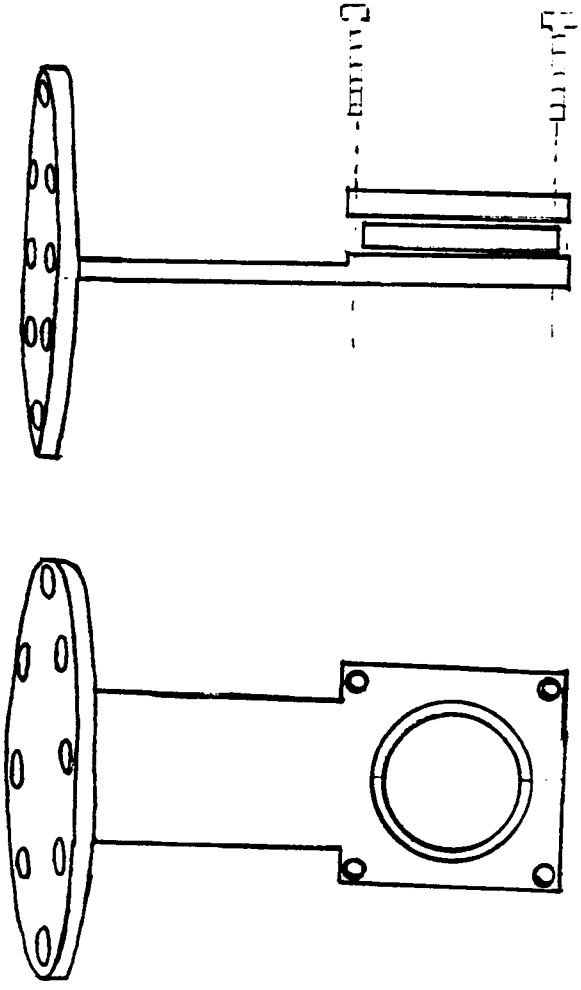


Figure 9. Front and side views of CsI sample window holder.

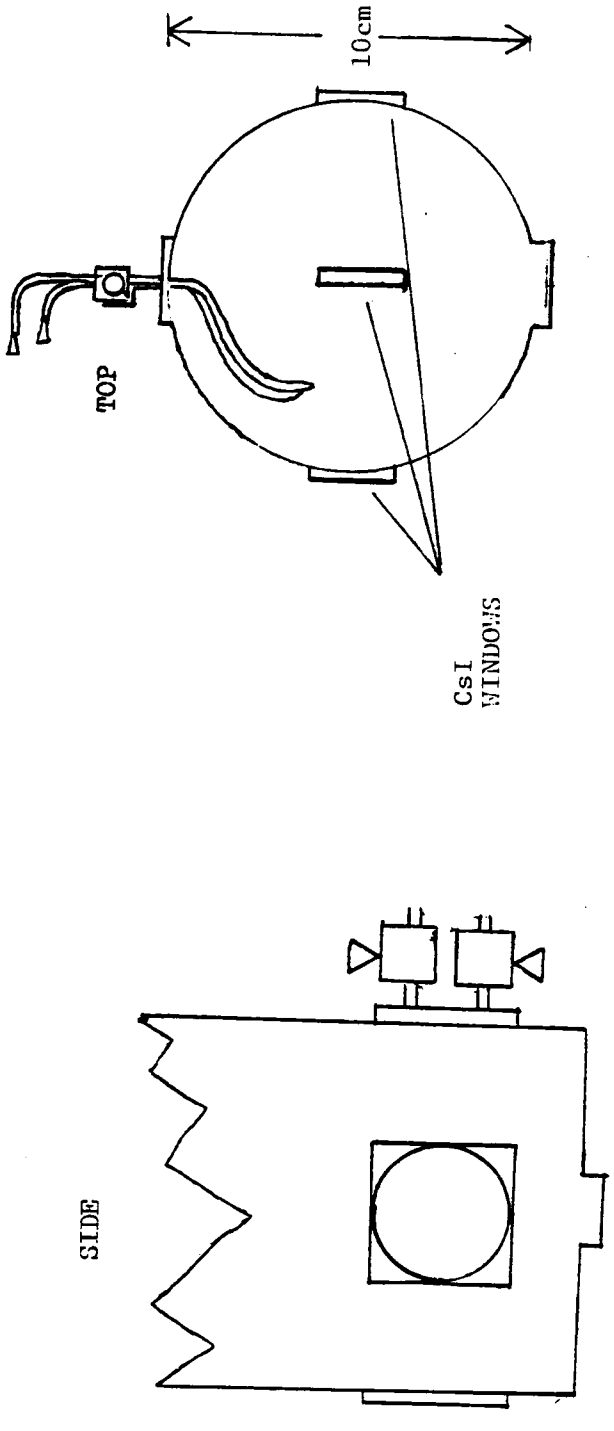


Figure 10. Side and top views of refrigeration unit cover and deposition port.

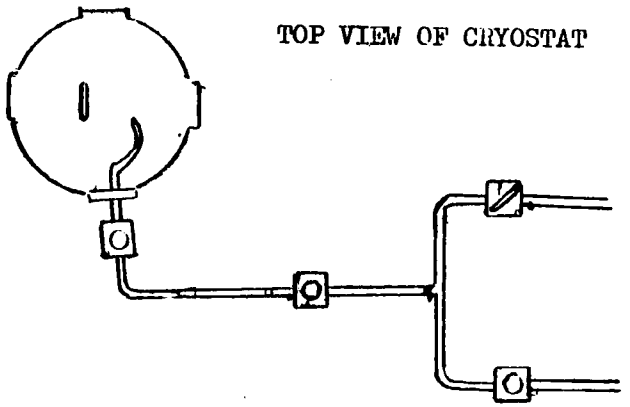


Figure 11. Arrangement used to merge and mix UF_6 and H_2O sample streams.

inserted into the fittings in order to alter the conditions of the experiments, namely the mixing time of the sample stream. Then the sample mixture could be fed into either deposition tube on the deposition port.

The post-deposition port mixing nozzle was constructed of aluminum (Figure 12). It was approximately 1/2-inch in diameter and one inch long. It was constructed so that it would fit over the ends of the deposition tubes in the sample chamber and consequently merge the two sample streams into one prior to deposition. The exit outlet was only about 1/16-inch in diameter. When the post-deposition port mixing nozzle was secured in position, it rested only about 1/2-inch away from the CsI window.

The deposition port constructed for the UOF_4 vapor studies consisted of a brass plate (see Figure 13) similar to the original deposition port. However, instead of holding two stainless-steel tubes, this plate consisted of one 1/8-inch stainless-steel tube and a Cajon 3/8-inch Bore-Thru adapter. A 3/8-inch copper tube containing a sample furnace could be inserted through the adapter. The copper tube (see Figure 13) was approximately 18 inches long, and on one end a trough was hollowed out in order to hold the small platinum-resistance heating-type furnace. On the other end a Ceramaseal (Ceramaseal, N.Y., N.Y.) 800 series straight-wall insulator was connected to a rod that traveled through the tube and connected to the furnace. The rod was insulated from the tube by small Viton (Kontes) O-rings placed around the rod. A variable rheostat was used to regulate the current through the platinum-wound furnace.

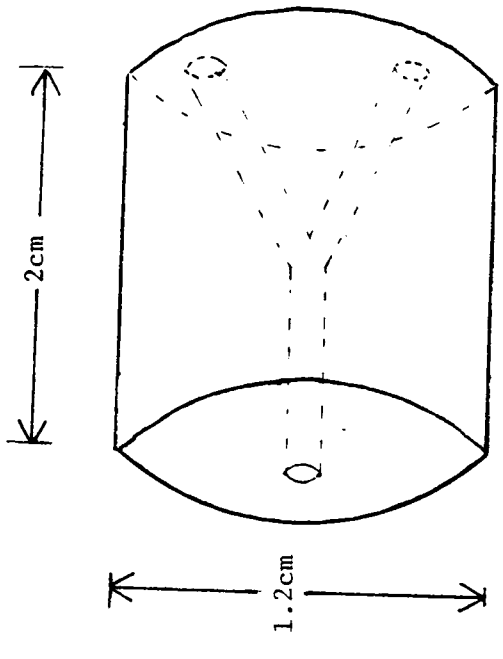


Figure 12. Post-deposition port mixing nozzle.

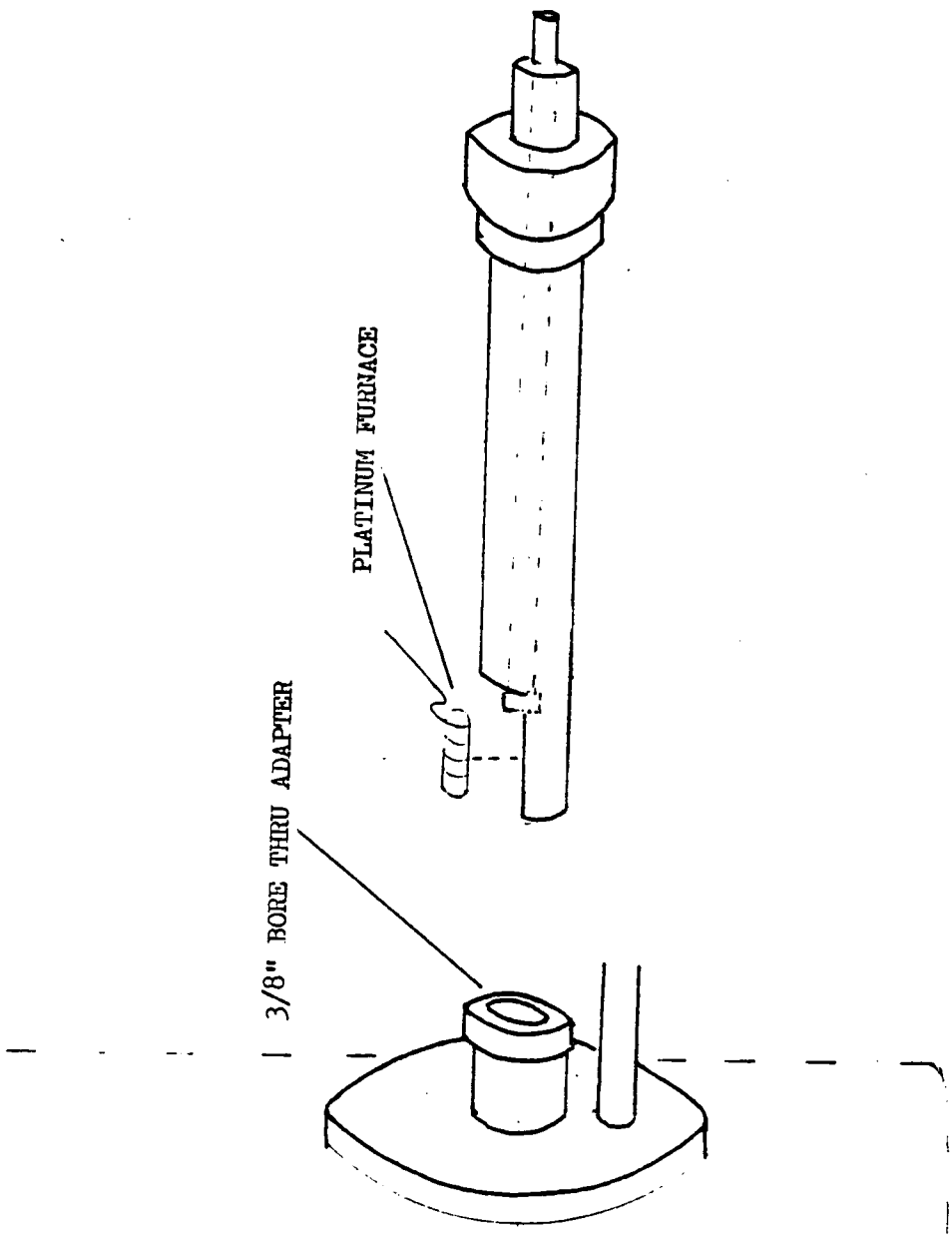


Figure 13. Deposition port and sample holder for UOF_4 vapor studies.

CHAPTER III

EXPERIMENTAL PROCEDURE

A. Gas Phase Experiment

An initial study was done with UF_6 to test its propensity to react with air at room temperature. In this study a small cylinder was constructed from Teflon and fitted on the end with CsI windows and sealed with Viton O-rings; a 1/4-inch stainless-steel tube fitted with an Autoclave Engineers valve was used to admit and remove the sample gas from the cylinder. First, the cylinder was evacuated to a very low pressure (ca. 10^{-6}torr) and then pressurized with a small amount of UF_6; pressures from 10 to 50 torr were admitted to the cylinder. The sample compartment of the Digilab FTS-20C/V spectrometer was sealed with plastic, and the cylinder was placed in the sample compartment with the stainless-steel tube directed through a slit in the plastic. Nitrogen gas was pumped through the sample compartment in order to purge the compartment of atmospheric gases which absorb in the infrared. The flow of nitrogen gas was continued during the course of the experiment. First, the pure UF_6 gas sample was scanned with approximately 500 scans at a resolution of 1 cm^{-1}. After the initial scan, a small amount of air was admitted to the cylinder. This was accomplished by opening the valve on the tube for approximately one second. This new mixture was then scanned at the same resolution as the initial mixture. The air-admission procedure was repeated several times until the UF_6 was depleted. Two variables that were controlled during the

course of the experiment were the initial pressure of the UF_6 gas and the length of time that the regulating valve was opened. As stated earlier, initial UF_6 pressures of 10 to 50 torr were used. The time lengths used were from one to five seconds; the time lengths could be kept constant through the course of the experiment or they could be changed.

B. Matrix-Isolated Water in Argon

The initial matrix-isolation experiments were performed with water and argon. In order to obtain the cleanest spectrum possible, it was necessary to degas the water. This was accomplished by freezing the water with liquid nitrogen and then pumping on the bulb while the water was frozen. After the presure gauge had stabilized, the bulb was shut-off and the water was allowed to heat up. When the water had melted, it was refrozen with liquid nitrogen and the process repeated. Doing this several times removed most of the gas from the water. A 1000:1 $Ar:H_2O$ mixture was made. This was done by using a carbon tetrachloride slush bath (-23°C). Carbon tetrachloride was placed in a Dewar and then cooled down to its freezing point by pouring in small amounts of liquid nitrogen, then stirring with a wooden stick. It is important to stir the slush bath while adding the nitrogen in order to achieve the proper consistency. When the proper consistency was achieved the Dewar was placed around the water bulb. The Dewar remained there for about 30 minutes to ensure that a proper equilibrium was reached. Since the temperature of the carbon tetrachloride slush bath was about -23°C,

this produced an ice vapor pressure of about 0.58 torr. The water side of the manifold was evacuated and then the water bulb was opened to the mixing tank for about five minutes to allow the pressure to stabilize. Then about 580 torr of argon (Matheson, 99.9995%) was allowed into the mixing tank and this gave a 1000:1 ratio.

The temperature controller was calibrated and zeroed in the low temperature range (up to about 25°K) by using an H_2 vapor pressure gauge which was located on the cryostat. It was calibrated in the high range (room temperature) when the refrigeration unit was shut-off. It had to be recalibrated periodically.

The temperature read 15.5°K after the cooldown was completed. About 30 torr of the mixture was deposited on the CsI window in about forty minutes. In matrix-isolation experiments it is important to deposit the sample as "cleanly" as possible to ensure maximum transmittance of the infrared beam. A fast deposit sometimes leads to a "cloudy" matrix. Therefore, as the sample was being deposited, it was examined intermittently with a flashlight. A glassy appearance usually indicated a good deposition. Also, in these experiments, the amount of sample which was deposited during the course of the experiment was measured using a Robertshaw Acragage. If it is stated that 30 torr was deposited, then the pressure dropped 30 torr in the manifold during the deposition. The sample was scanned at a resolution of 1 cm^{-1} with 500 scans.

After the initial spectrum was recorded, an annealing experiment was performed. The compressor was turned off momentarily and

the sample was allowed to warm to approximately 25°K and then recooled. (The diffusion point of argon is approximately 35°K). This sample was then rescanned under the same conditions. The procedure was then repeated except that the sample was warmed a little higher each time up to a temperature of about 35°K.

This experiment was repeated several times with several variables. The matrix gas-water ratio was changed from 1000:1 to 100:1. The smaller ratios were made by using an ice-slush bath. The deposition time and the amount deposited were also varied. Longer deposition times usually led to cleaner looking sample deposits. Amounts were varied so that the percent transmittance varied from about 20% to about 30%.

C. Matrix-Isolated UF_6 in Argon

The UF_6 side of the manifold was passivated with pure fluorine. This was accomplished by filling a small stainless-steel vessel with fluorine gas. The mixing tank on the UF_6 side was heated while being evacuated. The vessel was cooled with liquid nitrogen and connected to the utility outlet on the UF_6 side. The heating was continued while the fluorine was opened to the manifold for approximately two days.

The initial Ar:UF_6 ratio made was approximately 100:1. This was easily accomplished since the vapor pressure of UF_6 at room temperature is about 110 torr, and the lead UF_6 container had a regulating valve. The sample window was cooled to about 16°K, and about 50 torr of the initial mixture was deposited in 30 minutes. The

same annealing procedure that was performed for the H_2O:Ar experiments was also repeated here. The same variables that were present with the water experiments were also present here.

D. Matrix-Isolated UF_6 and Water in Argon

The same procedures that were followed in the independent deposition experiments on matrix-isolated UF_6 and water were performed simultaneously in the next series of experiments. Initially, a Ar:UF_6 ratio of 500:1 and an Ar:H_2O of 100:1 were used. The mixtures were deposited simultaneously at approximately the same deposition rates and approximately the same amounts. The amount deposited was solely determined by trial and error. The criterion was a moderately strong transmittance between 20 and 50 percent. It must be noted that there are many more parameters associated with co-deposition experiments than with single-deposition experiments. Not only can one vary the deposition time, matrix ratio, and amount deposited of each sample mixture, but one can also vary their concentrations in relation to one another. For example, one can have the same rate of deposition, etc., for both mixtures or change one and leave the other the same or change both in the same or opposite directions. Another variable that was not used initially but which was incorporated into the experiments later was the temperature of the window at the time of deposition. The initial deposit was usually scanned at a resolution of 1 cm^{-1} and 500 scans. After the sample was annealed and then recooled, subsequent spectral measurements involved only 200 scans. There were two different modes of

temperature control used during the annealing studies. The first method was previously described; the cooling compressor would be momentarily shut-off while the temperature rose, and then would be restarted, and the spectrum would not be recorded until the sample had recooled to 16°K. Another method of performing the annealing studies was to use a heating tape which was cemented to the refrigeration unit and controlled by the temperature controller. The controller could be dialed to the approximate temperature desired up to about 50°K. The controller would then heat the sample window up to this temperature and hold it there indefinitely. Using this method the spectra were recorded while the temperature was elevated to about 35°K.

E. Matrix-Isolated Water in Nitrogen

In the matrix-isolation studies involving H_2O and nitrogen, the same matrix ratios, deposition times, and sample amounts as in the H_2O and argon studies were used. However, there were some additional problems which the new matrix material presented. First, the liquid-nitrogen trap was much less efficient since the nitrogen carried much of the sample through the trap with it. Second, since the nitrogen matrix allowed guest molecules to diffuse easier than in the argon, the CsI window would contain debris that was left over after the experiment was completed, and, consequently, the CsI window would have to be cleaned and polished more often.

In the annealing experiments, the compressor would be shut-off or the temperature controller would be activated and the sample

allowed to warm for a few moments. The sample was then recooled and a spectrum recorded. Also, if the controller was fed only small amounts of current, the spectra could actually be recorded while the sample was warming. At a resolution of 1 cm^{-1}, the spectrum could be scanned and the data computed in approximately 15 minutes. This time would correspond to about a 15 degree rise in temperature. Since sample debris did remain on the window after the diffusion point of nitrogen was reached, it was felt that the annealing experiments could be continued past the diffusion temperature in order to see if any reaction would occur. Also, the compressor could be restarted for a few minutes during the course of the annealing experiment with the purpose of slowing down the warming process.

F. Matrix-Isolated UF_6 in Nitrogen

The same general procedures were followed in the UF_6:N_2 studies that were used in the H_2O:N_2 studies.

G. Matrix-Isolated UF_6 and Water in Nitrogen

In the co-deposition experiments involving nitrogen as the matrix material the same conditions used in the co-deposition studies with argon were utilized here. Also, the procedures used in the annealing experiments with N_2:H_2O and N_2:UF_6 were utilized here.

H. Matrix-Isolated UF_6 and Water in Xenon

No independent UF_6-in-xenon or H_2O-in-xenon experiments were performed, only studies in which they were deposited simultaneously. The Xe:UF_6 and Xe:UF_6 matrix ratios were both approximately 100:1. The deposition times and amounts were approximately one hour and 50 torr respectively. The initial deposition temperature was at 16°K and the annealing studies were performed to about 200°K.

I. Pure UF_6 and Water

In this series of studies pure UF_6 and pure water were deposited on the CsI sample window simultaneously and mid-IR spectra recorded. In this series of experiments the mixing tanks were not used; on the water side of the manifold, the flask (water bulb) was opened to the manifold during the course of the experiment. This would only cause a slight deflection on the Robertshaw pressure gauge, but, since the vapor pressure of water is approximately 17 torr at about 298°K this figure was used. On the UF_6 side, about 25 torr of UF_6 gas would be leaked into the tubing and usually the deposition would end as soon as all the UF_6 was gone.

Several problems arose with these studies that were not present with the matrix-isolation studies. First, since the water flask was opened to the line continuously it would be difficult to approximate how much water had actually been deposited. It was assumed therefore that if the deposition rates were kept approximately equal then the same amounts would be deposited on the sample window. But, this

assumption entails another problem. That is, how does one set the deposition rate equal to that of the UF_6 if the pressure on the water is continuously maintained? This problem was eliminated by the following procedure. First, the water flask was opened to the manifold, and the flow meter set to a previously-decided flow rate. As the sample was being deposited, the pressure in the cryostat would rise slightly and would give a deflection on the Penning gauge. When the pressure stabilized, the gauge reading would be recorded and the flow stopped on the water side. Next, the flow would be started on the UF_6 side and adjusted so that the pressure on the Penning gauge matched the previously recorded reading. Then the flow on the water side would be restarted, and the flow meter would be set to its original rate. Therefore, the flow on both sides should be approximately equal.

Another problem which arose is that since no matrix gas was being used which could provide a protective layer between the CsI window and the reacting material, there would be some material left on the window after the experiment was finished. Therefore, the windows had to be repolished after each experiment.

After the sample was deposited at 16°K, the compressor was turned off and the sample allowed to warm. Scans were started at about 100°K; the temperatures were recorded at the beginning and ending of each spectrum.

J. Merging Streams of UF_6 and Water

In this series of experiments, dilute samples of argon and UF_6 and argon and water were merged into one deposition tube prior to being deposited on the CsI window in the cryostat. Matrix ratios of 100:1 were used for both UF_6 and H_2O. The apparatus used is shown in Figure 11 and described in Chapter II, Section B.

The methods for making the sample mixtures and deposition procedures were basically the same as in the previous experiments. However, some unexpected problems did occur. It was believed that when the streams merged at the "t" intersection, that they would be cryo-pumped toward the sample window. This, in fact, was difficult to achieve. In order to achieve a clean deposition with as little spectral band broadening as possible, it was necessary to adjust the deposition rates on each side to be as nearly equal as possible. Also, the deposition rates had to be slow in order not to overrun the single line's capacity. If one mixture was being deposited at a slower rate than the other, then this tended to cause one of the lines to back-up and reacted material would be absorbed on the inner surface of the deposition line. This material would usually be freed by passing pure argon through the lines, baking the lines with heating tape, and then evacuating for several days.

In the initial experiments the length of tubing from the "t" intersection to the deposition port was approximately 30 cm. Later, sections of tubing that ranged from 100 cm in length to 300 cm in length were installed in order for the mixtures to have more time to react. Also, the tubing was heated while the deposition was

occuring in order to prevent any material from being adsorbed on the inner surfaces of the deposition lines. After the sample was deposited at 16°K, the CsI window would be warmed and spectra recorded in order to see if any additional reaction would take place.

K. Low-Ratio Deposition Studies

In the low-ratio deposition experiments sample ratios for $Ar:UF_6$ and $Ar:H_2O$ ranged from 2:1 to 6:1. The apparatus was the same as in the original deposition experiments except that the deposition tubes inside the cryostat sample chamber were angled toward one another to insure that good mixing of the sample streams occurred in the small space between the tubes and the CsI window. The mixtures were made inside the manifold lines, and the mixing tanks were not used because only very small volumes were made; in fact, they were so small that the entire mixture was deposited on the window in a single experiment. Much of the work in this series of experiments was more art than science, because the apparatus was not designed to manipulate mixtures of such a small volume. The entire volume would be deposited in about 40 minutes and would usually give IR transmittance of about 30 to 40 percent. After the sample was deposited at 16°K it was then warmed to about 200°K and IR spectra recorded as in the previous experiments.

Actually, when this series of experiments was started, it was hoped that a reaction sequence could be produced by merely manipulating the sample ratios and deposition rates. (Only a single spectrum would be recorded after the deposition, and no annealing

experiment was to be performed.) When it was discovered that this could not be accomplished with this apparatus, then the experiment was redesigned. Sample mixtures having ratios of 3:1 (Ar:X, X=UF_6, H_2O) were deposited on the window at 16°K, and then a series of annealing experiments were performed similar to previous annealing series. In this case, the only purpose of the matrix gas was to act as a solvent. The initial spectrum recorded at 16°K was one of a matrix-isolated sample, but since argon's diffusion point occurs at approximately 35°K and the boiling point occurs at 87.3°K, the subsequent spectra recorded during the annealing experiments were not matrix-isolated or possibly only partially matrix-isolated.

L. Low-Ratio Mixing Nozzle Experiments

This series of experiments was mainly designed in order to verify the low-ratio deposition studies. In these experiments low-ratio samples were used as in the case of the previous low-ratio experiments. The only alteration to the apparatus was a small aluminum nozzle (Figure 12) that essentially insured that the two streams were well mixed before they reached the CsI window. The same conditions were used in the annealing studies as in previous annealing experiments. The only problem encountered in this experiment was that the radiation shield that almost totally surrounded the CsI window was removed to allow room for the nozzle.

M. UOF_4 Volatility Study

Uranium oxide tetrafluoride was prepared from UF_6 in the laboratory by means of the procedure described by Paine and associates.[10] An IR spectrum of the sample in a KBr disc correlated very well with the IR spectrum by Paine and associates.[10]

UOF_4 was transferred from an air-tight container to a glass sample cell in a dry bag flushed with dry nitrogen. The glass sample cell had been heated in an oven at 350°C for several hours to remove water. The cell was transferred to a platinum-wire resistance-heating furnace located on the tip of the conductor rod. The furnace was then inserted through the deposition port on the cryostat head by means of a Cajon Bore-Thru adapter. While transfering the furnace from the dry bag to the cryostat, it was covered with a small plastic bag in order to keep the sample dry. Also, the cryostat had been continuously flushed with dry argon in order to exclude moisture. After the furnace had been located in the deposition port, the cryostat was evacuated and then the CsI window was cooled. The furnace was then heated and the sample vaporized onto the CsI window. An FT-IR spectrum was then recorded at 4 cm^{-1} resolution.

CHAPTER IV

RESULTS AND DISCUSSION

A. Results

1. Preliminary UF_6 Vapor Experiments

The following discussion pertains to the experiments on the interaction of UF_6 vapor with ambient (moist) air, and the experimental prodcedures are those discussed in Chapter III, Section A.

Figure 14 represents a spectrum of a sample of UF_6 gas at 10-torr pressure placed in a sample cell. There are many sharp peaks occupying the 3960-3540 cm^{-1} region, two weak peaks between 3000 and 2800 cm^{-1}, two weak peaks surounding 2360 cm^{-1}, many sharp peaks occupying the 1920-1400 cm^{-1} region, a broad band with several spikes out the top in the 1400-1240 cm^{-1} region, a weak peak at 1160 cm^{-1}, a weak peak at 1030 cm^{-1}, a weak peak at 821 cm^{-1}, a weak peak at 667 cm^{-1}, a strong peak at 619 cm^{-1}, and a broad band from 600 to 480 cm^{-1}. The sharp peaks in the 3960-3540 and 1920-1400 cm^{-1} region are typical H_2O gas-phase absorptions quite comparable to numerous other data in the literature.[65] No obvious assignment can be made of the two weak peaks between 3010 and 2800 cm^{-1}. The two weak peaks surrounding 2360 cm^{-1} and the peak at 667 cm^{-1} fit the pattern for CO_2 absorptions which are well-known.[65] The weak peak at 1160 cm^{-1} is due to UF_6[1-3], and the one at 1030 cm^{-1} is characteristic of absorption by SiF_4,[66] both the wavenumber and shape fitting previous observations. The peak at 821 cm^{-1} could

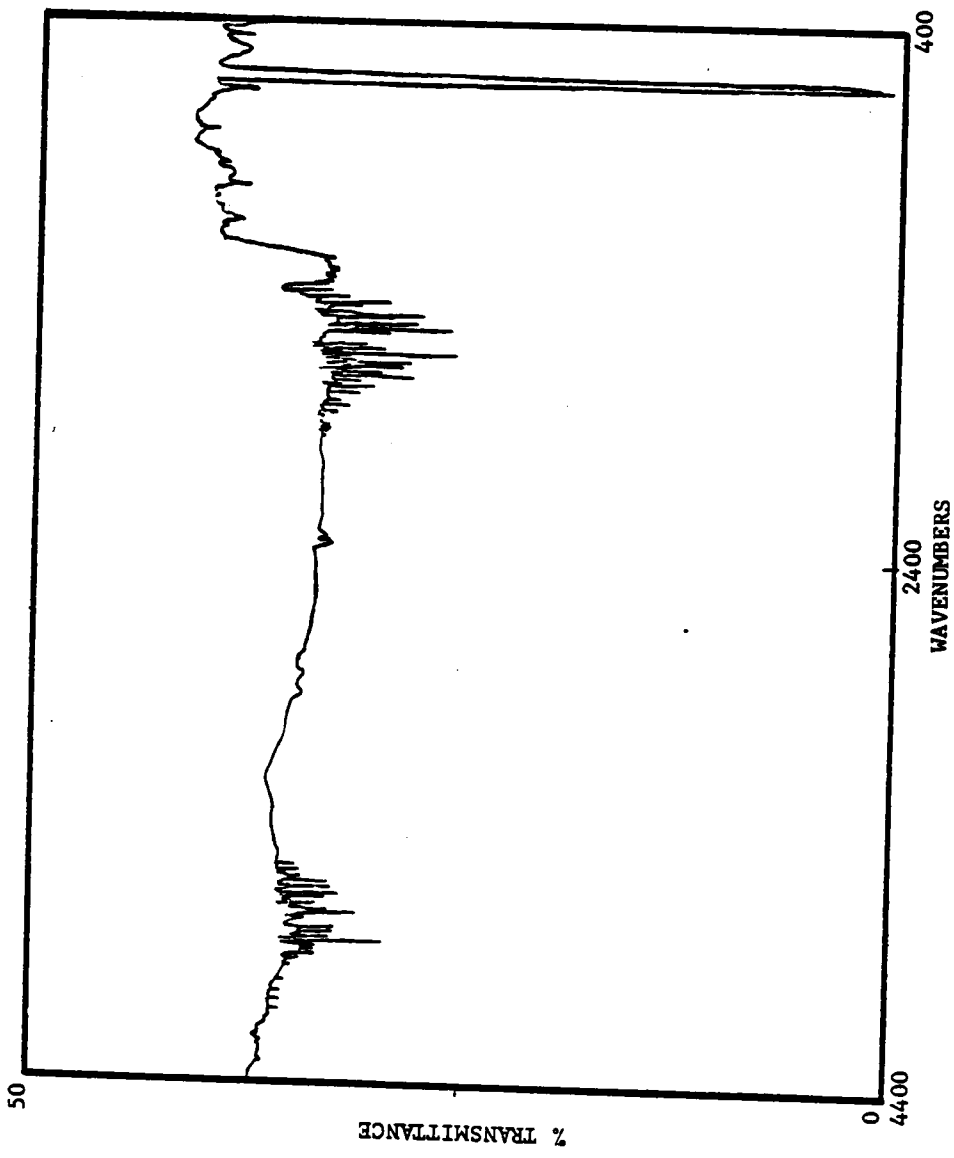


Figure 14. FT-IR spectrum of initial sample of UF_6 gas at 10-torr placed in sample cell.

not be characterized, but the strong absorption at 619 cm^{-1} is believed to be due to UF_6. Previous investigations on UF_6 have assigned absorptions to the U-F stretch in UF_6 to values very close to 620 cm^{-1} (± no more than 7 cm^{-1}).[1-3] Because no appreciable reaction of UF_6 with water has yet taken place one could probably conclude that the H_2O absorptions are due only to water that is in the spectrometer beam but not in the sample. After several admissions of relatively small amounts of air into the cell (see Figure 15), there seem to be only slight changes in the subsequent spectra; the water and CO_2 absorptions are apparently disappearing somewhat. Also, small sharp bands are apparently appearing between 4000 and 4200 cm^{-1}. Bands having these shapes and appearing in this region have been previously assigned to HF absorptions by other investigators.[67] In addition, bands in the 1200-800 cm^{-1} region have apparently been growing. Figure 16 represents the sample after several large pulses of air were introduced into the cell. The bands between 4200 and 3600 cm^{-1}, and the bands in the 1200-800 cm^{-1} region have continued to grow. Also, the UF_6 peak has decreased somewhat in intensity. The final spectrum (Figure 17) shows that the UF_6 band (619 cm^{-1}) has decreased markedly and the bands between 1200 and 800 cm^{-1} have increased, the greatest increase occuring at 1030 and 980 cm^{-1} where two sharp bands are located. Again, the band at 1030 cm^{-1} is typical of an SiF_4 absorption that has been assigned previously to an Si-F stretch by

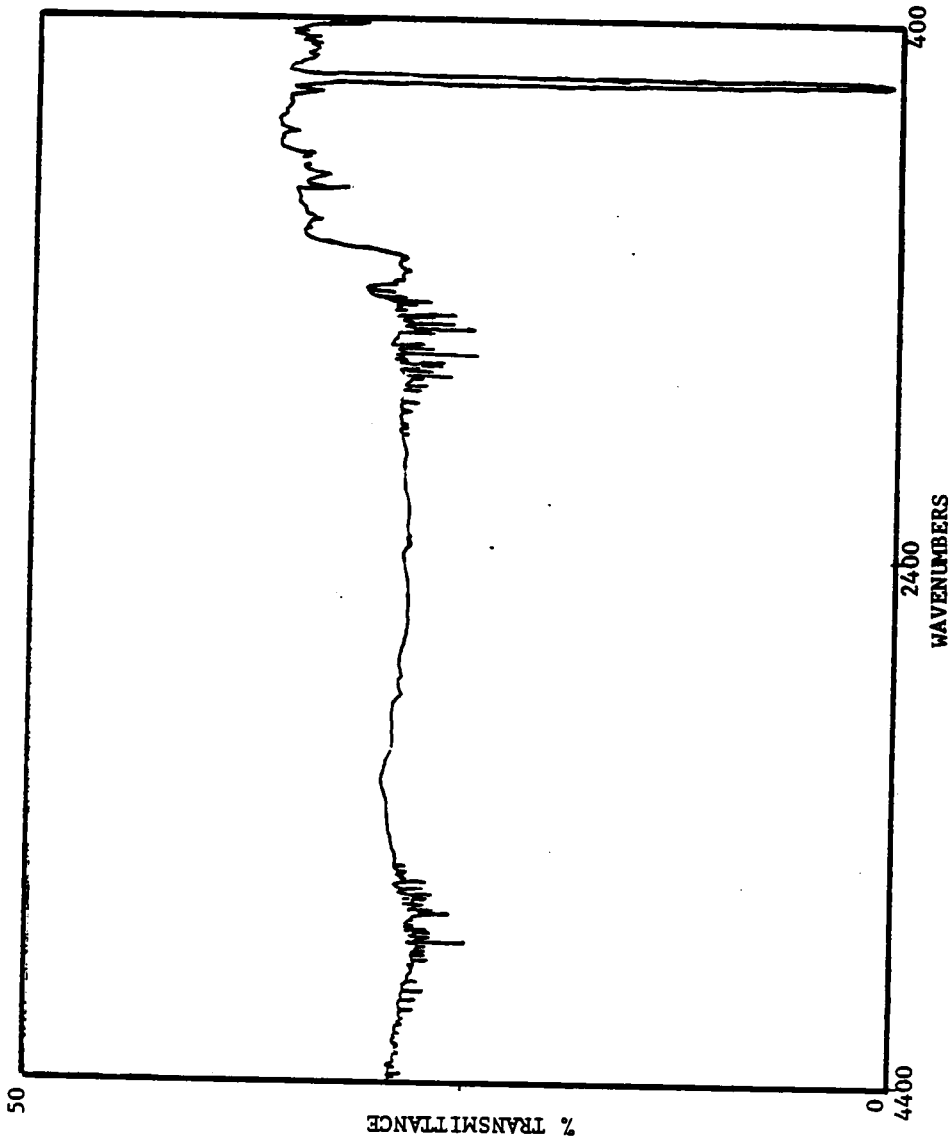


Figure 15. FT-IR spectrum after several admissions of small amounts of air.

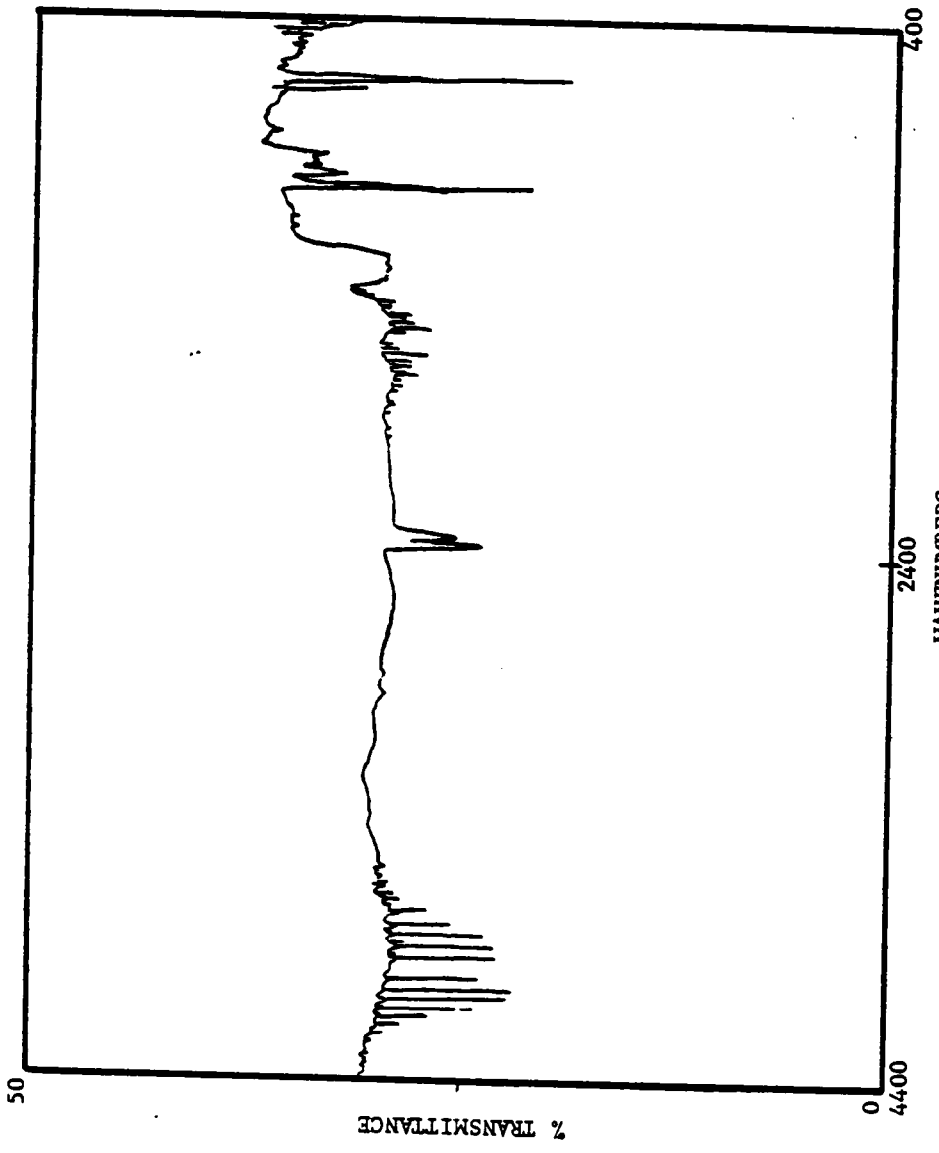


Figure 16. FT-IR spectrum after several large pulses of air.

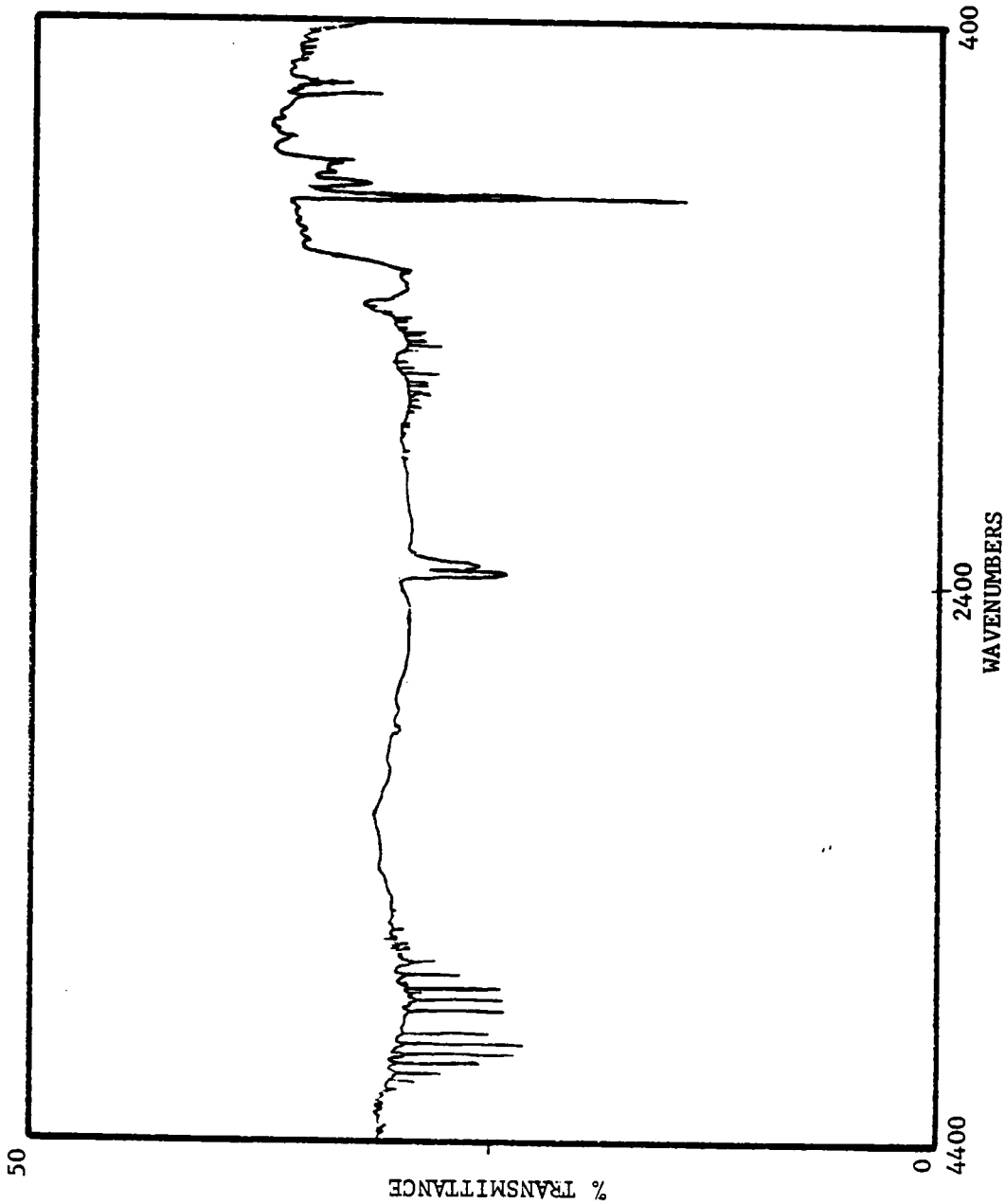


Figure 17. FT-IR spectrum after cell was pressurized to atmosphere.

numerous investigators.[65] Silicon tetrafluoride, which might be present, was probably generated from UF_6 or HF reacting with the silicon-based stopcock grease that was used to lubricate the Viton O-rings which sealed the CsI windows. The emerging band at 980 cm^{-1} could possibly be assigned to a UO_2 stretch arising from UO_2F_2, which is a product of the reaction of UF_6 with water. Several investigators have previously assigned bands in that region (990-930 cm^{-1}) to a UO_2 stretch.[20] Clearly, these experiments were somewhat primitive, but they were instructive. It must be noted here that a very important parameter which could not be controlled with the apparatus employed was the water content of the air. The main purpose of this primitive experiment was to try to obtain some idea of the reactivity of UF_6 with moist air. It also must be noted that no detectable reaction of UF_6 occurred until larger amounts of air were admitted into the cell.

The next series of spectra represent a 50-torr sample of UF_6 interacting with moist air. The first spectrum (Figure 18) was one taken before any air had been admitted, and it shows some HF to be present (4200-3600 cm^{-1}).[67] Two new sharp bands appear at 1292 and 1158 cm^{-1} which are probably due to UF_6.[1] Other weaker bands appear at 1030, 938, 855, 821 cm^{-1} and finally two strong bands appear at 667 and 620 cm^{-1}. As in the case of the 10-torr experiment, only relatively small amounts of air were introduced into the sample cell initially. However, unlike the 10-torr sample, the 50-torr sample (Figure 19) seemed to react when only small amounts of air were admitted. The HF bands continued to grow.

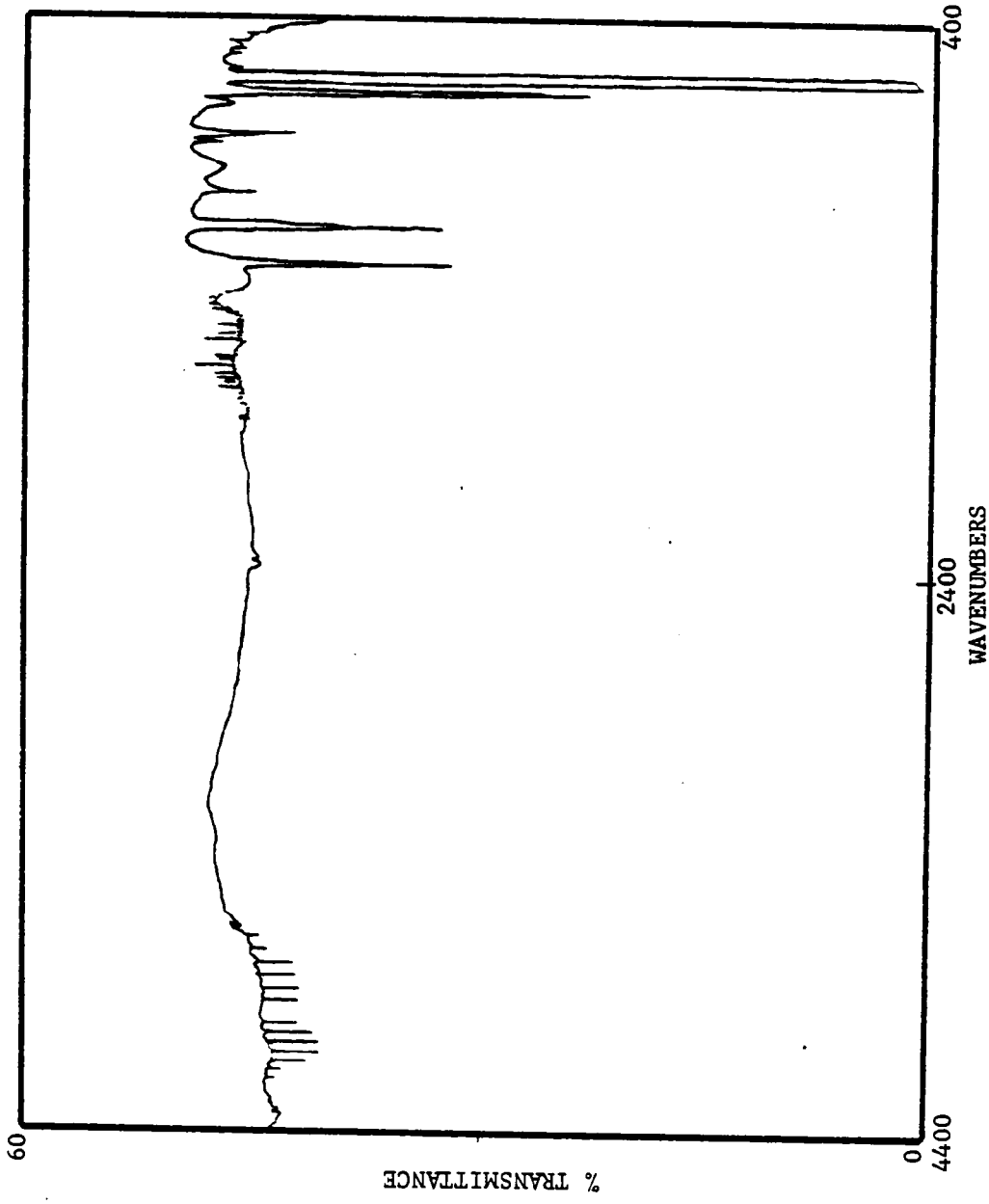


Figure 18. FT-IR spectrum of initial sample of UF_6 gas at 50-torr placed in sample cell.

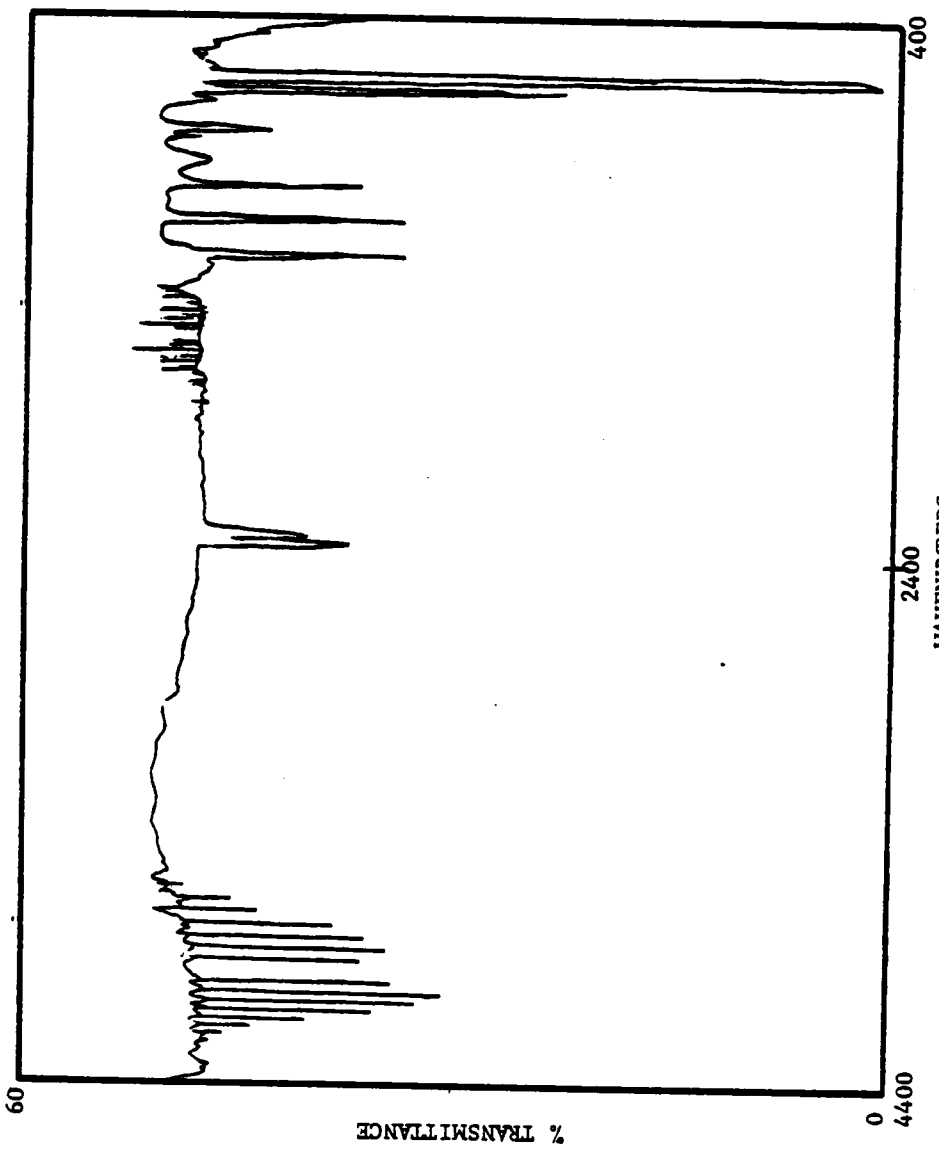


Figure 19. FT-IR spectrum of sample after only small pulses of air were admitted.

Later, (Figure 20) larger amounts of air were admitted into the cell, and after the sample had been exposed to air for a relatively long time (1 min), the spectrum showed that the HF bands had continued to grow as had the 1030 cm^{-1} band. The bands at 1292 and 1158 cm^{-1} are due to UF_6.[1] The bands at 855, and 821 cm^{-1} are not immediately identifiable. Again the 1030 cm^{-1} band can be assigned to SiF_4. The new band at 935 cm^{-1} is in a region in which investigators have assigned similar bands to a UO_2 stretch. The 667 and 620 cm^{-1} bands can again be assigned to CO_2 and UF_6, respectively.

The easiest observation that can be made when comparing these two samples is that the 50-torr sample reacted more readily when only small amounts of air were introduced into the sample cell. Also, although there were many similarities in the two different sets of spectra, there were several dissimilarities. New bands appeared at 1292, 1158, 855, and 821 cm^{-1} in the higher-concentration sample, but they do not seem to change much in their intensities as the experiment progresses. Also, another interesting aspect of the experiment is the 980 cm^{-1} band in the 10-torr experiment, and the absence of a band at this wavenumber in the 50-torr experiment, but the emergence of a new band at 935 cm^{-1}. According to past investigations,[10,20] either or both bands could possibly be assigned to a UO_2 stretch, but no obvious reason for the change in wavenumber can be given. It can be further noted that the bands are approximately the same shape (breadth and general contour).

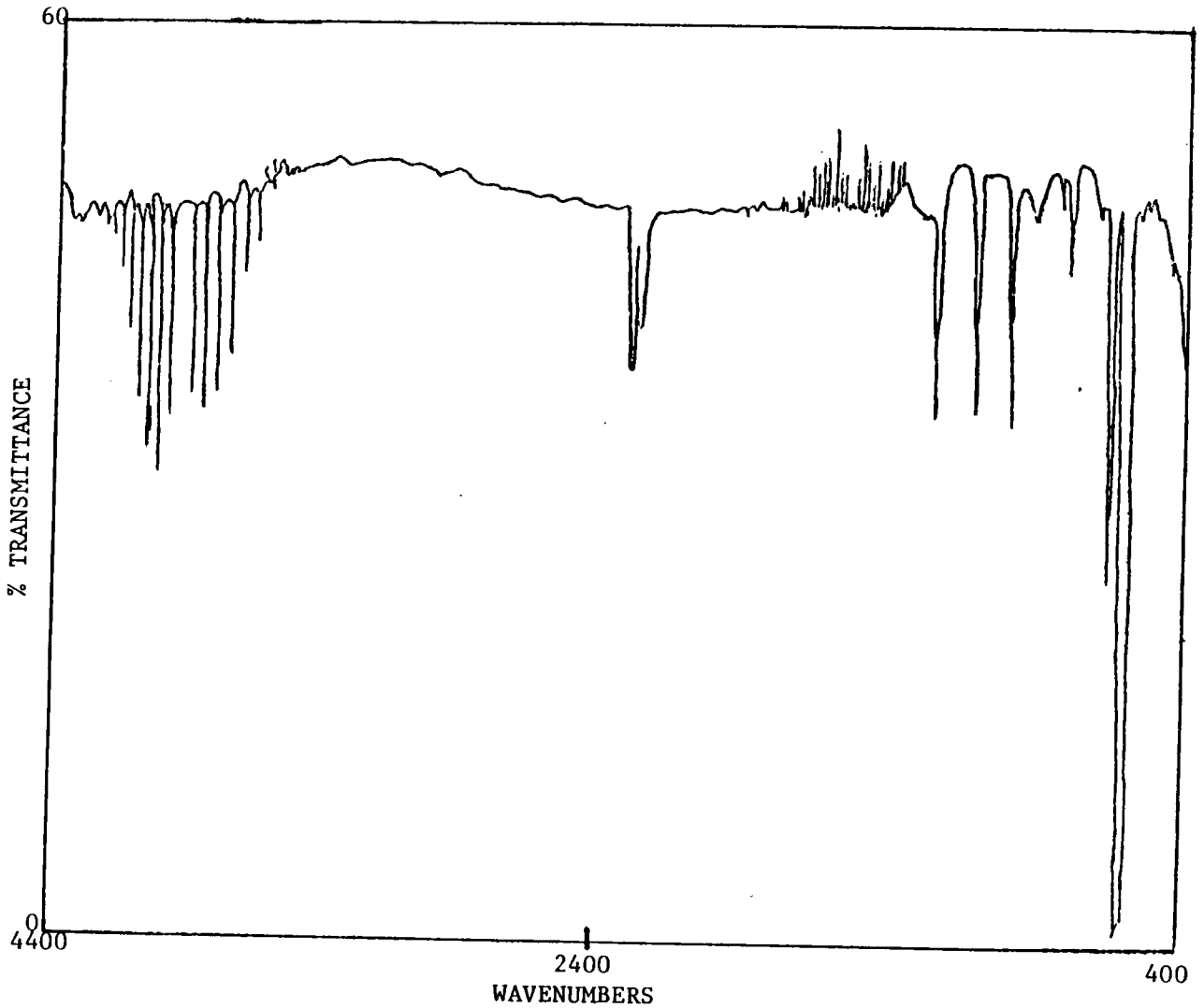


Figure 20. FT-IR spectrum of sample which was recorded after the sample cell was exposed to air for approximately one minute.

2. UF_6-Ar Matrix-Isolation Studies

A series of UF_6:Ar matrix-isolation studies were performed under conditions discussed in Chapter III, Section C. The first spectrum (Figure 21) is of a UF_6-argon sample which had an Ar-to-UF_6 (Ar:UF_6) ratio of 500:1. A close inspection of the spectrum reveals that there were some impurities in the sample. The weak bands between 4000 and 3600 cm^{-1} are characteristic of H_2O absorptions. Also, there are traces of CO_2 impurity (peak at 2340 cm^{-1}). There are also a few weak bands in the 1200-800 cm^{-1} region. And, finally there is the strong UF_6 band which occurs at 619 cm^{-1}.

On closer inspection of an enlargement of the UF_6 band at 619 cm^{-1} (Figure 22), one can see that it actually is composed of a strong band at 619 cm^{-1} surrounded by six weaker satellite bands. They occur at 627, 623, 621, 617.5, 614, and 609 cm^{-1}. Also, an enlargement of the spectral region between 1000 and 700 cm^{-1} can be seen in Figure 23. This permits one to see the unidentified bands which occur at 935, 901 and 820 cm^{-1}.

Next, annealing experiments were performed. The temperature of the sample was elevated to about 35°K, but no significant changes in the spectrum were noticed. If diffusion had occurred, one would expect that the UF_6 molecules might form aggregates and the band at 619 cm^{-1} might broaden, and its fine structure become obscured.

Figure 24 represents a spectrum of a Ar:UF_6 sample having a ratio of 100:1. If one compares this spectrum to Figure 21, one can see that the intensities of the impurities have increased somewhat. There is also an additional band at 1030 cm^{-1} which is due to SiF_4.

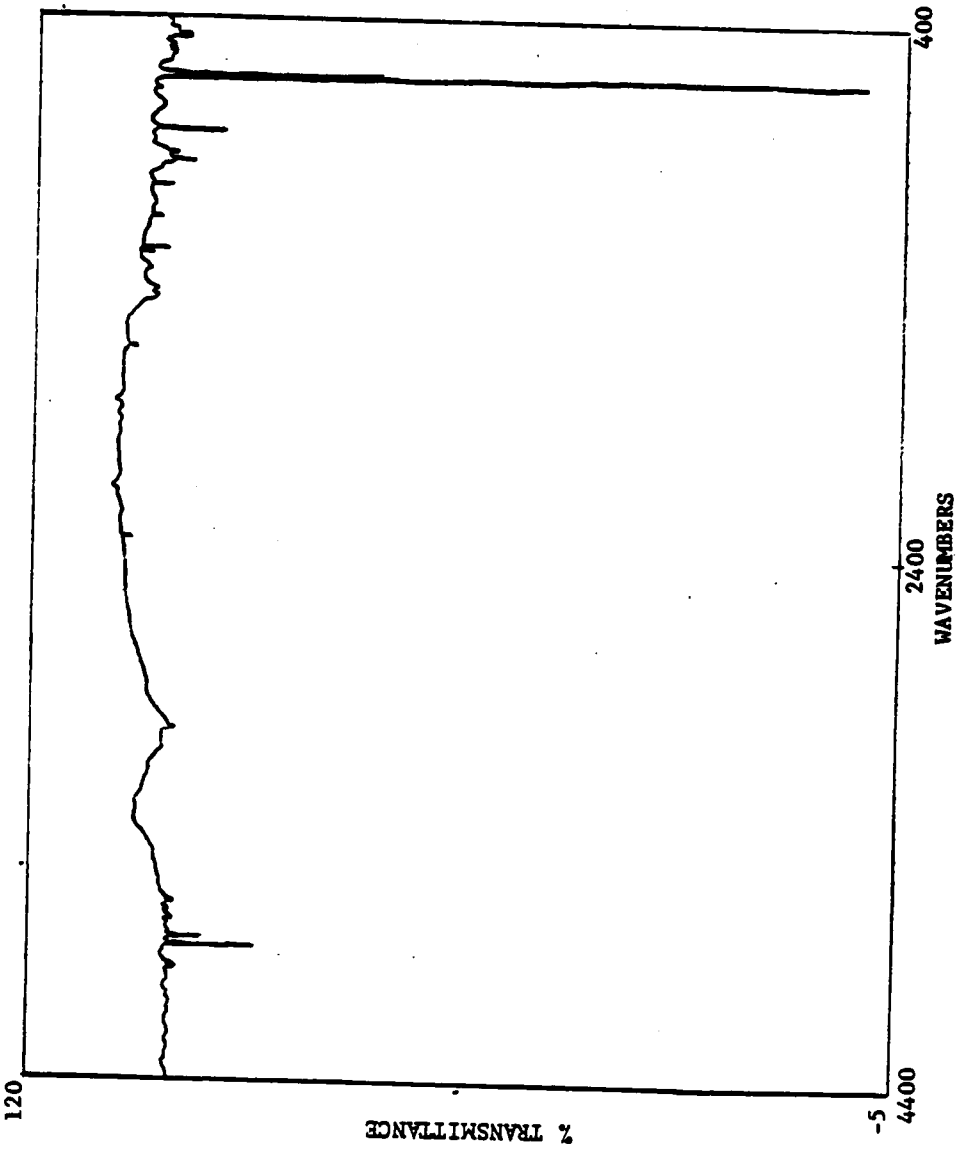


Figure 21. Matrix-isolated FT-IR spectrum of Ar:UF_6 at 500:1.

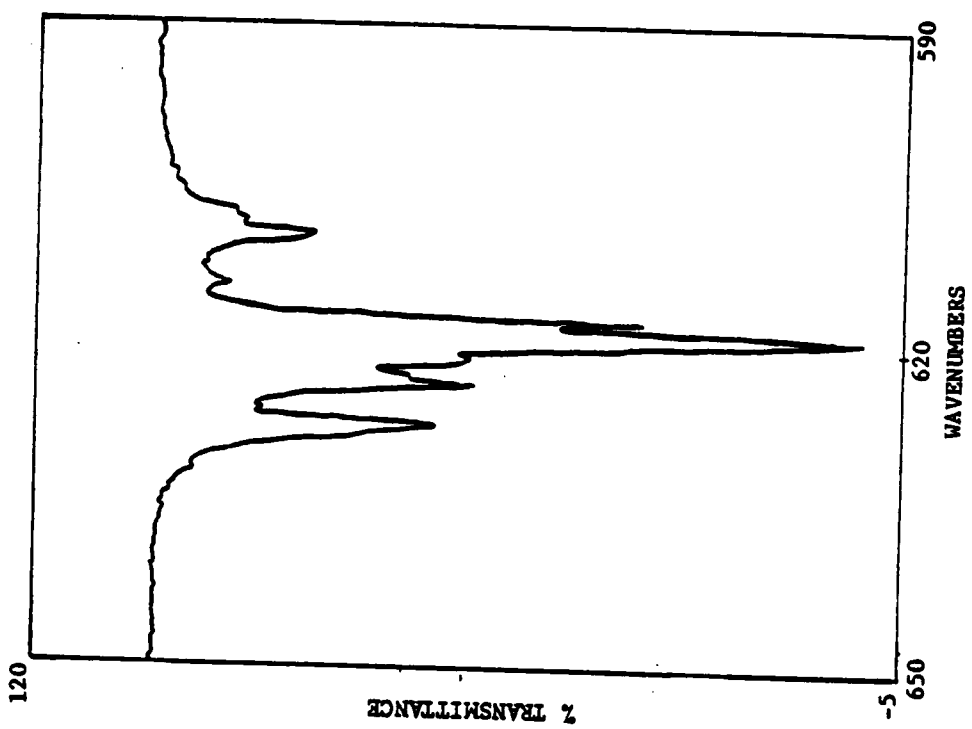


Figure 22. Enlargement of UF_6 absorption.

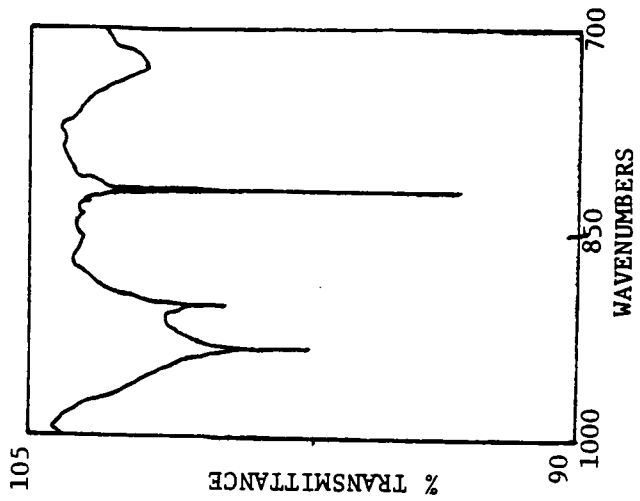


Figure 23. Enlargement of impurity region.

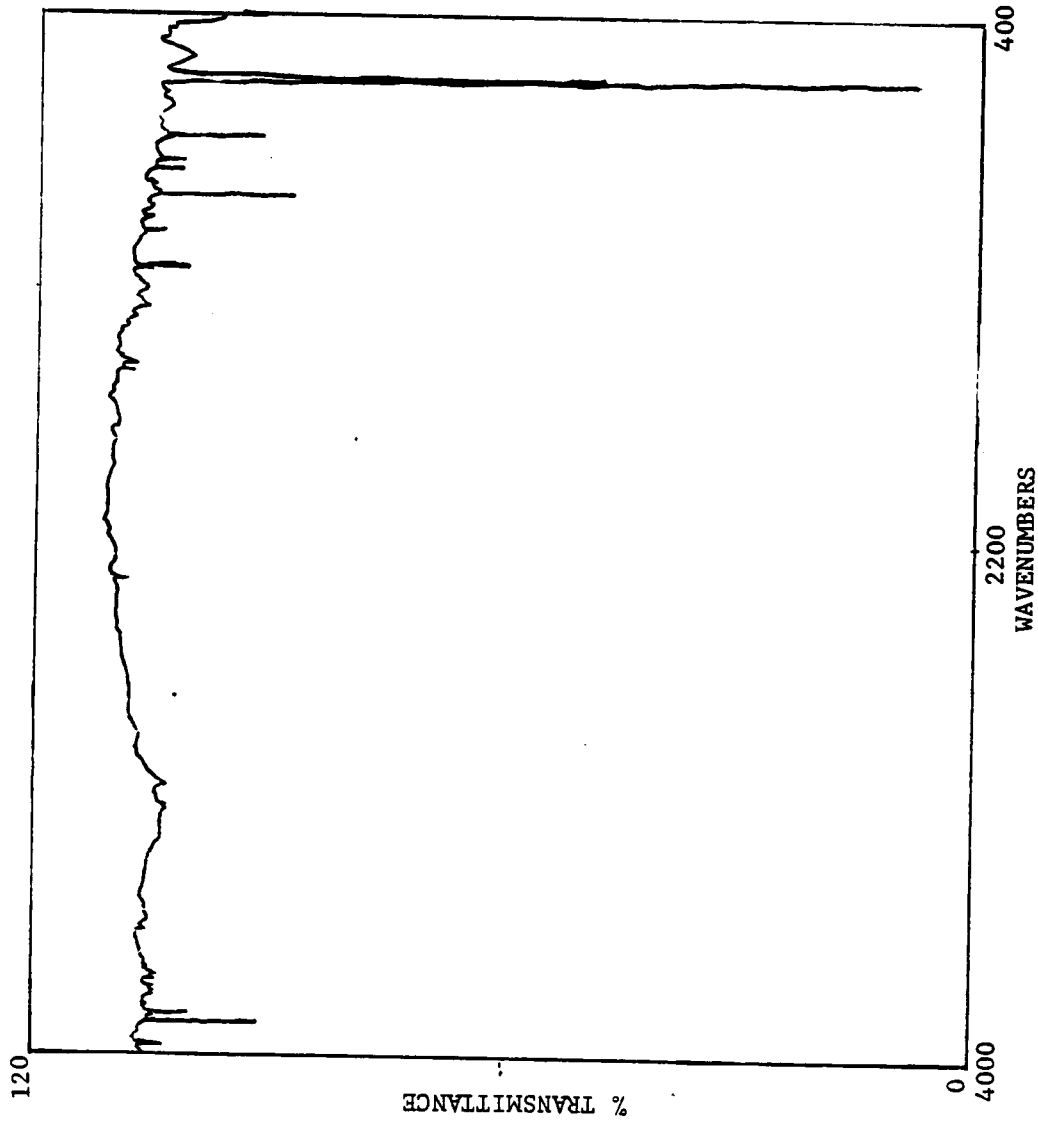


Figure 24. Matrix-isolated FT-IR spectrum of Ar:UF_6 at 100:1.

Close inspection of the UF_6 band at 619 cm^{-1} (Figure 25a) indicates that the satellite bands surrounding the 619 cm^{-1} peak have increased in intensity.

The spectrum of the same sample after having been annealed to 25°K is shown in Figure 25b. One can see that the spectrum is basically the same. There are no intensity changes or peak shifts.

One or two conclusions can be drawn from these experimental results. A characteristic of annealed samples in which clustering occurs is that the spectral bands tend to broaden and lose their sharpness. Keeping this fact in mind, one can probably conclude that no significant aggregation of matrix-isolated UF_6 molecules occurs in argon in these temperature ranges. Another interesting feature of this experiment is the resemblance of the unidentified impurity bands in the 1000 to 600 cm^{-1} region to the unidentified bands in the same region in the UF_6-vapor interaction with moist air experiment. It will be instructive to keep this phenomenon in mind as one reads further.

3. Matrix-Isolated H_2O in Argon

Next, a series of H_2O:Ar matrix-isolation experiments were performed under experimental conditions discussed in Chapter III, Section B. Figure 26 is a spectrum of a 1000:1 matrix-isolated sample of Ar:H_2O. In previous investigations of matrix-isolated IR experiments with water, most authors examined two spectral regions.[68,69] They are the 4000 to 3000 cm^{-1} and the 1650 to 1550

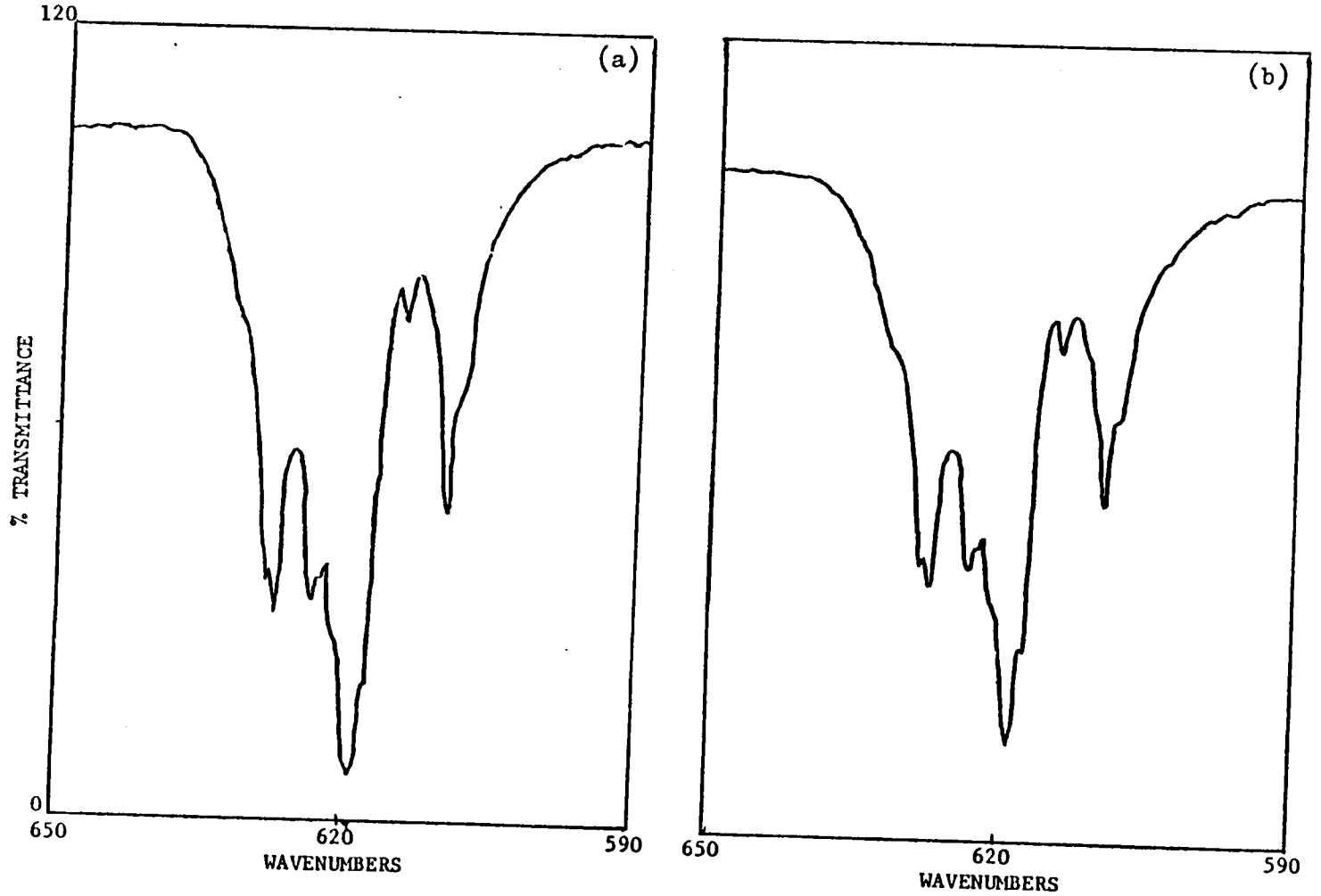


Figure 25. (a) Enlargement of UF_6 absorption before annealing. (b) Enlargement of UF_6 absorption after annealing to 25 K.

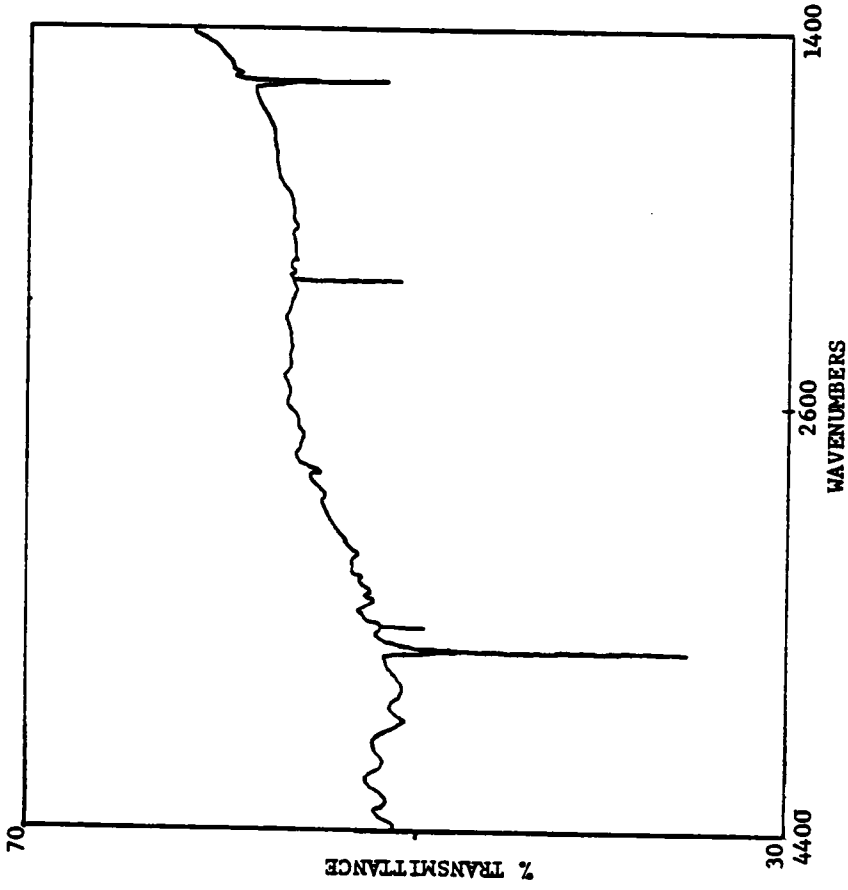


Figure 26. Matrix-isolated FT-IR spectrum of a 1000:1 sample of Ar:H_2O.

cm^{-1} regions. Figure 27 is an enlargement of the 3800-3500 wavenumber region. Two bands appear at 3730 and 3640 cm^{-1}. These bands have previously been assigned by other investigators to Ar matrix-isolated water molecules.[68,69] The next spectrum (Figure 28) is an enlargement of the 1650 to 1550 cm^{-1} spectral region. Absorptions appear at 1611.5, 1601, 1599, and 1593 cm^{-1}. These bands are also similar to absorptions that have been previously assigned to Ar matrix-isolated water molecules.[68,69] The next two spectra (Figures 29 & 30) show enlargements of the same two regions after the samples had been annealed to 32°K. The peak intensities and shapes are roughly the same as in the initial spectra.

The next spectrum (Figure 31) is of a 100:1 matrix-isolated sample of $Ar:H_2O$. The two aforementioned spectral regions will be analyzed. In the 3800-3400 cm^{-1} region (Figure 32) several new bands have emerged that were not present with the 1000:1 sample. Peaks at 3776, 3755, 3730, 3724, 3705, 3699, 3696, 3633, 3573, 3565, 3563, 3556, 3552, 3523, and 3516 cm^{-1} are present and the most intense seem to be the 3705, 3699, and 3696 cm^{-1} peaks. In the other region (Figure 33) several new peaks have also emerged. They are at 1623, 1613.5, 1611.5, 1608.5, 1604, 1603, 1601, 1597, 1593 and 1572 cm^{-1}. These bands closely resemble and are in relatively good agreement with matrix-isolated IR spectra of H_2O that were obtained by Brentwood and associates.[69] They assigned most of the bands in the 3800-3400 cm^{-1} region to dimers and trimers and the bands in the 1650-1580 cm^{-1} region were assigned mostly to monomers and dimers. Figures 34 and 35 reveal that after annealing to 30°K

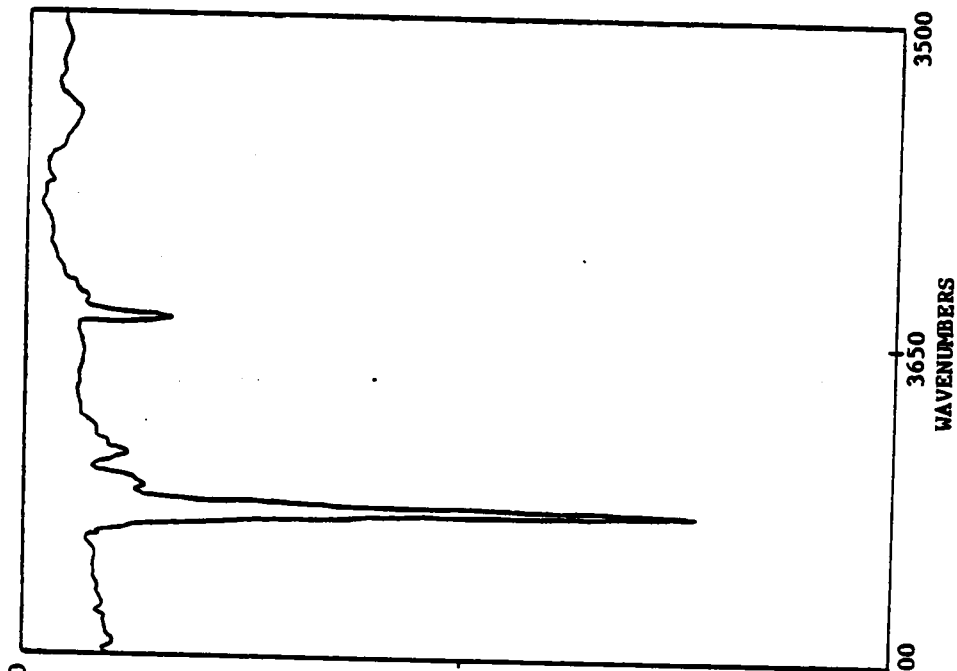


Figure 27. Enlargement of 3800-3500 wavenumber region.

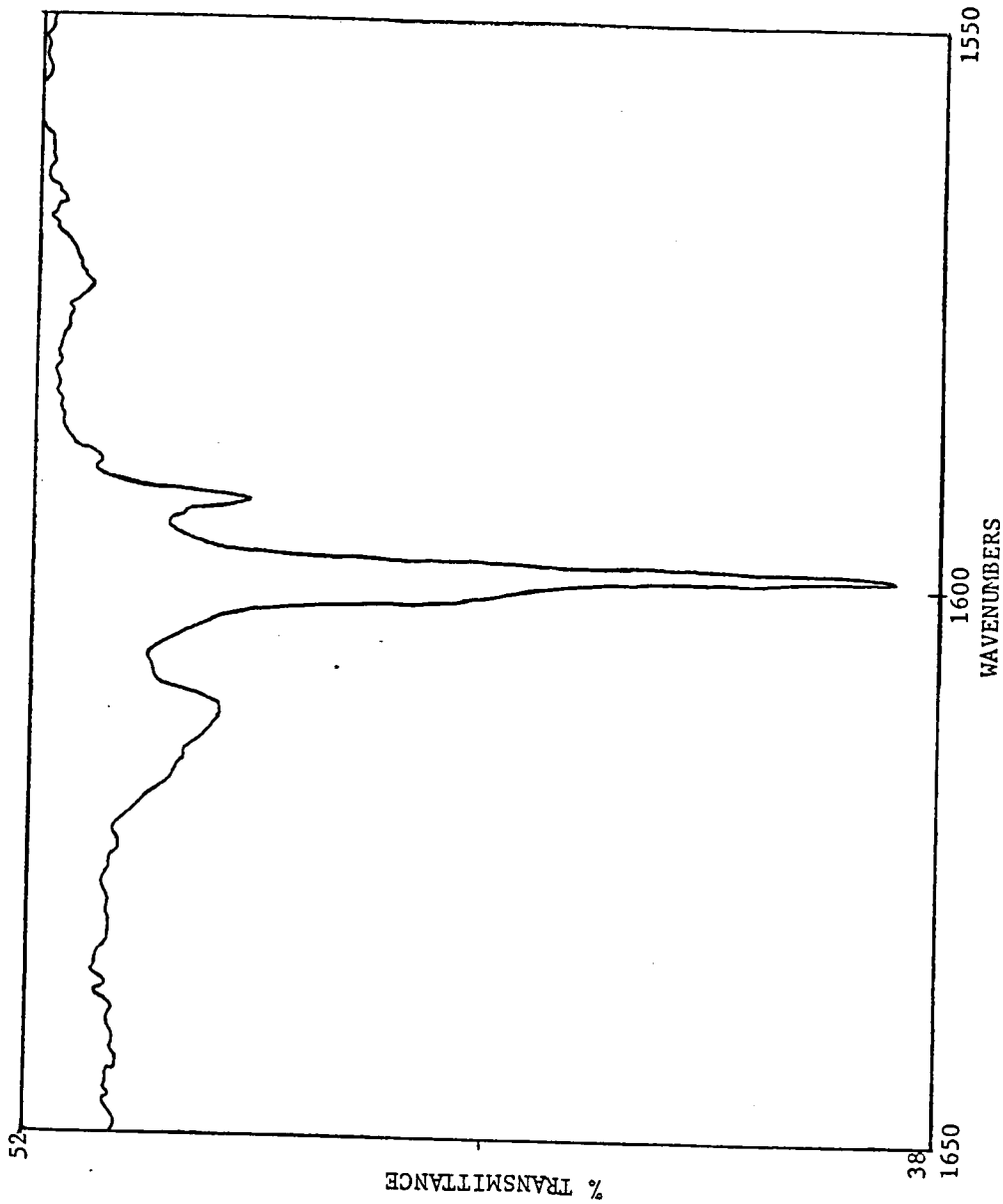


Figure 28. Enlargement of the 1650-1550 wavenumber region, Ar:H_2O = 1000:1.

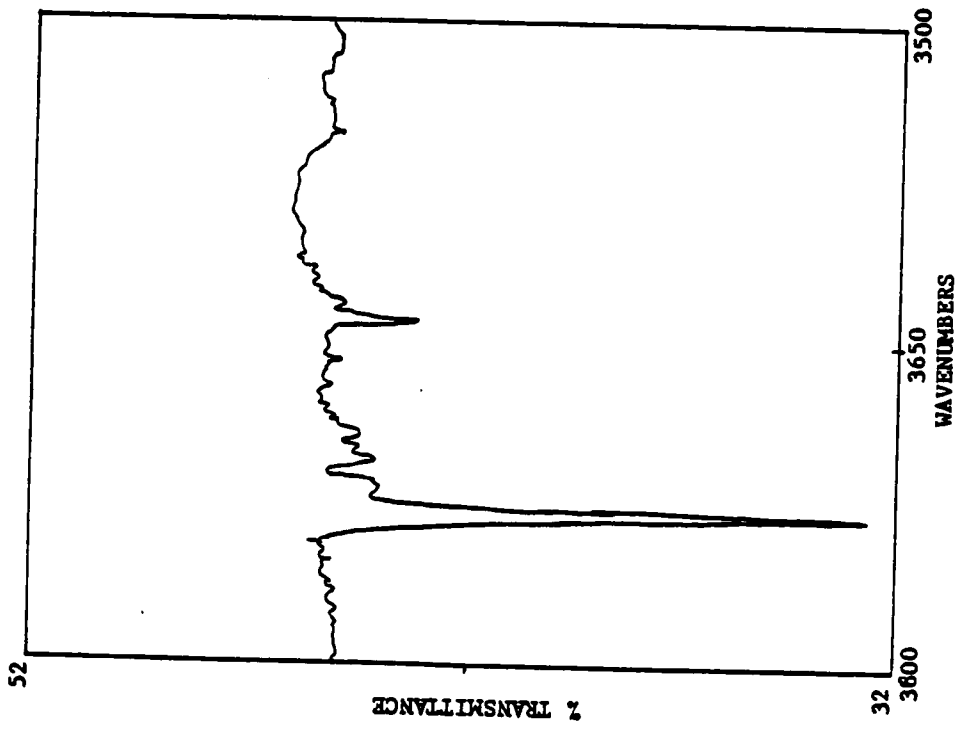


Figure 29. Enlargement of 3800-3500 wavenumber region after annealing to 32°K.

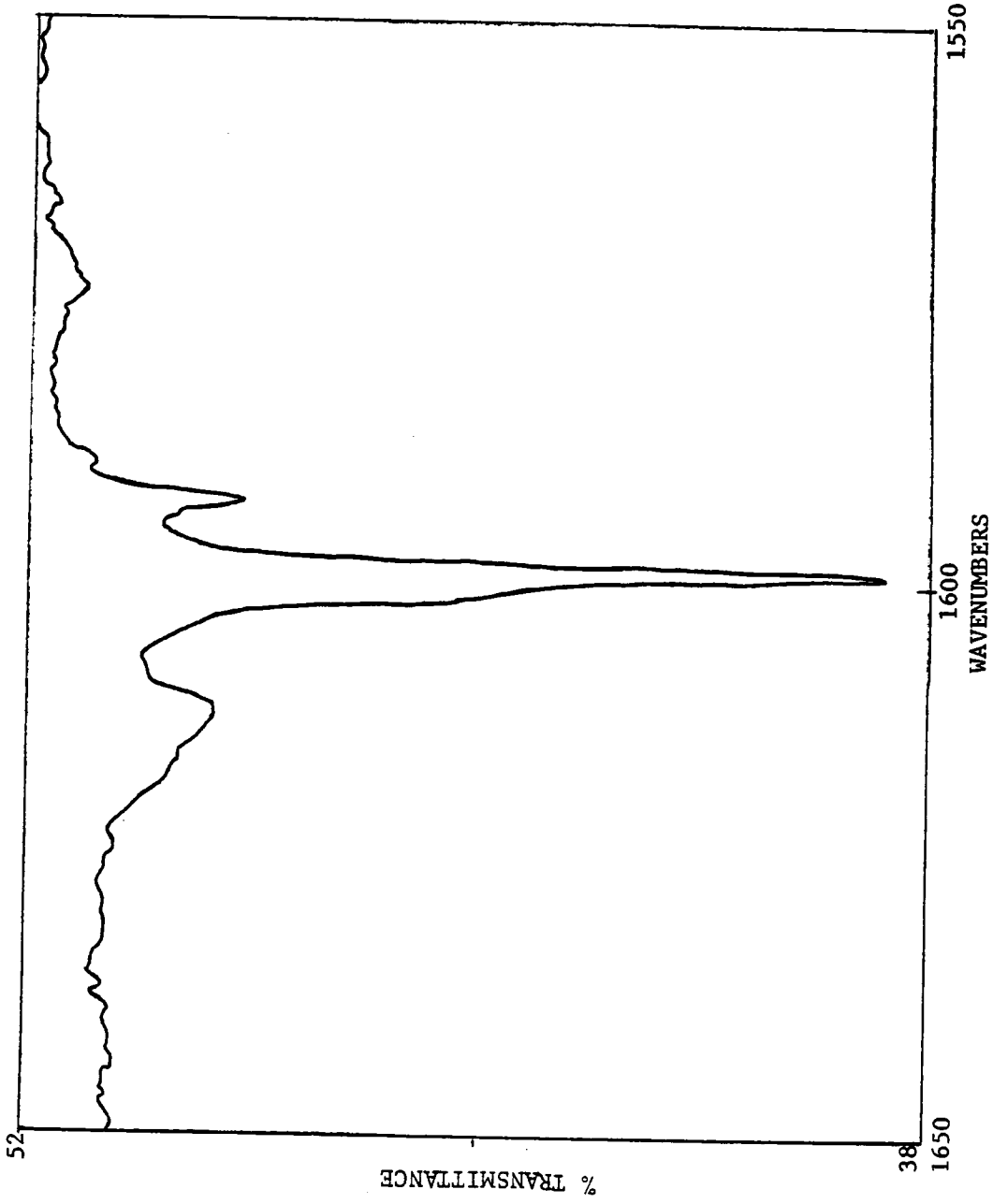


Figure 30. Enlargement of 1650-1550 wavenumber region after annealing to 32°K.

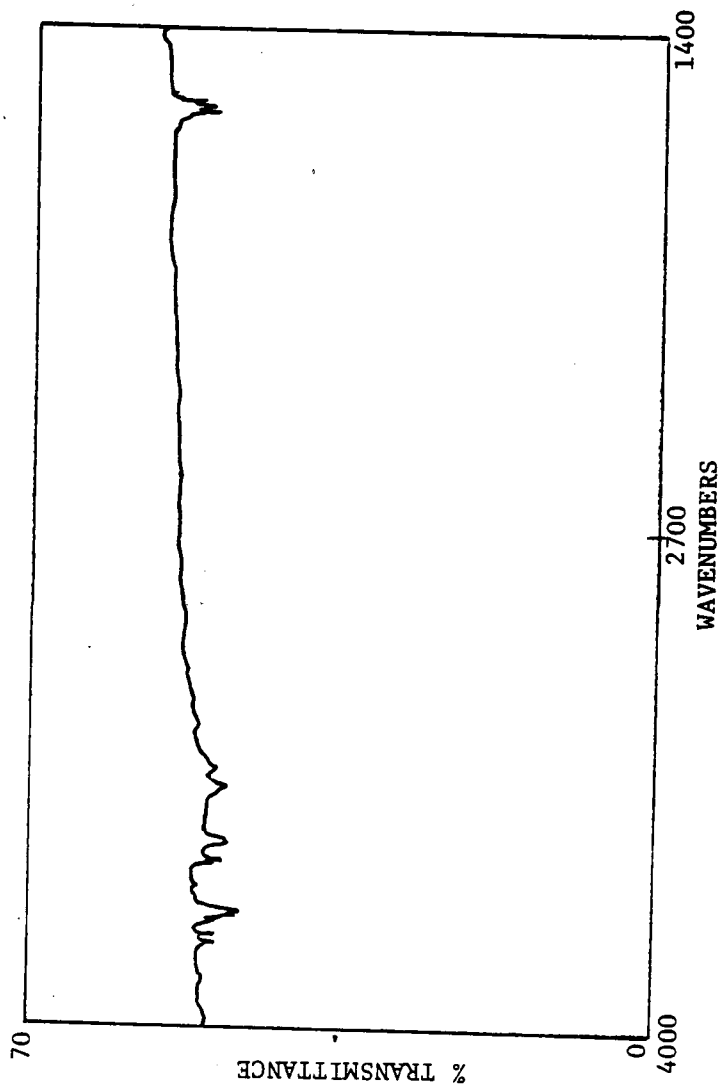


Figure 31. Matrix-isolated FT-IR spectrum of a 100:1 sample of Ar:H_2O.

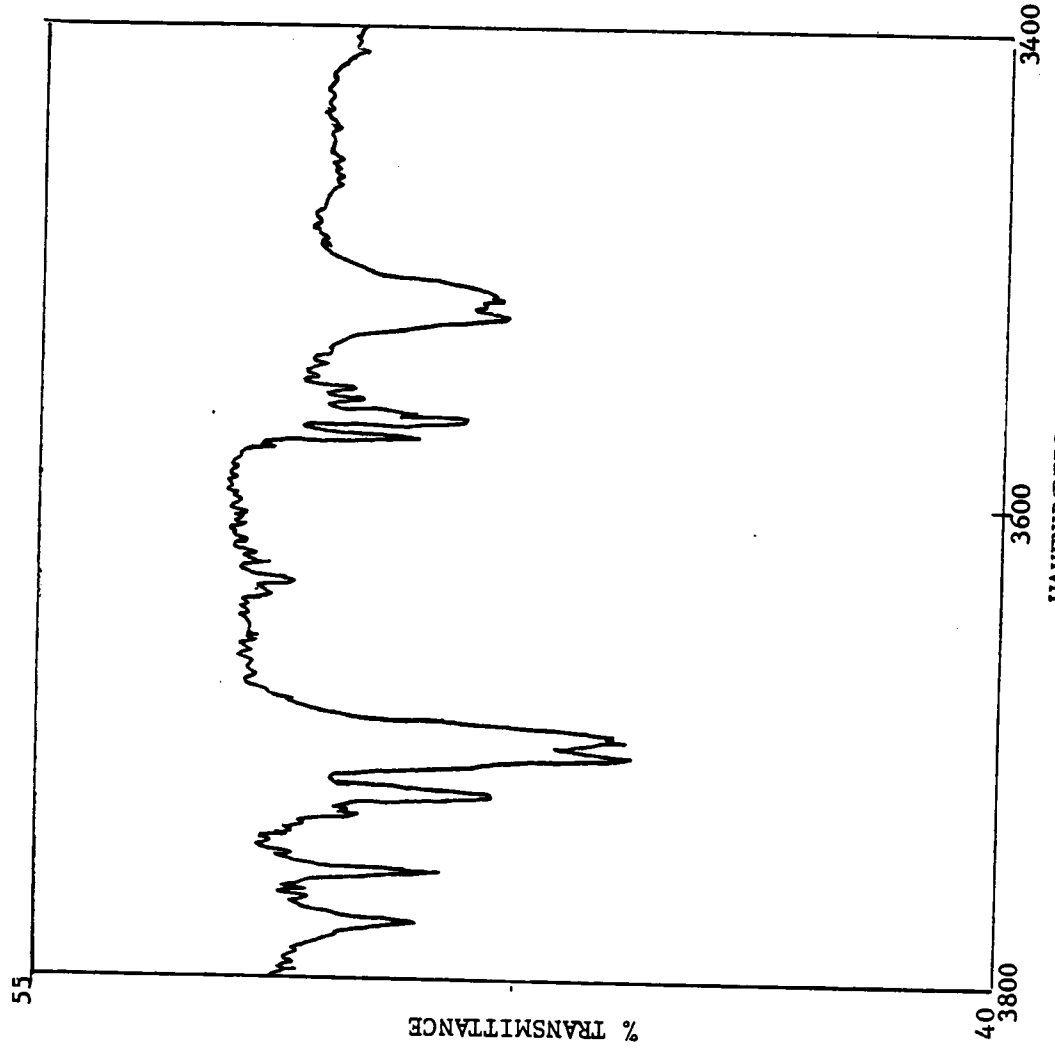


Figure 32. Enlargement of 3800-3400 wavenumber region.

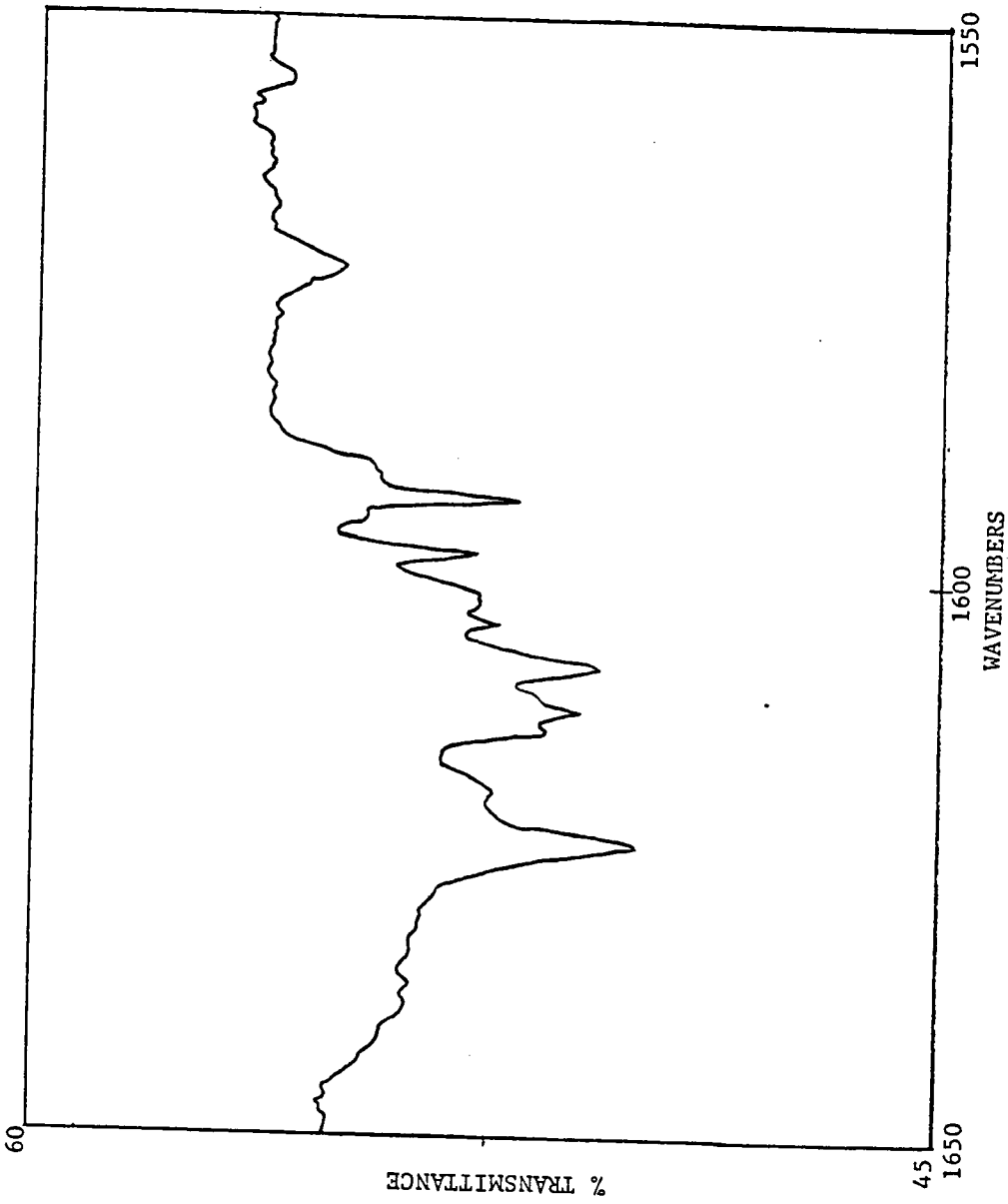


Figure 33. Enlargement of the 1650-1550 wavenumber region, $Ar:H_2O$ = 100:1.

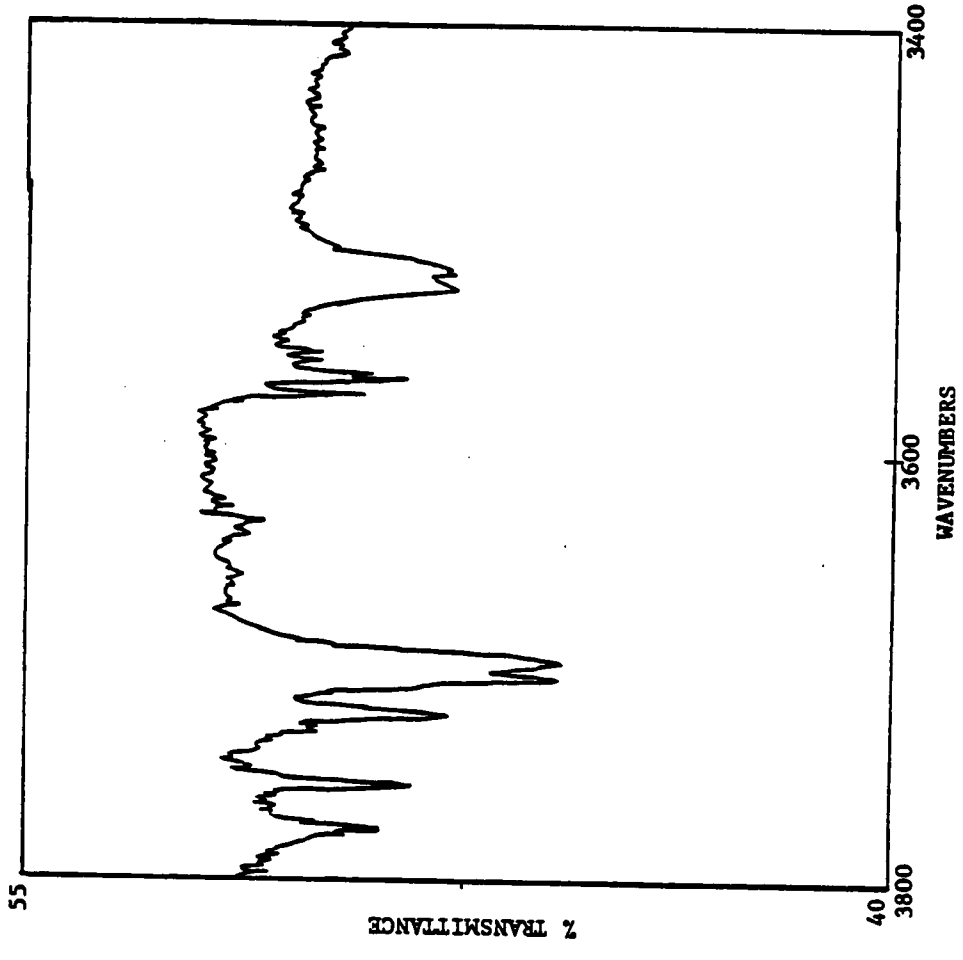


Figure 34. Enlargement of 3800-3400 wavenumber region after annealing to 30°K.

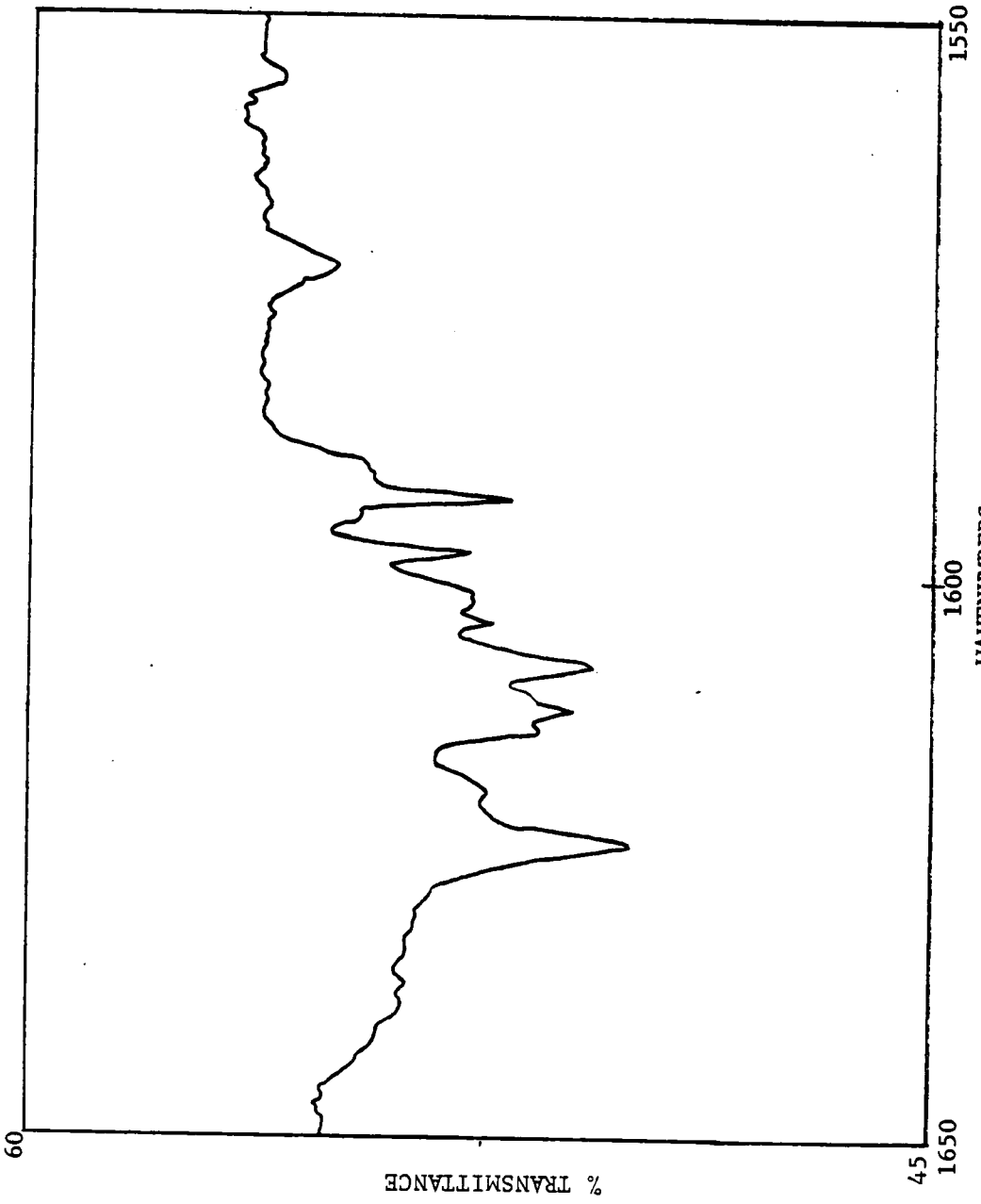


Figure 35. Enlargement of 1650-1550 wavenumber region after annealing to 30°K.

most of the peaks lose some intensity but no new peaks seem to appear. Also, the peaks remain relatively sharp.

Figure 36 represents a spectrum of a 20:1 Ar:H_2O sample. The two aforementioned spectral regions will be examined. Figure 37 is an enlargement of the 3800-3100 cm^{-1} region. There is a strong absorption located at 3697 cm^{-1} and also a broad band that ranges from 3600 to about 3100 cm^{-1} with spikes appearing at 3573, 3516, 3375, 3325, and 3205 cm^{-1}. Also, in the other region (Figure 38) there is a broad band ranging from about 1650 to 1605 cm^{-1} and other weaker bands located at 1601.5 and 1593 cm^{-1}. Annealing the sample to 35°K leads to little change in the spectra.

Several observations can be made from these experimental results. First, as one progresses from the 1000:1 Ar:H_2O sample to the 20:1 ratio sample, more peaks begin to appear in the two aforementioned spectral regions (namely the 3800-3400 and 1650-1553 cm^{-1}). As mentioned earlier, these peaks are due to agglomerated water molecules. The bands in these two regions tend to broaden and coalesce as the concentration increases. A 20:1 sample is very similar spectrally (IR) to a pure water sample. Also, since aggregation of sample molecules upon annealing usually leads to broader, less-resolved peaks, one can probably conclude that little or no diffusion or aggregation occurs in argon in these temperature ranges.

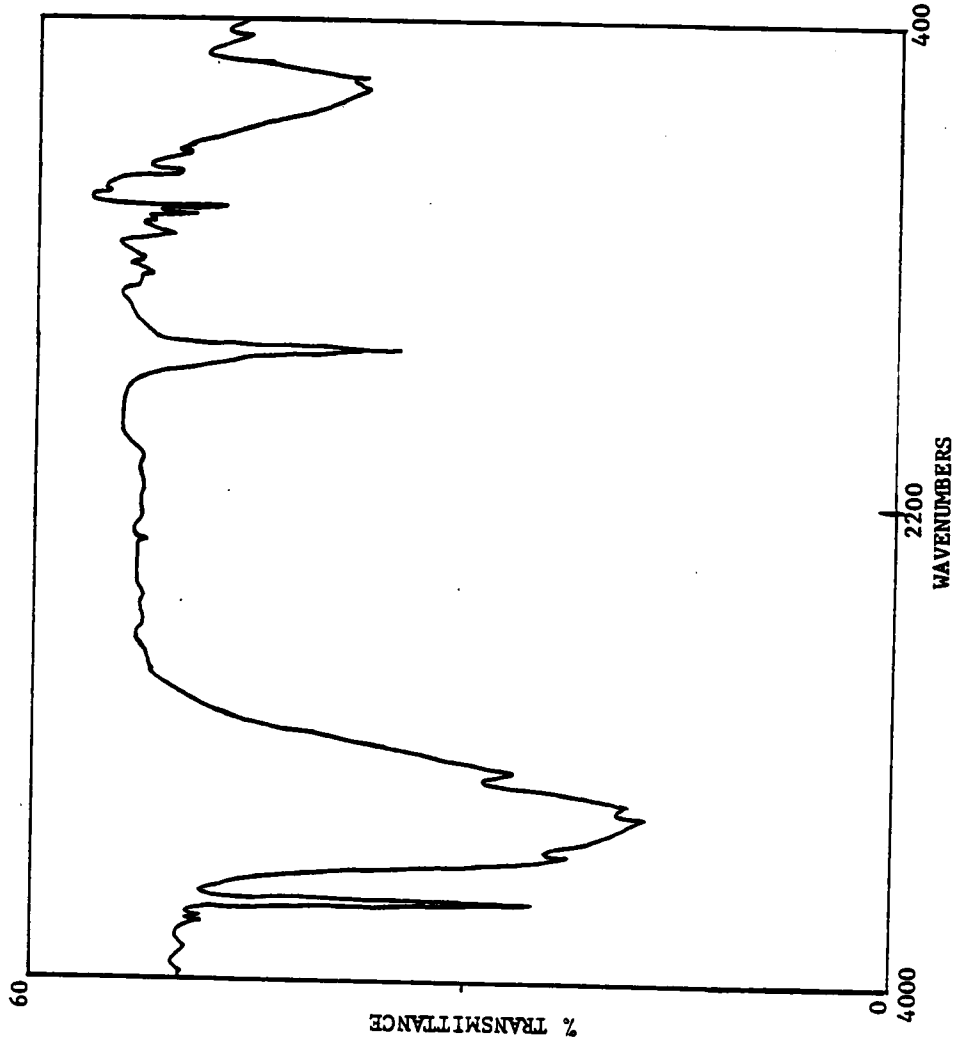


Figure 36. Matrix-isolated FT-IR spectrum of 20:1 sample of Ar:H_2O.

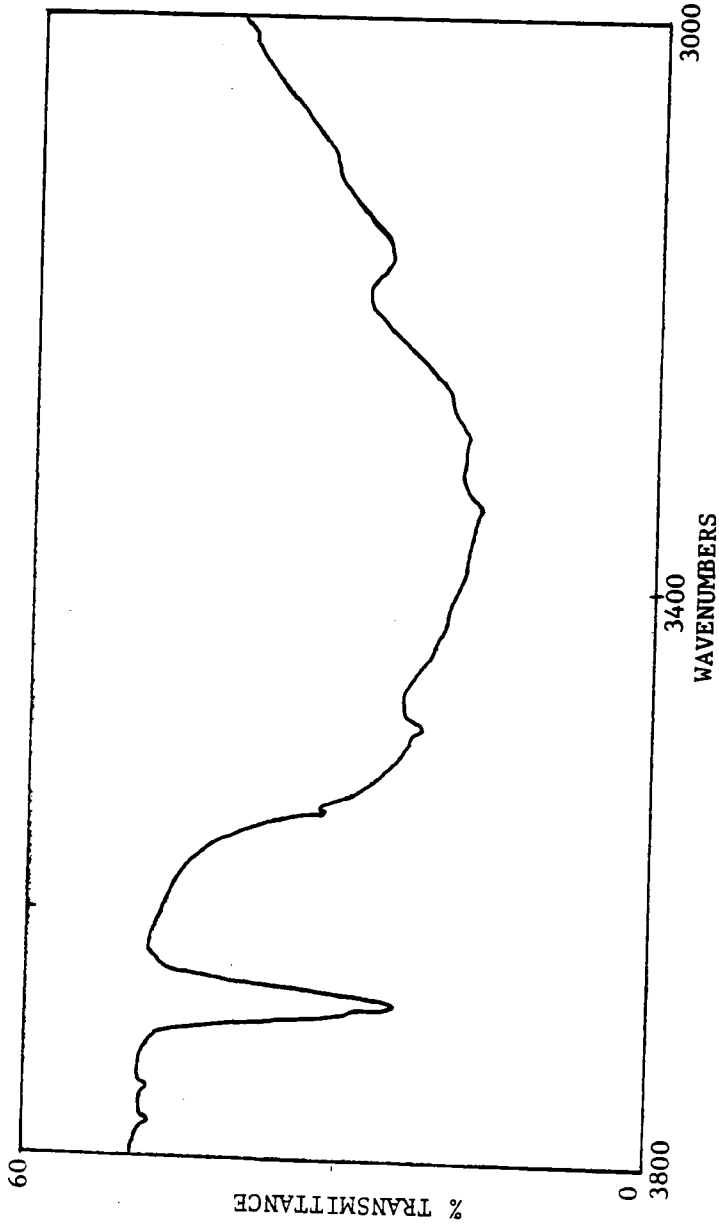


Figure 37. Enlargement of 3800-3000 wavenumber region.

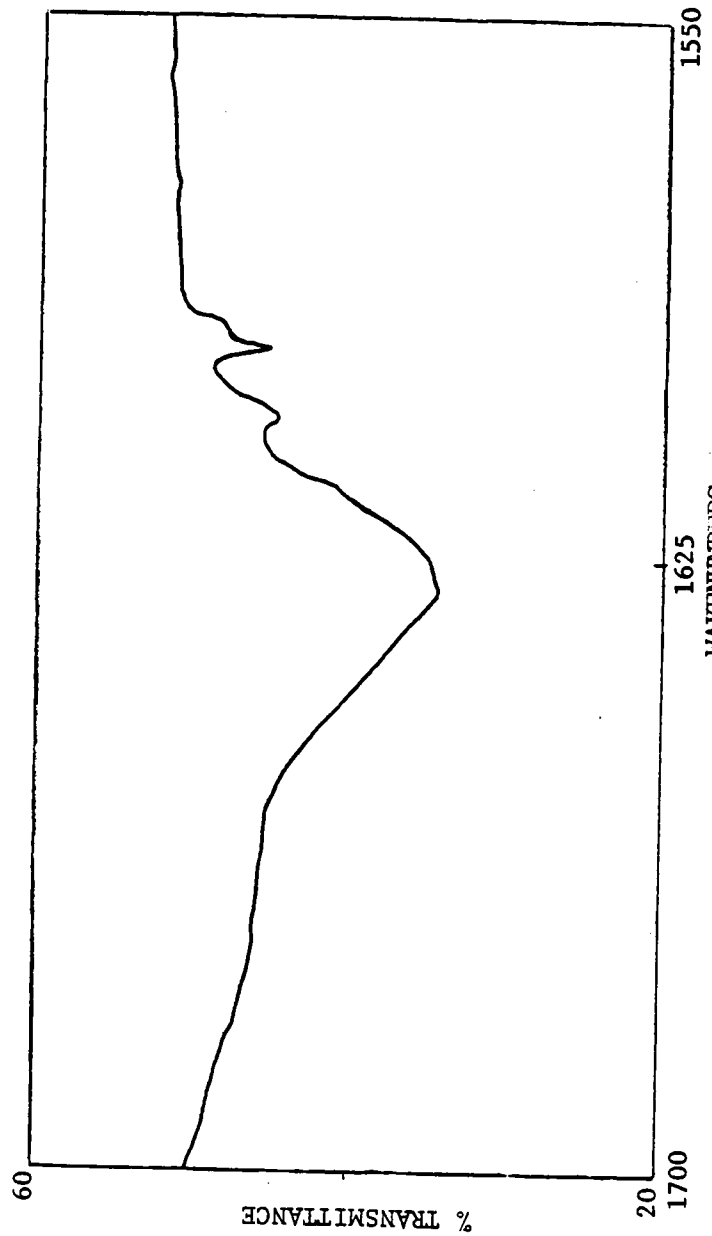


Figure 38. Enlargement of 1700-1550 wavenumber region.

4. UF_6 and H_2O Co-deposited in Argon

This section will detail the results obtained from the co-deposition of UF_6 and H_2O in an argon matrix. The experimental details are those discussed in Chapter III, Section D. Only one series of spectra will be analyzed. The matrix-to-sample ratios were 500:1 for $Ar:UF_6$ and 100:1 for $Ar:H_2O$. This series of spectra was chosen because the deposits were made "cleanly" and most of the spectral bands which need to be examined are fairly well resolved. The UF_6:Ar and H_2O:Ar samples were deposited in approximately equal amounts. The first spectrum shown (Figure 39) is of the initial deposit before any annealing was done (16°K). Upon examination of the spectrum, one readily notices the strong UF_6 absorption at 619 cm^{-1}. Also, one can compare the 3800-3400 cm^{-1} and 1650-1550 cm^{-1} regions in Figure 39 to the ones that were previously examined in Section 3 and realize that they compare very well to a 100:1 $Ar:H_2O$ sample. In order to allow easier examination of the annealing experiments, only the 1800-500 cm^{-1} region will be plotted. Figure 40 is a spectrum of the initial deposit in the 1800-500 cm^{-1} region. Figure 41 represents the sample after having been annealed to 26°K. If one compares this spectrum to Figure 40, one can see that the sample has remained virtually unchanged. The next spectrum (Figure 42) was taken after the sample had been annealed to 34°K. Clearly the intensities of both the water bands and the UF_6 bands are diminishing somewhat. However, no new bands seem to be appearing in this spectral region. Finally, Figure 43 represents the sample after it had been annealed to 37°K. Both the

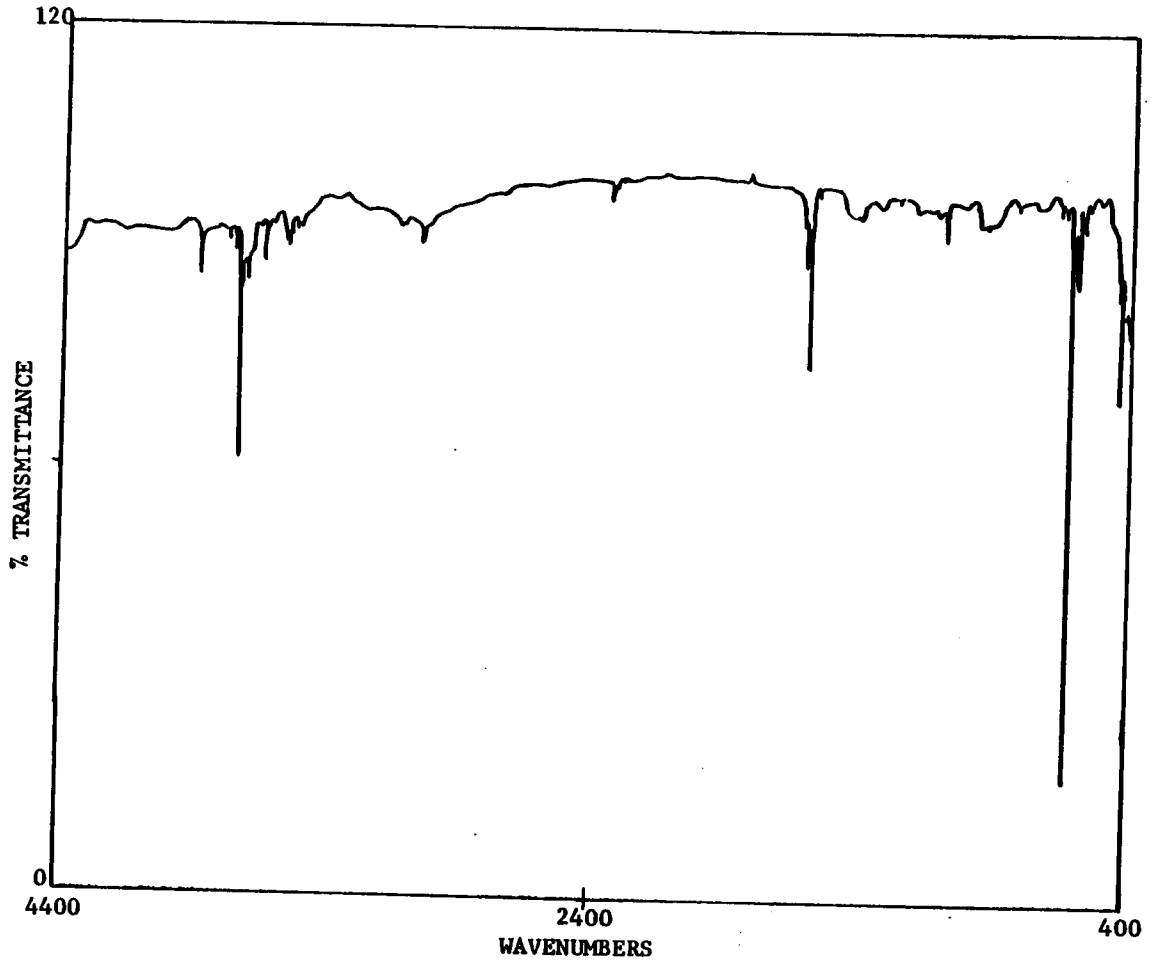


Figure 39. Matrix-isolated FT-IR spectrum of Ar:UF_6 (500:1) and Ar:H_2O (100:1) held at 16°K.

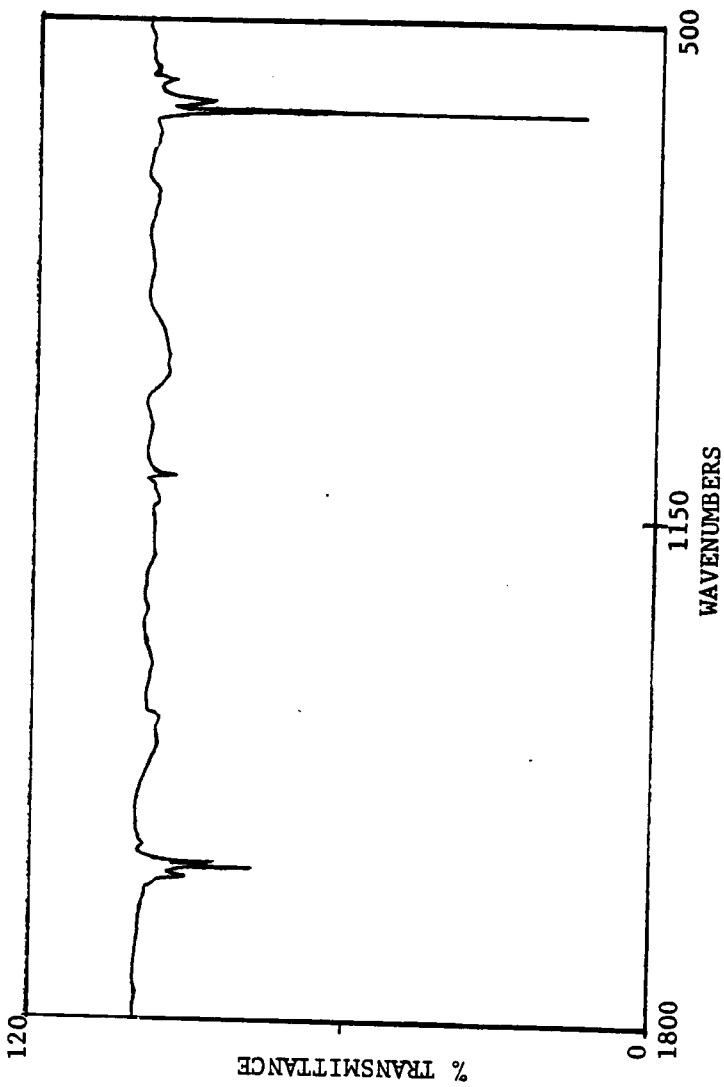


Figure 40. Enlargement of the 1800-500 wavenumber region at 16°K.

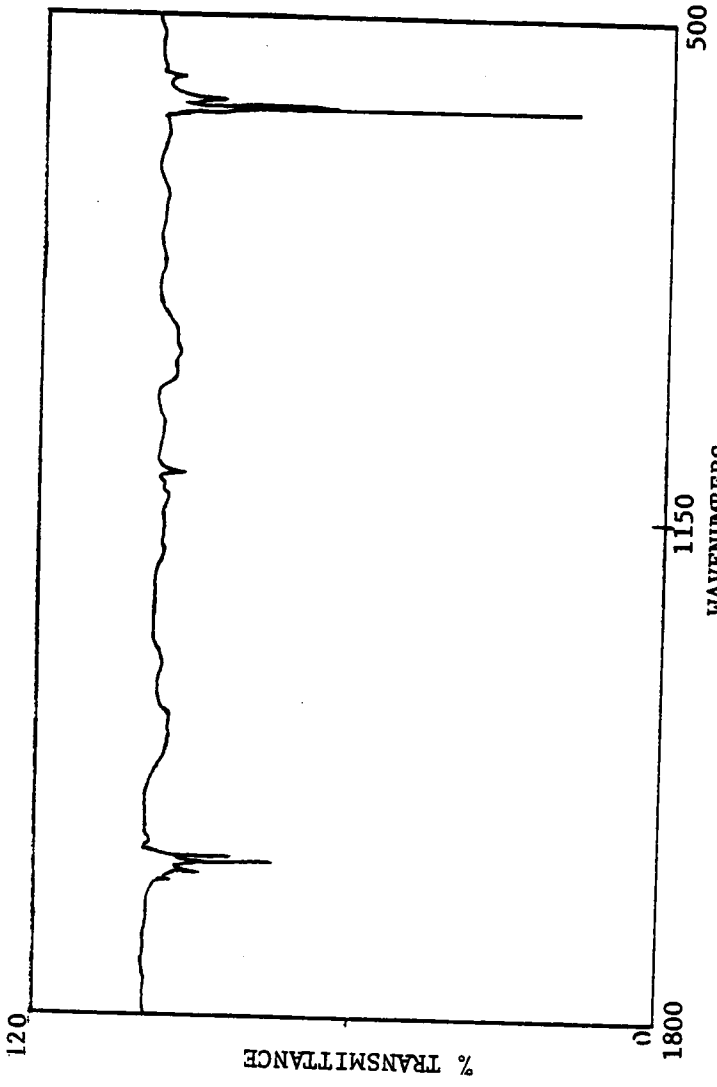


Figure 41. Enlargement of 1800-500 wavenumber region after annealing to 26°K.

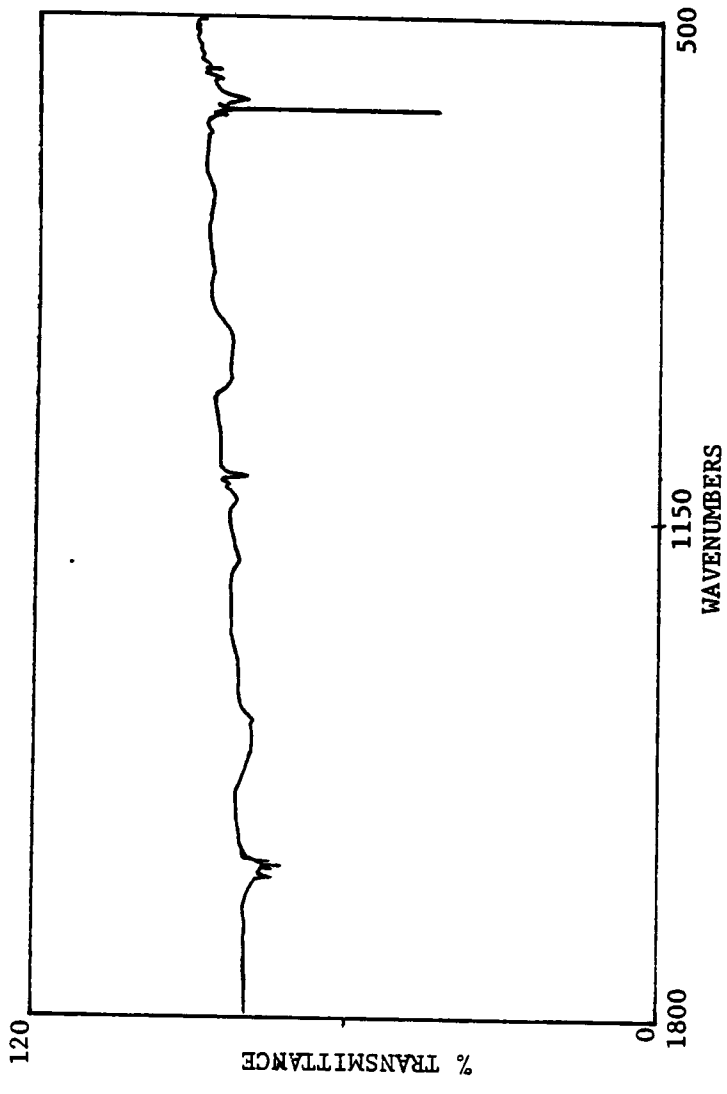


Figure 42. Enlargement of the 1800-500 wavenumber region after annealing to 34°K.

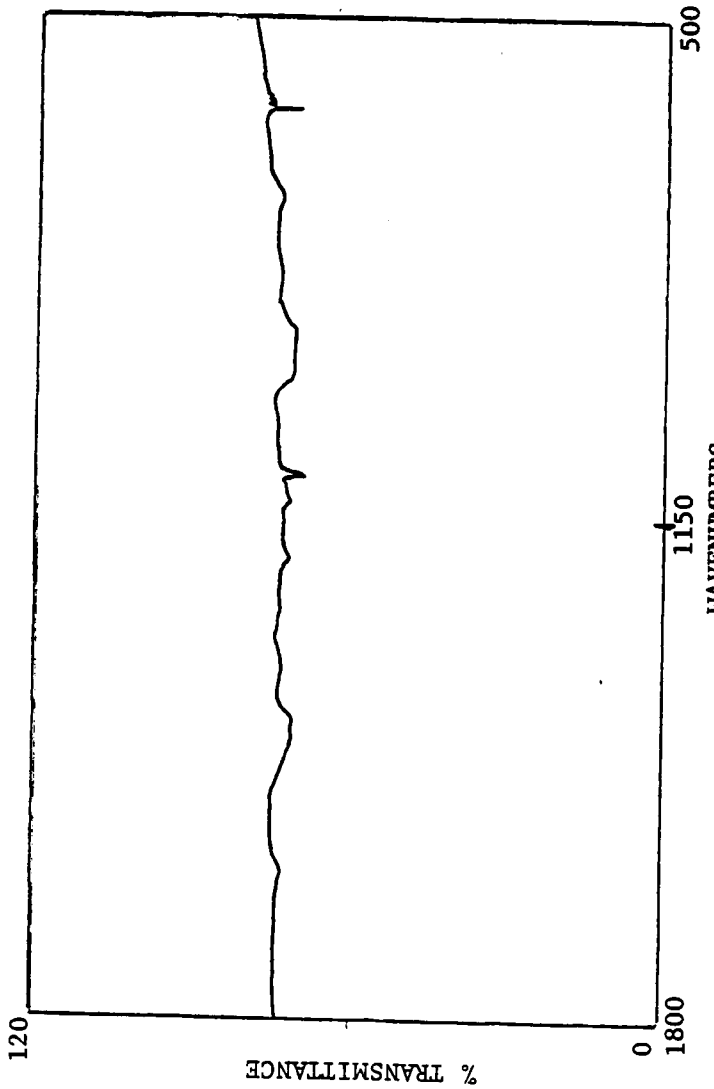


Figure 43. Enlargement of the 1800-500 wavenumber region after annealing to 37°K.

water bands and the UF_6 band have virtually disappeared. Again no new bands have shown up in this spectral region.

A few conclusions might be drawn from this experiment; that is, there might be several reasons that no UF_6 and water reaction was observed. Among the several possibilities are: (1) they reacted to produce species that are not IR active, (2) the reacted species were evacuated away from the window (with the argon), (3) they did not react. If the third conclusion is correct, then there could be several reasons for it. These reasons are: (1) they did not react because no diffusion occurred, (2) they did not react because higher temperatures might be needed thermodynamically, and (3) they did not react because their concentrations might be too low. Some of these conclusions might be eliminated if pure water and pure UF_6 are deposited simultaneously and subsequent annealing experiments performed.

5. Matrix-Isolated UF_6 in Nitrogen

The following discussion pertains to the experiments on the matrix isolation of UF_6 in nitrogen which were performed under experimental conditions discussed in Chapter III, Section E. Figure 44 represents a spectrum of a N_2:UF_6 sample having a ratio of 100:1. Again, the UF_6 absorption in the 650-600 cm^{-1} spectral region will be detailed. The UF_6 absorption actually consists of five peaks under these experimental conditions. There is a weak peak at 627 cm^{-1}, a strong peak at 624, a strong peak at 623, a medium peak at 617.5, and a weak peak at 610 cm^{-1}. If one compares this spectrum

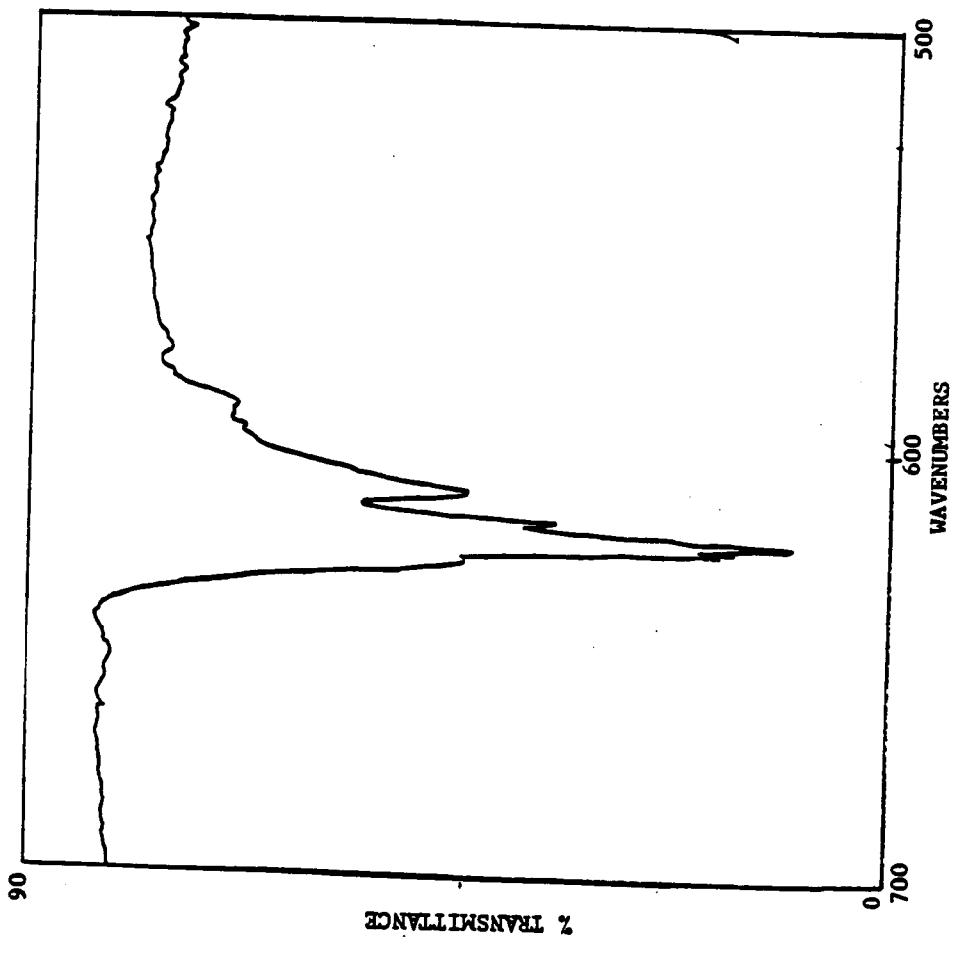


Figure 44. Matrix-isolated FT-IR spectrum of 700-500 wavenumber region of 100:1 sample of N_2:UF_6.

to Figure 21 one can see that the UF_6 in argon and UF_6 in nitrogen IR absorptions are somewhat dissimilar. Frequency shifts for molecules in different matrix materials have been previously discussed by Moskovits and Ozin.[70] Figure 45 shows a spectrum after the sample had been annealed to 24°K. One can see that the peak intensities have slightly decreased but are also slightly better resolved. Figure 46 is a spectrum of the same sample after it was annealed to about 28°K. The band previously assigned to the UF_6 stretch and its satellites has undergone considerable broadening. It was then decided that the matrix ratio would not be increased because spectra were already being complicated by sample aggregation. It was therefore decided to proceed with a co-deposition experiment of UF_6 and H_2O in nitrogen.

6. UF_6 and H_2O Matrix-Isolated in Nitrogen

The following is a discussion of the UF_6 and H_2O co-deposition experiments in nitrogen which were performed under experimental conditions discussed in Chapter III, Section G. Figure 47 is a spectrum of a sample of UF_6:N_2 at 1:100 and H_2O:N_2 at 1:500 which was recorded at 16°K. Again, bands in the 3800-3200 cm^{-1} and 1650-1550 cm^{-1} regions are typical of water absorptions that have been observed by previous researchers.[68,69] The strongest peaks appear at 3730, 3795, 3360, and 1598 cm^{-1}. The peak at 2360 cm^{-1} is consistent with an absorption which has previously been assigned to CO_2. There are also peaks at 1395, 1350, and 1235 cm^{-1} that have

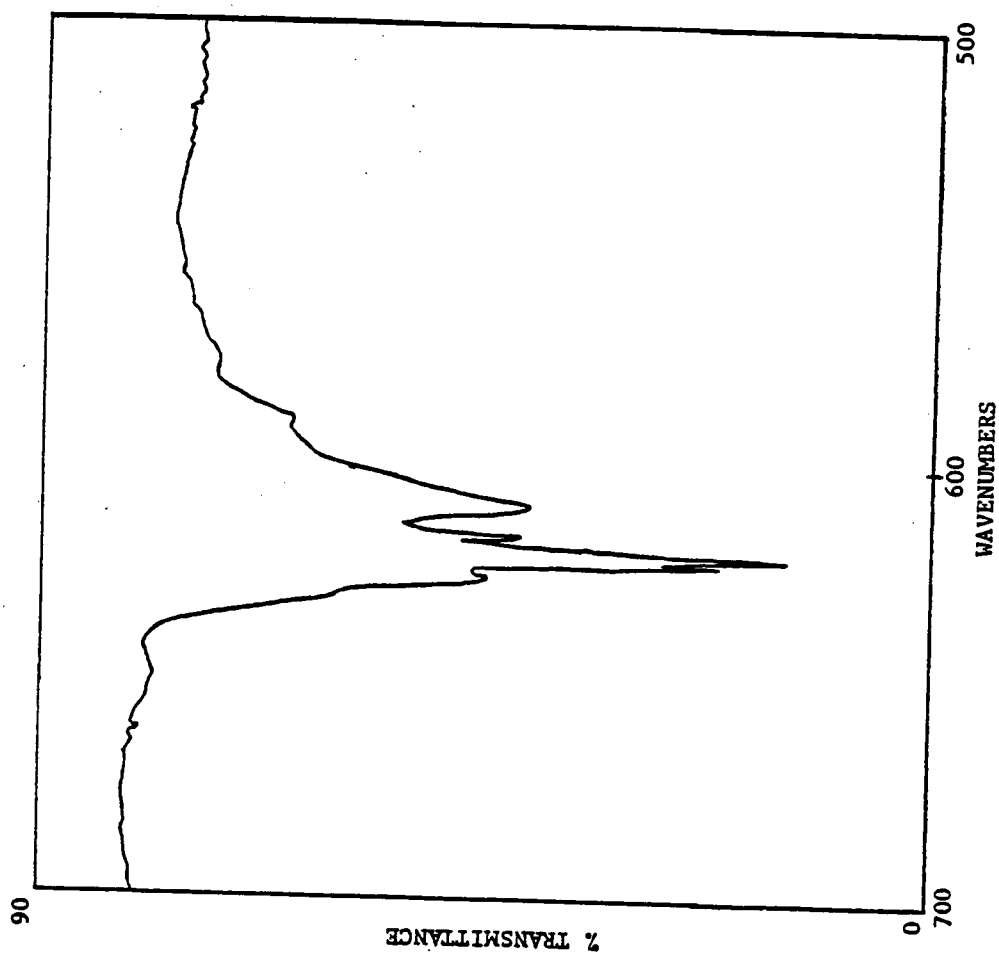


Figure 45. Same region after sample was annealed to 24°K.

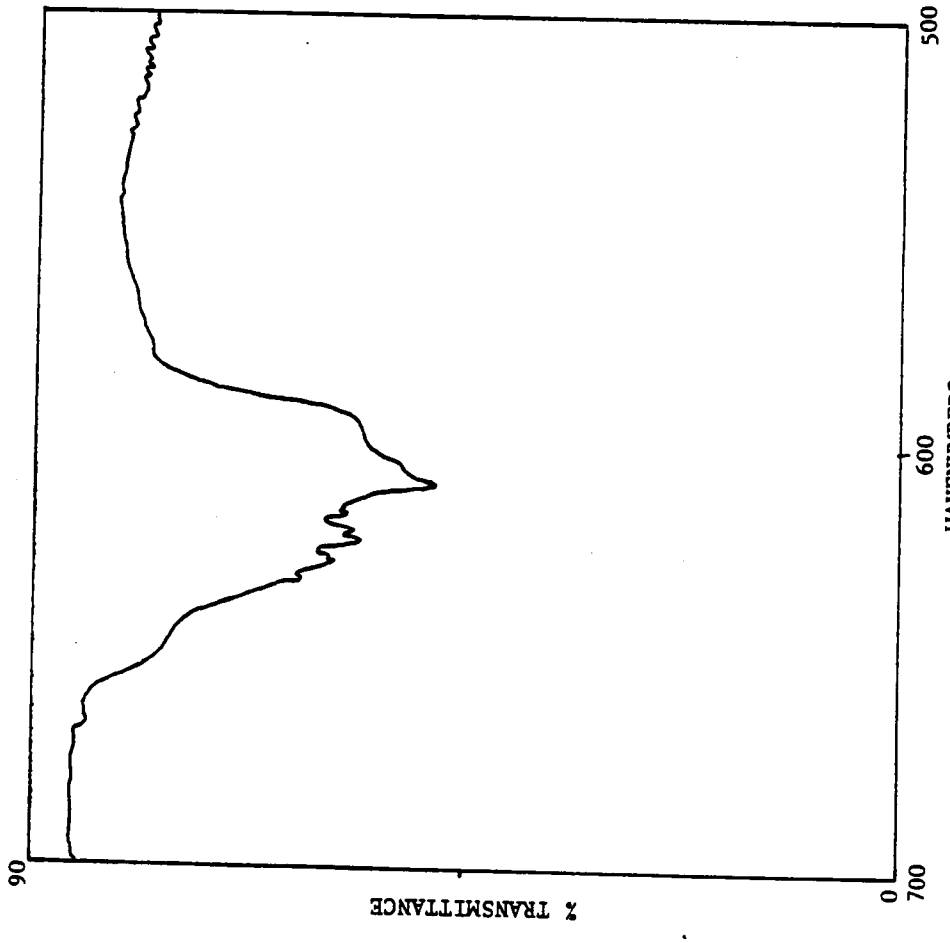


Figure 46. Spectrum of same sample after it was annealed to 20°K.

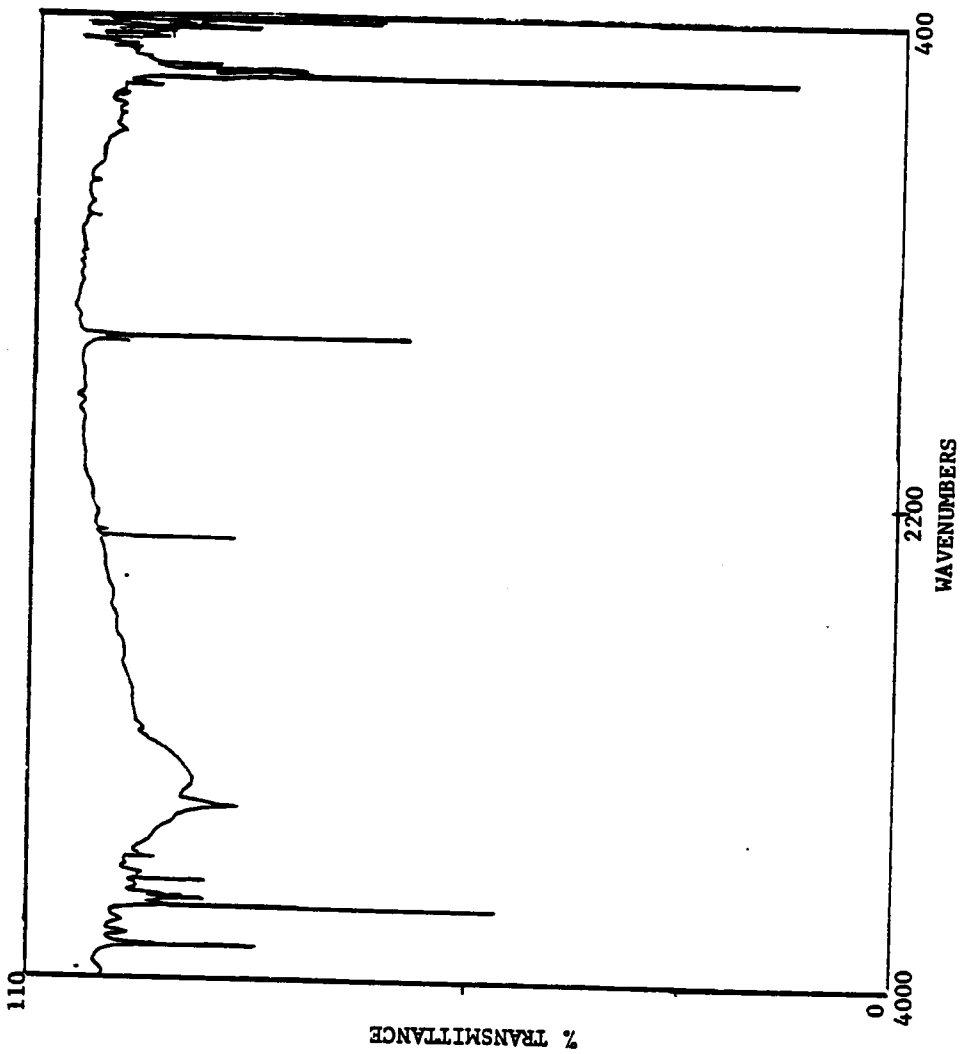


Figure 47. Matrix-isolated FT-IR spectrum of UF_6:N_2 (1:100) and H_2O:N_2 (1:500) at 16°K.

yet to be identified. And, finally there is the strong UF_6 absorption which occurs at 623 cm^{-1}. Figure 48 is an enlargement of the H_2O absorption at 1598 cm^{-1}. If one compares it to Figure 28, which is an enlargement of the 1650-1550 cm^{-1} region of water isolated in argon, then one can see that it is somewhat different. The next spectrum (Figure 49) was taken after the sample had been annealed to approximately 30°K. One can see that there is a striking difference between this spectrum and the one shown in Figure 48. In the 3800-3200 cm^{-1} region (not pictured) there is only one broad band centering at 3250 cm^{-1}. One can see that the band at 1598 cm^{-1} has diminished somewhat. Although the UF_6 absorption is not included, the original spectrum showed that it had disappeared.

Some hypotheses might be drawn from these results. The UF_6 band at 623 cm^{-1} is obviously disappearing and it might be because the UF_6 is not diffusing or reacting and is being carried away as the sample is evacuated away from the window. Another conclusion might be that the UF_6 is reacting with the CsI window because, after the experiment was completed, there was usually some debris remaining on the window. And, one can conclude that the H_2O is probably also diffusing because the absorptions in the 3800-3200 cm^{-1} region are broadening and coalescing. A strong, broad absorption in this region is indicative of agglomerated water.[65] It also must be noted here that the changes in the water bands are occurring while the UF_6 band still remains intact. Therefore, it is possible that UF_6 and water molecules are coming into contact with one another during the annealing experiment. However, no UOF_4 or

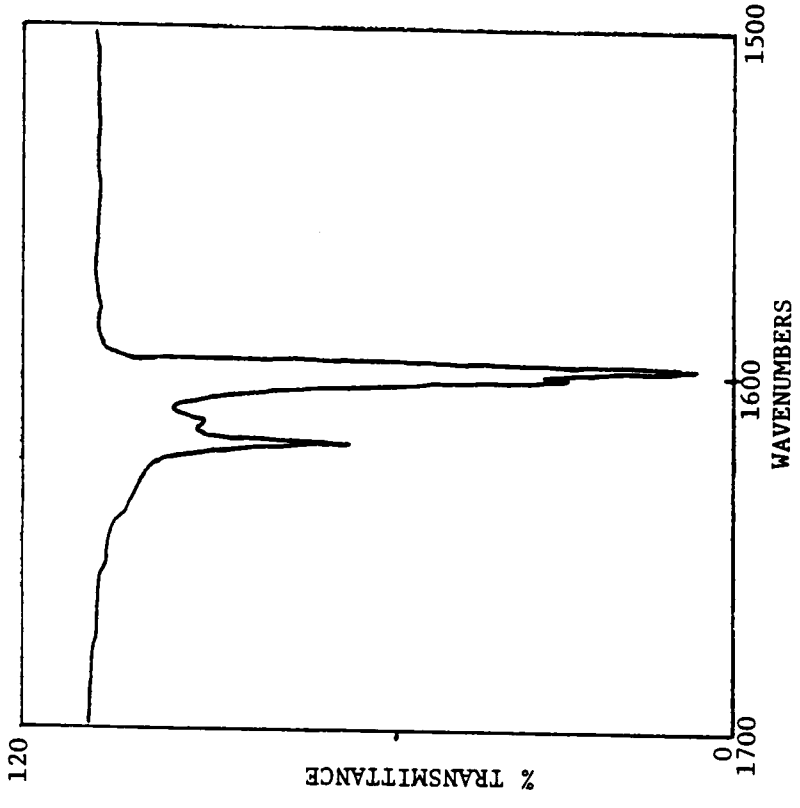


Figure 48. Enlargement of H_2O absorptions.

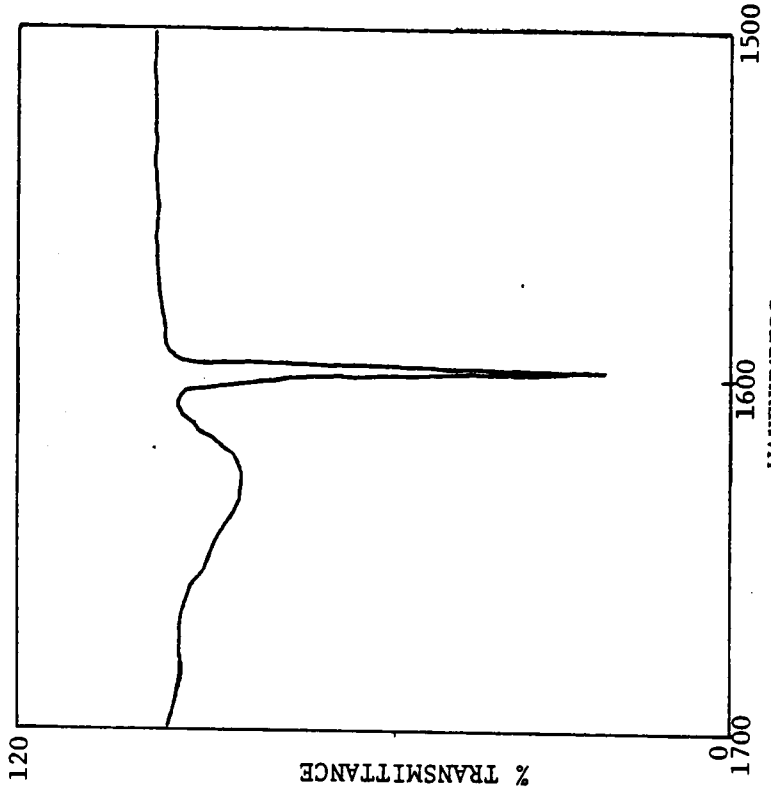


Figure 49. Enlargement of 1700-1500 wavenumber region after sample was annealed to 30°K.

UO_2F_2 molecules are apparently forming since no bands appear in the 1000-700 cm^{-1} region.

7. Co-deposition of UF_6 and H_2O Sans Matrix

The following section will detail the result obtained in the experiments in which UF_6 and H_2O were deposited simultaneously and then annealing experiments performed. The experimental details were those discussed in Chapter III, Section I. Figure 50 represents a spectrum of the sample held at 16°K prior to any annealing. If one examines the 3800-3200 cm^{-1} and 1650-1550 cm^{-1} regions one can see the broad absorptions that are characteristic of agglomerated water.[65] There are also absorptions located in the 1000-400 cm^{-1} spectral region. Figure 51 is an enlargement of this region. There is a strong band located at 865 cm^{-1} and two weaker absorptions centering at 780 and 710 cm^{-1}. Finally, there is the strong UF_6 absorption located at 620 cm^{-1}. The next spectrum (Figure 52) was taken after the sample had been warmed to about 150°K. The changes in the spectrum are that the absorption at 865 cm^{-1} has increased, the absorption in the 600-550 cm^{-1} region has decreased, and the 780 and 710 cm^{-1} absorptions may have receded somewhat. The next spectrum (Figure 53) was taken after the sample had been warmed to about 165°K. There is a slight absorption appearing at about 940 cm^{-1}. The other bands seem to be the same, but the shoulder on the right side of the UF_6 absorption, located at about 590 cm^{-1}, seems to be decreasing. The next spectrum (Figure 54) was taken after the sample was warmed to about 180°K. Clearly the band located at

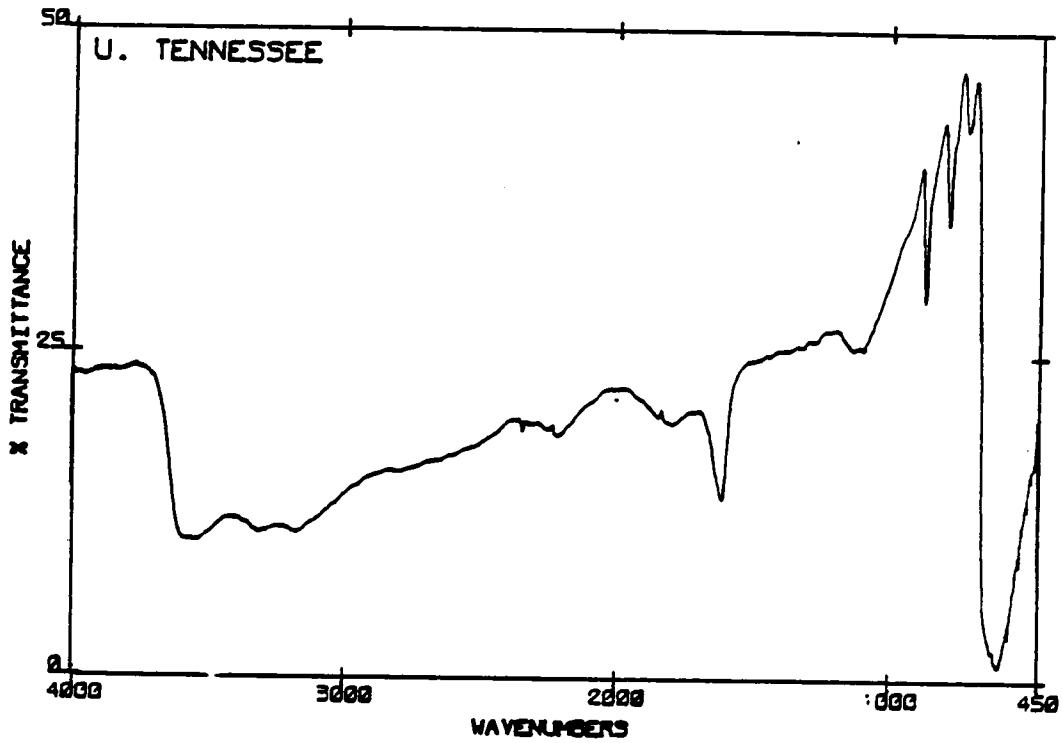


Figure 50. FT-IR spectrum of neat deposited sample of UF_6 and H_2O prior to any annealing.

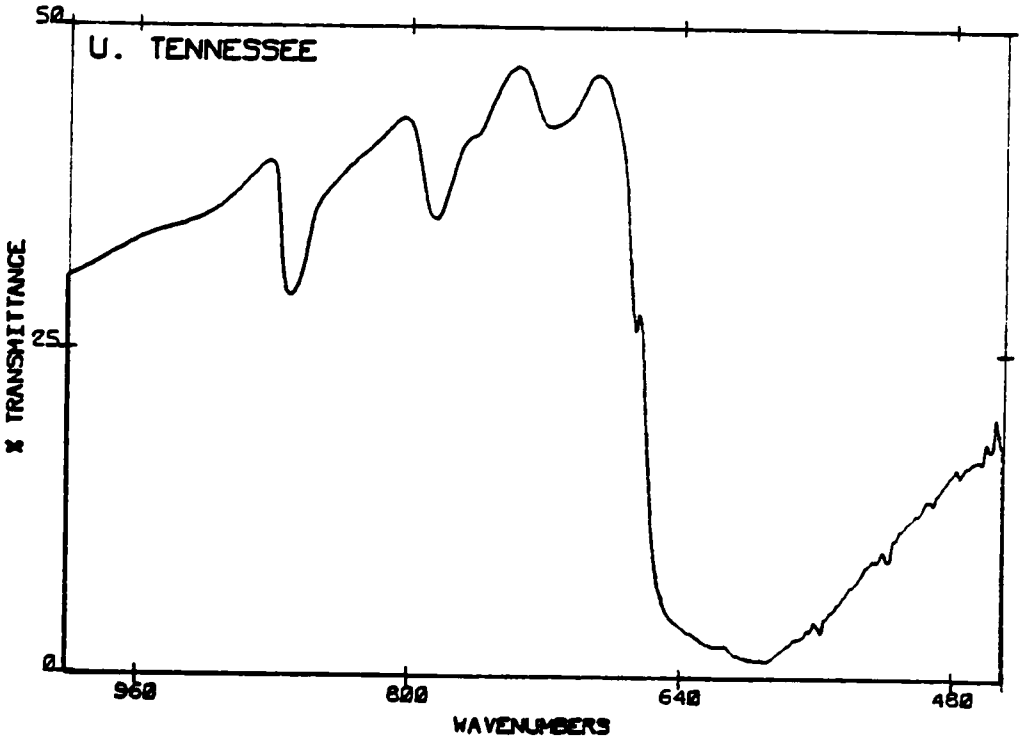


Figure 51. Enlargement of the 1000-400 wavenumber region prior to annealing.

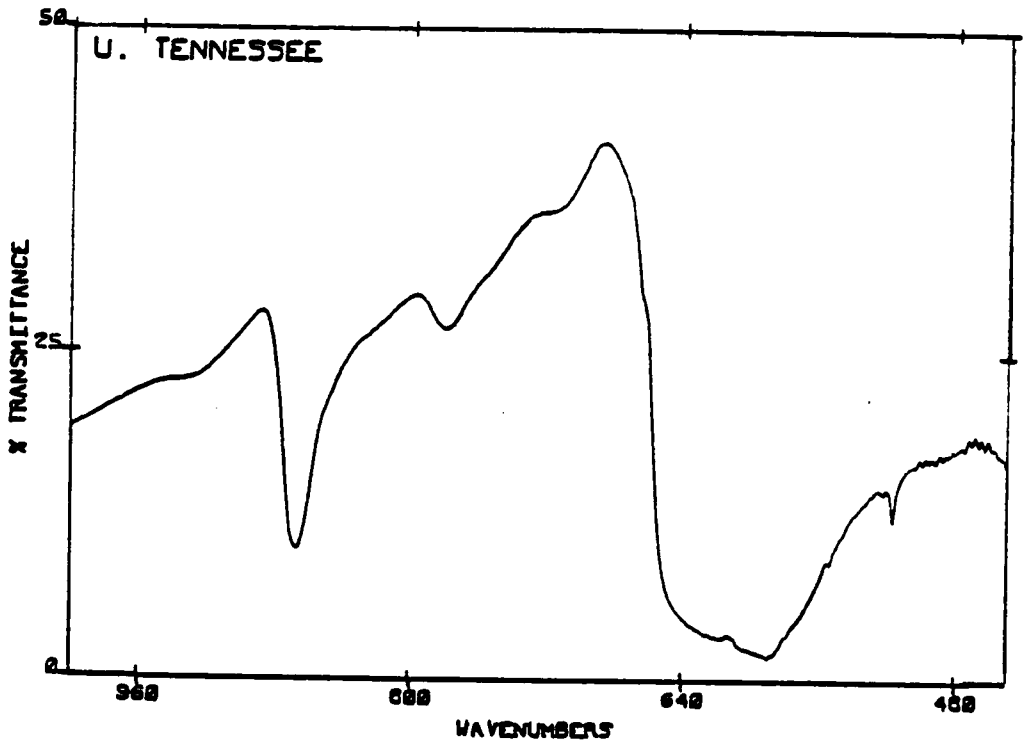


Figure 52. Enlargement of 1000-400 wavenumber region after sample had been annealed to 150°K.

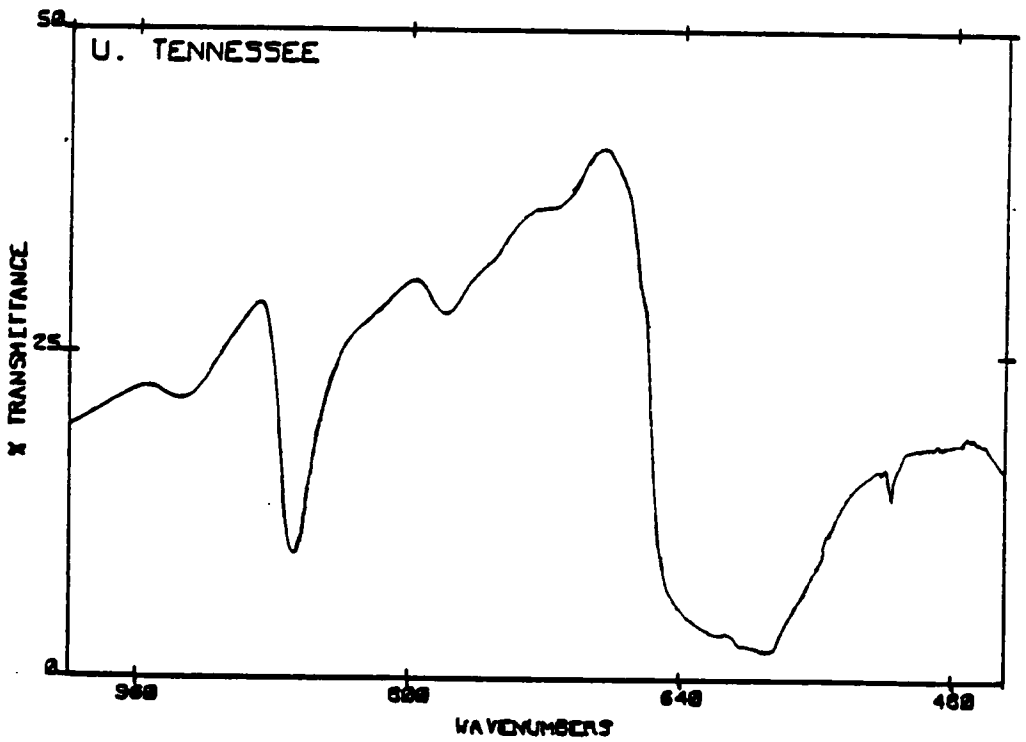


Figure 53. Enlargement of 1000-400 wavenumber region after sample had been annealed to about 165°K.

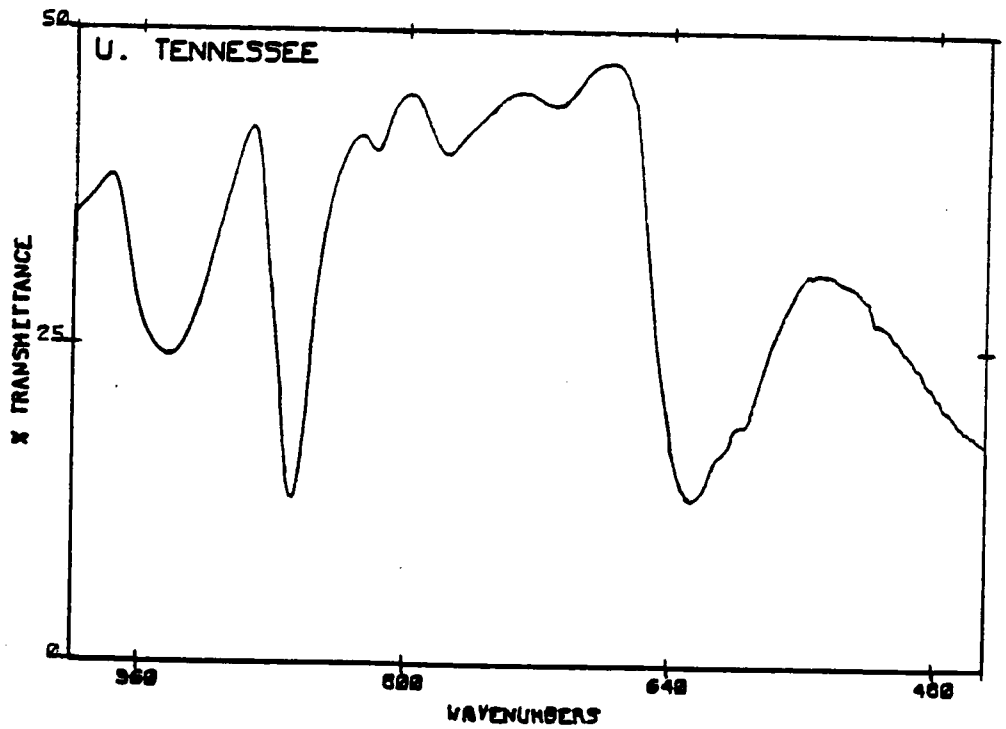


Figure 54. Enlargement of 1000-400 wavenumber region after sample had been annealed to about 180°K.

940 cm^{-1} has increased in intensity and likewise has the band at 865 cm^{-1}. The absorptions at 780 and 710 cm^{-1} have remained the same or possibly slightly decreased. Also, the shoulder at 590 cm^{-1} has disappeared. The next spectrum (Figure 55) was taken after the sample had been warmed to about 195°K. The band at 940 cm^{-1} is clearly the strongest absorption. The 865 cm^{-1} band is now smaller than the 940 cm^{-1} band and the bands at 780 and 710 cm^{-1} have receded. Also the UF_6 absorption at 620 cm^{-1} has decreased measurably in intensity. The final spectrum (Figure 56) was taken after the sample had been warmed past 220°K. The band at 940 cm^{-1} is very strong now. The band at 864 cm^{-1} may have receded and is overlapped by the 940 cm^{-1} band, but the bands at 780, 710, and 620 cm^{-1} cannot be located.

This experiment supports the belief that even, if diffusion had occurred in the co-deposition experiments in argon, no reaction would have occurred because of thermodynamic factors at those temperatures. The UF_6 and H_2O were obviously in contact with one another during deposition and on the window since they were both in concentrated form and also because products were formed on the initial deposit which is evidenced by the bands at 865, 780, and 710 cm^{-1}. These products were probably formed during the mixing of the UF_6 and H_2O streams between the deposition tubes and the CsI window, since no new bands appeared during the annealing experiment until the sample had been warmed to about 160°K; then, the new band at 940 cm^{-1} appeared, and the others receded. Obviously the band at 940 cm^{-1} acts independently of the 865, 780, and 710 cm^{-1} bands. But,

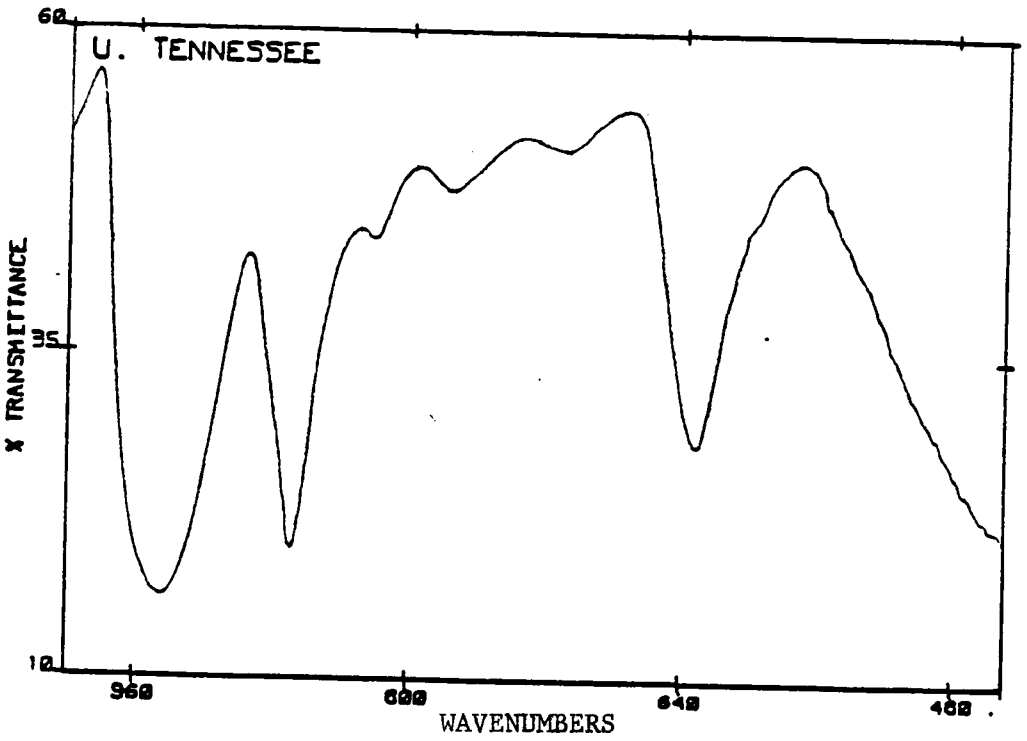


Figure 55. Enlargement of 1000-400 wavenumber region after sample had been annealed to about 195°K.

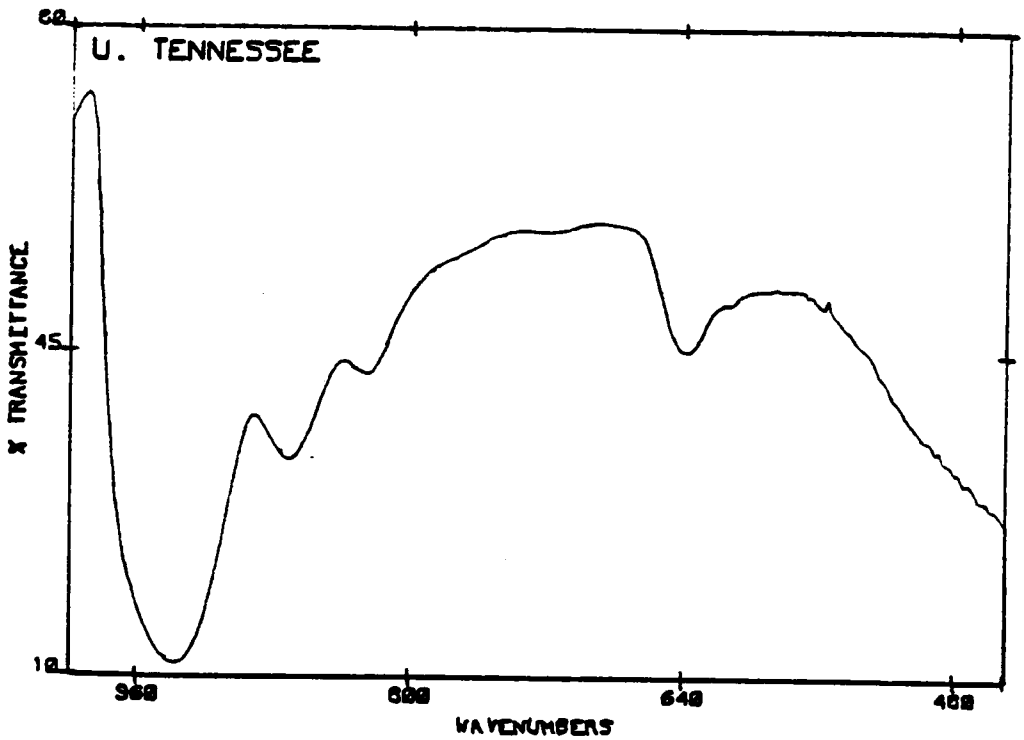


Figure 56. Enlargement of 1000-400 wavenumber region after sample had been annealed past 220°K.

how are the 865, 780, and 710 cm^{-1} bands interrelated? Also, the shoulder on the right-hand side (590 cm^{-1}) of the UF_6 band seems to act independently. The 940 cm^{-1} band is in a region and also has a shape that has been previously assigned to a UO_2 stretch by prior investigators.[10] In a study conducted by Hoekstra,[71] it was determined that uranyl fluoride dihydrate ($UO_2F_2 \cdot 2H_2O$) has a UO_2 stretch which occurs at 935 cm^{-1}. The other bands cannot be definitively assigned at this time. The nitrogen experiments helped to support the fact that probably little or no diffusion was observed during the argon-matrix experiments. The pure studies have supported the belief that there are thermodynamic factors involved also. But, is there also a concentration effect? This question cannot be answered at this point.

8. Matrix-Isolated UF_6 and H_2O in Xenon

The following is a discussion of the results obtained in the co-deposition experiment of UF_6 and H_2O in xenon which was performed under experimental conditions discussed in Chapter III, Section H. Before proceeding with the discussion, some reservations about the experiment must be noted. During the annealing, the pressure would sometimes start to rise drastically at about 30°K, and then lower to its initial value. This process would also tend to cause the annealing to proceed faster than was desired. It was felt that the xenon had some impurities, possibly wet air. Also, the experiments were difficult to duplicate. Sometimes when the matrix sublimed it carried the sample with it, and at other times some of the sample

remained. The few spectra that will be shown are examples of experiments in which some UF_6 and H_2O remained and subsequently underwent hydrolysis. The first spectrum (Figure 57a) was taken while the sample was being held at 16°K. The two peaks in the 1650-1600 cm^{-1} spectral region are indicative of H_2O absorptions. Other peaks occur at approximately 1250, 940, 850, and 615 cm^{-1}. The band at 615 cm^{-1} can be assigned to the UF_6 absorption. The next spectrum (Figure 57b) was taken after the sample had warmed past 150°K. Notice how the peaks at 940, 850, and 800 cm^{-1} have increased in intensity. But, also notice how the background baseline has shifted due to scattering. The next spectrum shown (Figure 58a) reveals that the UF_6 absorption has decreased in intensity relative to the peaks at 940, 850, and 800 cm^{-1}. The final spectrum (Figure 58b) shows that the UF_6 absorption at 615 cm^{-1} has almost gone, and the absorptions at 940, 850, and 800 cm^{-1} have apparently intensified.

The peaks in the 1000-600 cm^{-1} region in the xenon-matrix study are similar to the ones located in the same regions in the neat experiment (pure UF_6 and pure H_2O). In the neat experiment peaks were located at 940, 865, 780, and 710 cm^{-1}. It would probably be safe to assume that the peak located at 940 cm^{-1} in both experiments could be assigned to a UO_2 stretch. As for the others, no assignments can be made at this point.

9. UF_6 and H_2O Merging Streams Co-deposition Experiment

In this section the results of the UF_6-H_2O merging-streams study will be presented and discussed. The experimental details

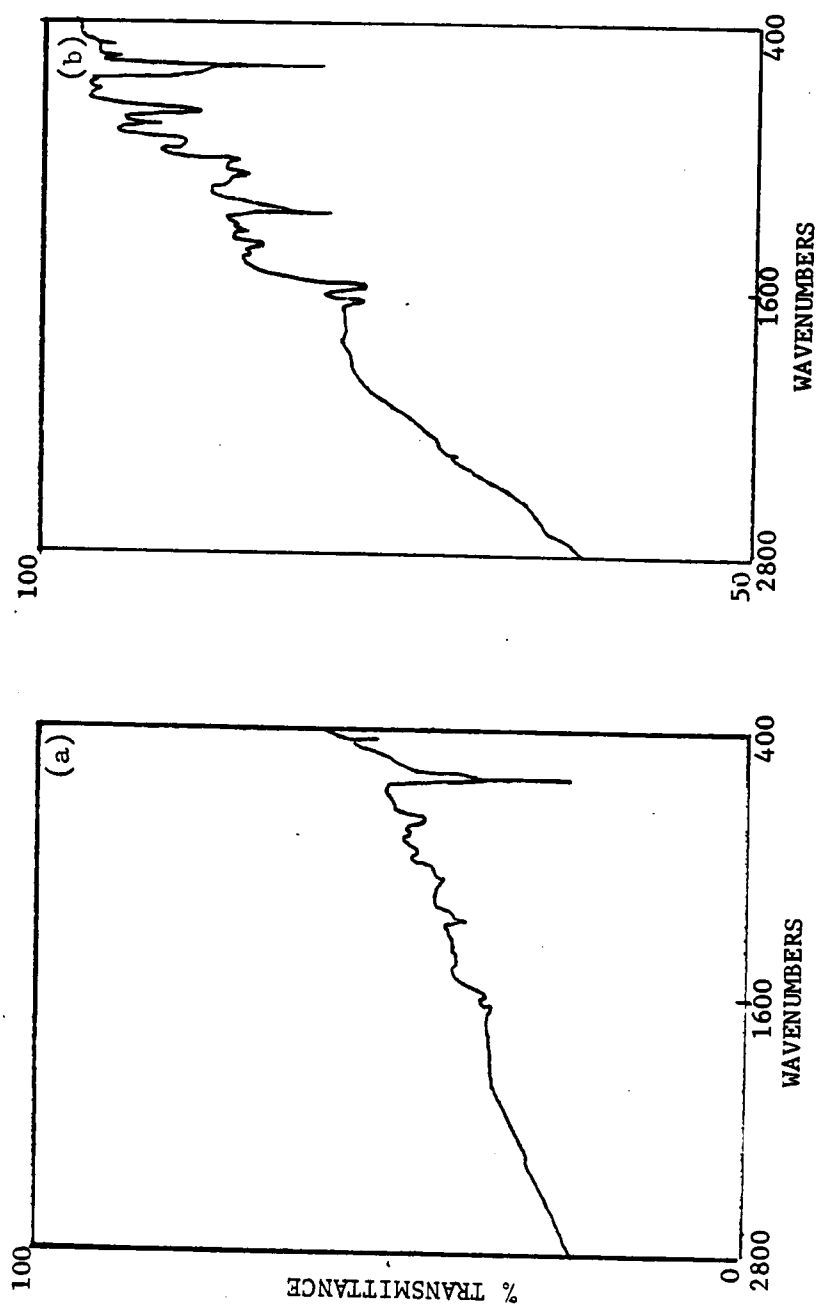


Figure 57. (a) Matrix-isolated FT-IR spectrum of Xe:UF_6 and Xe:H_2O held at 16°K. (b) Spectrum taken after sample was annealed past 150°K.

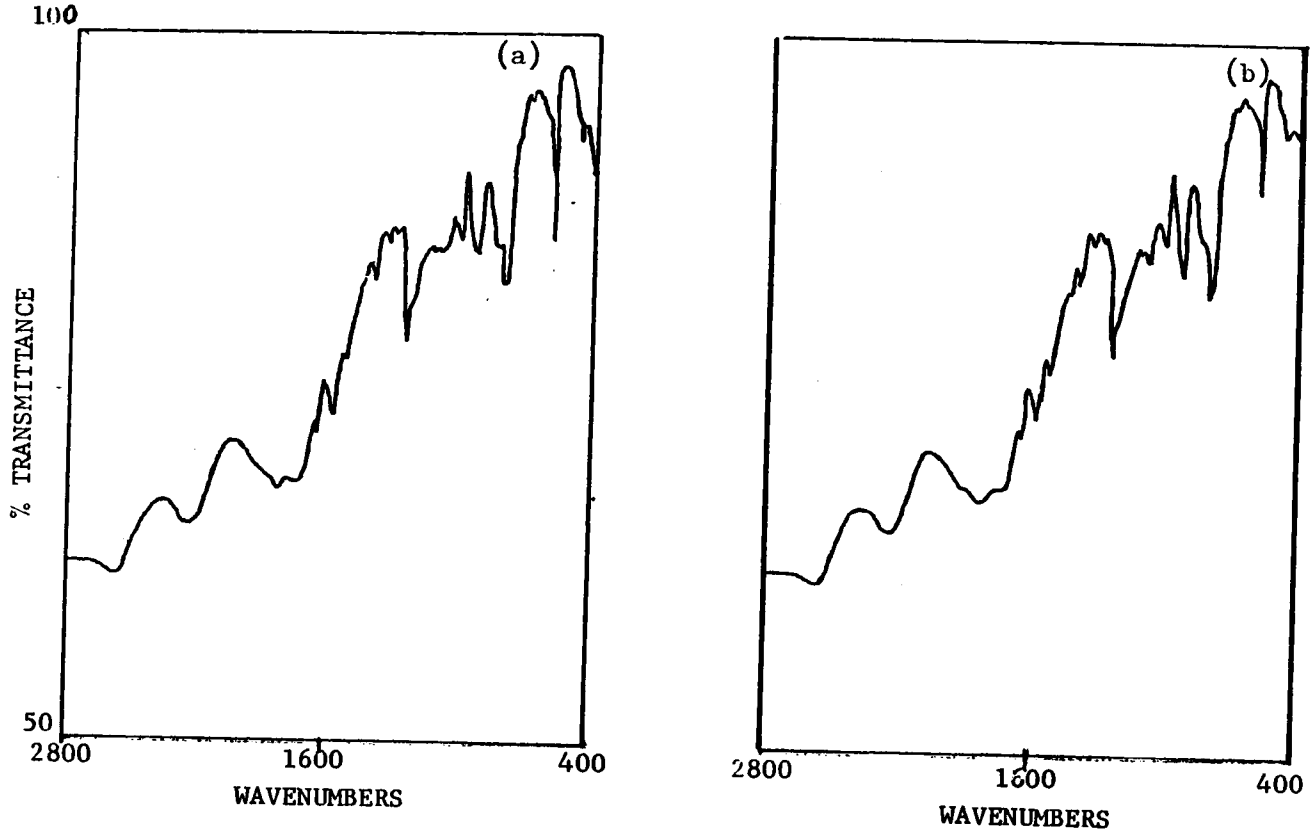


Figure 58. (a) Spectrum of same region after annealing further. (b) Spectrum of same region after annealing past 200°K.

were those discussed in Chapter III, Section J. The first spectrum (Figure 59) was taken after 100:1 samples of Ar:UF_6 and Ar:H_2O were mixed prior to deposition at 16°K in a tube back 30 cm from the deposition inlet. In order to simplify the discussion, only the 1000-500 cm^{-1} region will be examined. Figure 59 reveals only one peak in this region, and it is centered at approximately 800 cm^{-1}. The next spectrum (Figure 60) was also taken at 16°K after a 100:1 sample deposit, and it discloses the same 800 cm^{-1} band. After obtaining these results there was some uncertainty as to whether the samples were depositing cleanly. There was some fear that the streams might have been backing up and absorbing on the inner surfaces of the tubes since only a small peak was observed. Figure 61 represents a spectrum that was taken after the UF_6 and H_2O 100:1 argon samples were deposited separately. Notice the broad band which extends from about 950 to 750 cm^{-1}. It centers at about 850 cm^{-1} and, since the streams were deposited separately, the broad band should not have appeared. Since there were no water lines present in the spectrum (Figure 61), it was felt the H_2O was reacting with some debris that had been adsorbed on the inner walls of the H_2O deposition lines. There is also the UF_6 absorption located at about 600 cm^{-1}. The next spectrum (Figure 62) was recorded after only pure argon was passed through the H_2O side of the lines. Again, notice the broad peak. Since passing a UF_6:Ar sample through the UF_6 deposition tube produced a spectrum having only a UF_6 absorption, this indicated that there might be some contaminants in the H_2O deposition line and not in the UF_6 side. Therefore heating

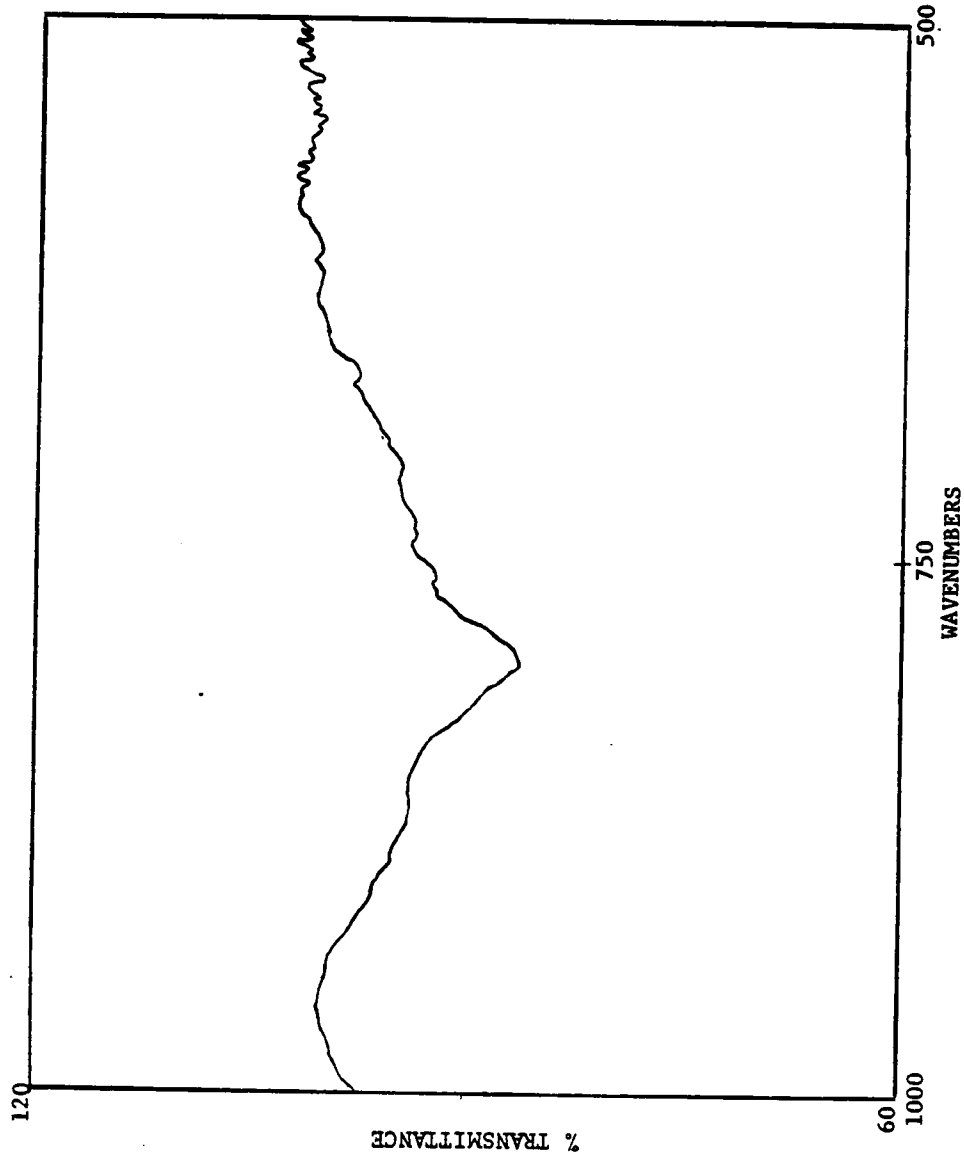


Figure 59. Matrix-isolated FT-IR spectrum of sample of UF_6:H_2O:Ar (1:1:100) that was mixed in-line prior to deposition.

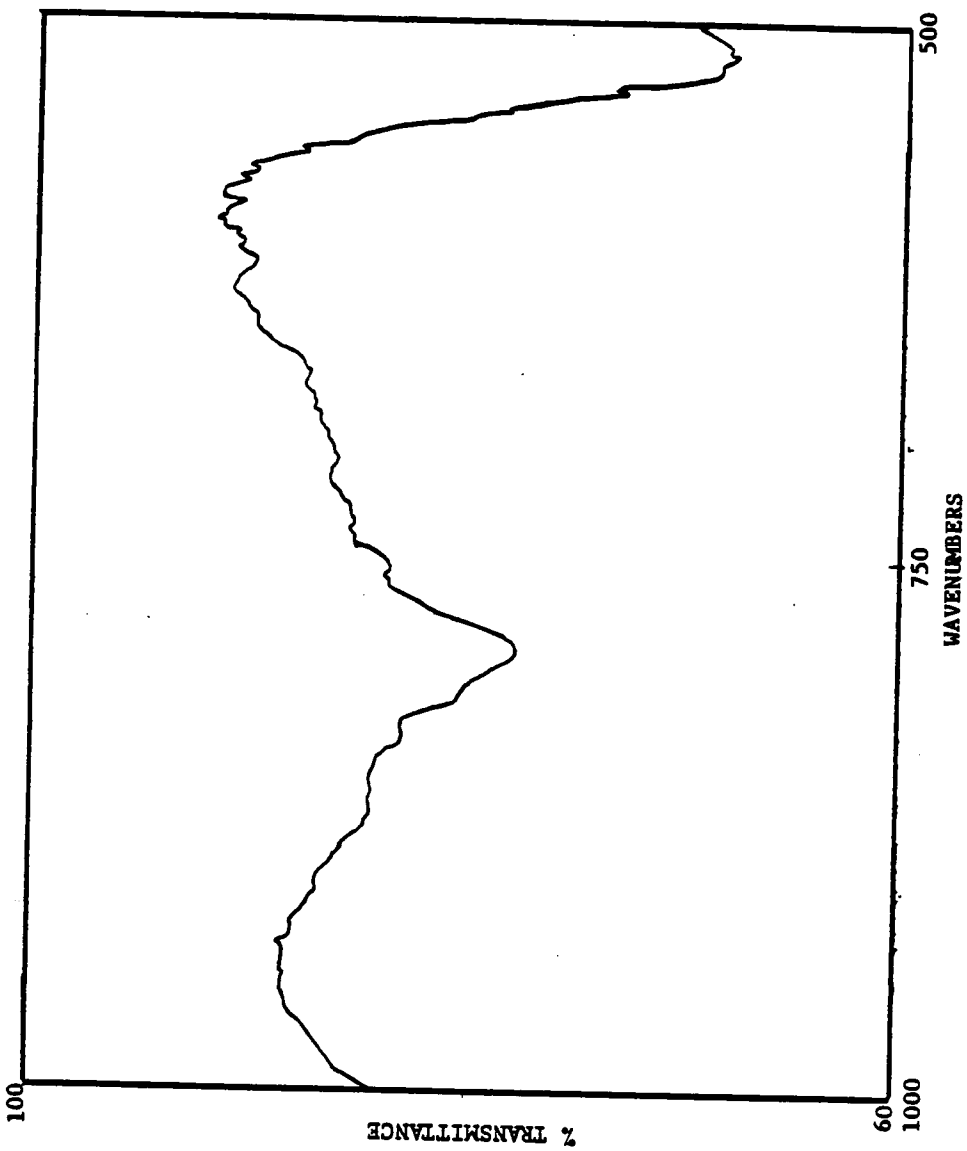


Figure 60. Matrix-isolated FT-IR spectrum of identical sample that was mixed in-line prior to deposition.

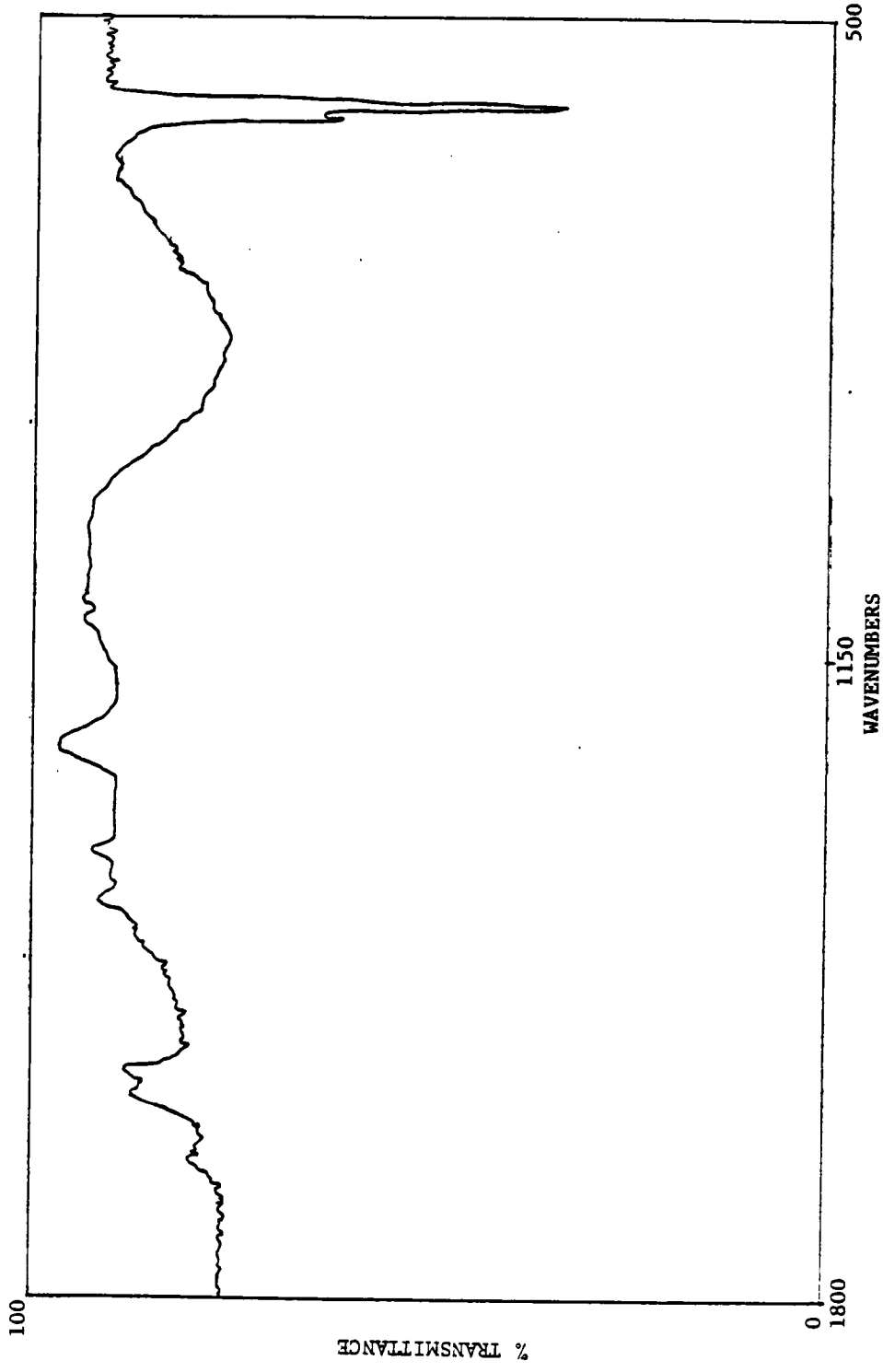


Figure 61. Matrix-isolated FT-IR spectrum of similar sample in which the UF_6 and H_2O were deposited sequentially.

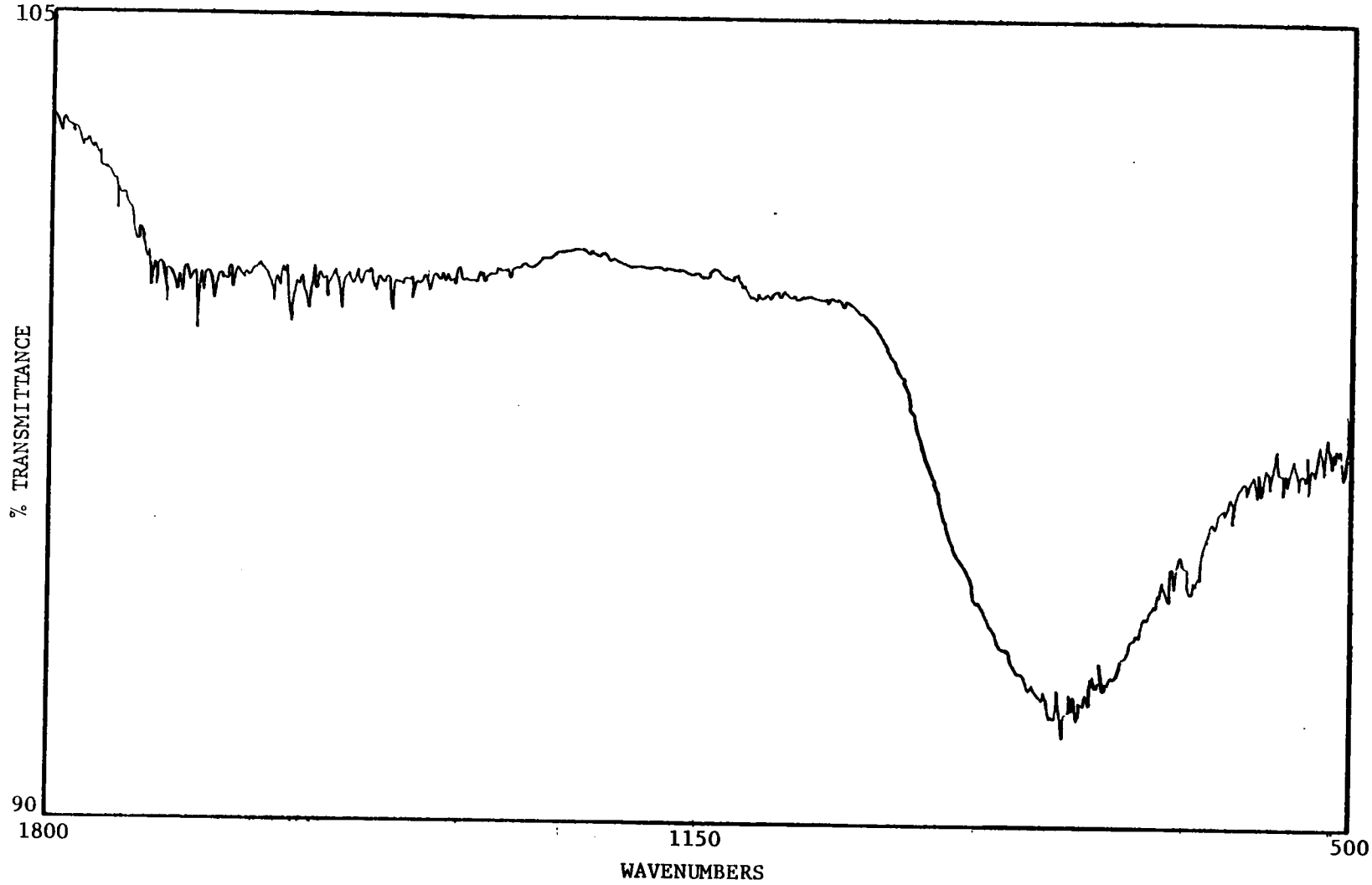


Figure 62. FT-IR spectrum that was recorded after only pure Ar was passed through the H_2O side and deposited.

tape was wrapped around the tube, and the tube was evacuated for several days in order to remove the debris. It was then decided to decrease the water concentration to possibly help eliminate some of the debris. The next spectrum (Figure 63) was recorded after 100:1 Ar:UF_6 and 1000:1 Ar:H_2O samples were merged and deposited at 16°K. Note the broad bands in the 3800-3200 cm^{-1} region indicating that some water had been deposited on the CsI windows. The only significant peak present in the 1000-600 cm^{-1} region is the UF_6 absorption.

Next, the 30-cm tube was lengthened to 100 cm. Figure 64 represents a spectrum that was taken after 100:1 samples of Ar:X (X=UF_6, H_2O) were merged and deposited at 16°K. There is a broad band which extends from about 950 cm^{-1} to about 750 cm^{-1} and is centered at about 840 cm^{-1}. (It must be noted here that the tubes were heated during this experiment in order to prevent any material from adsorbing on their inner walls since a higher concentrated water sample was used.) There are also two other peaks located at 625 cm^{-1} and 595 cm^{-1}. The next spectrum (Figure 65) was taken after the deposited sample had been warmed. The large band at 825 cm^{-1} has changed shape and possibly shifted somewhat (from 840 cm^{-1}), and the bands at 625 and 595 cm^{-1} have virtually disappeared. However, no new bands have emerged. The next three figures (66, 67, and 68) are basically a repeat of the same deposition and annealing experiment with esentially the same results. Later, 1000:1 samples of Ar:UF_6 and Ar:H_2O were tried with basically the same results (see Figure 69). It was then decided that the mixing tube would be

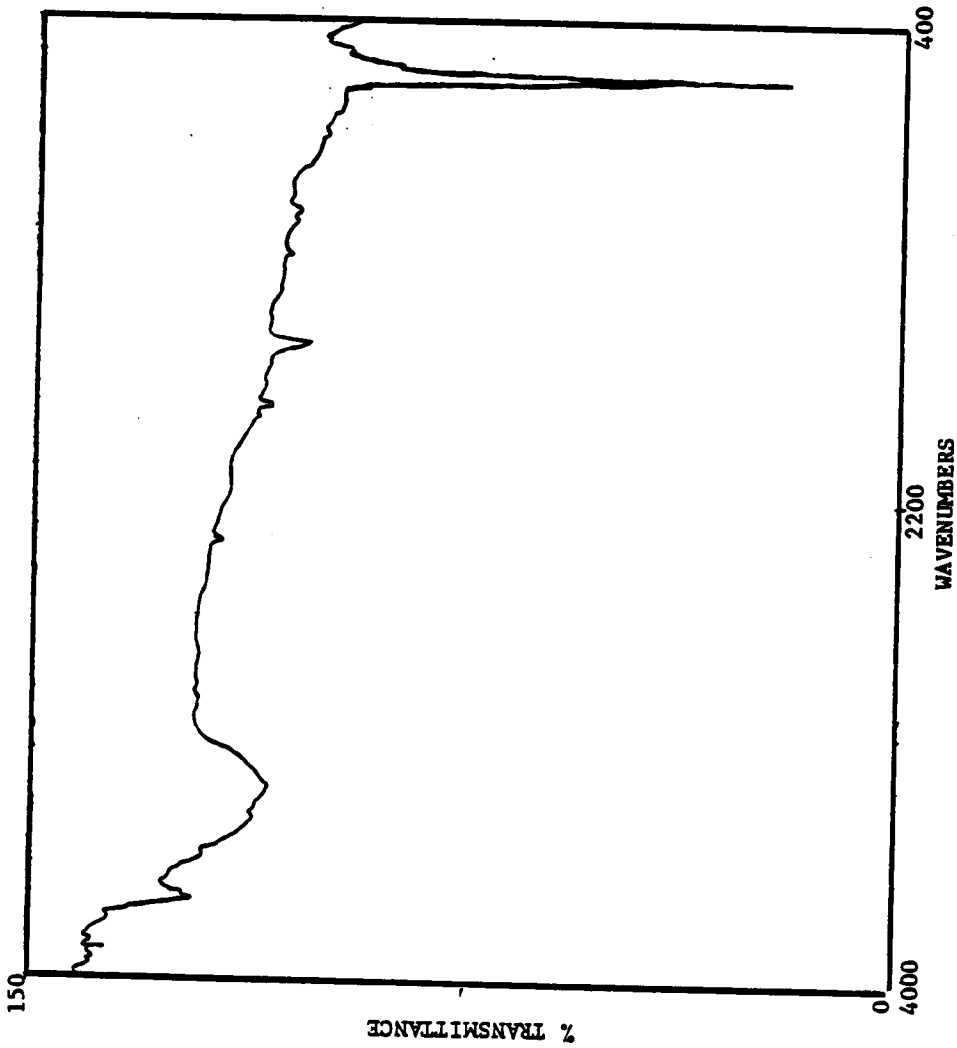


Figure 63. Matrix-isolated FT-IR spectrum of 100:1 Ar:UF_6 and 1000:1 Ar:H_2O samples were mixed and deposited at 16°K.

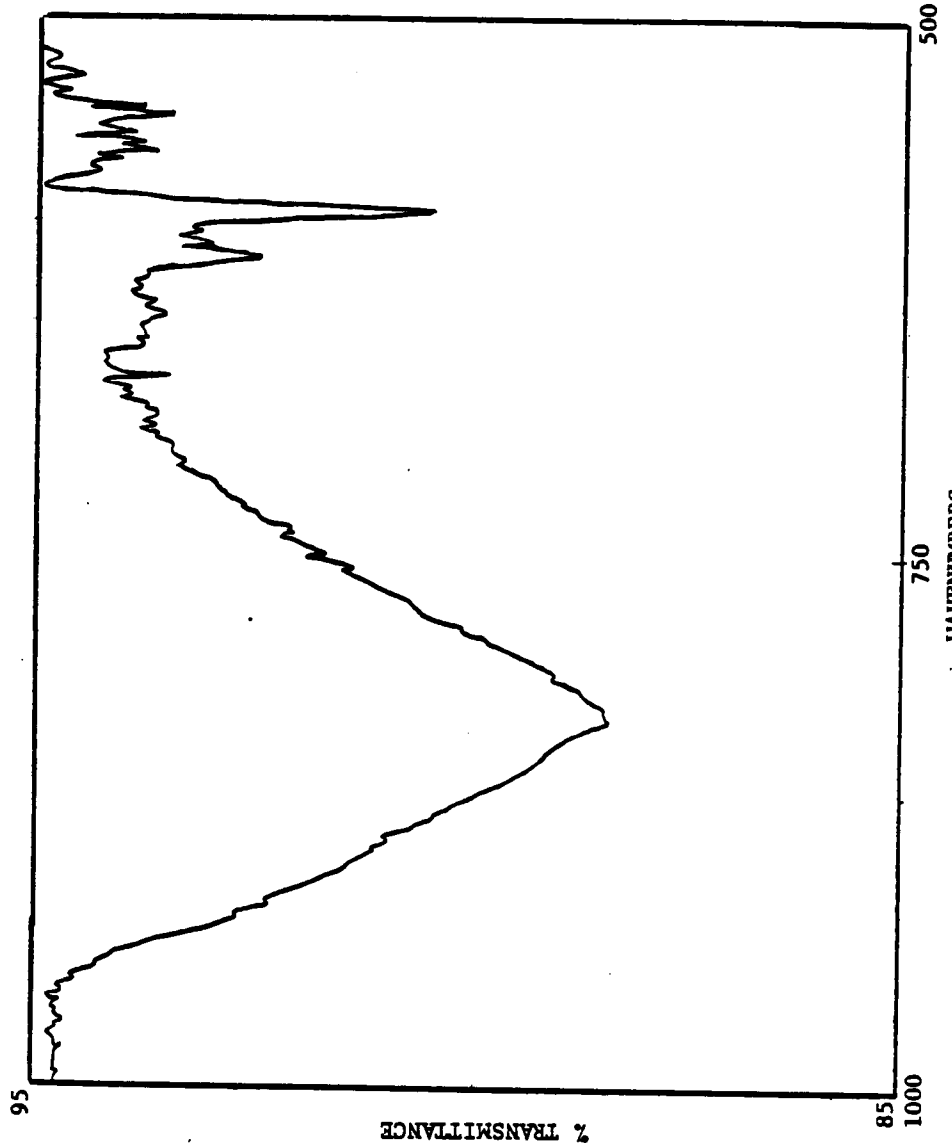


Figure 64. Matrix-isolated FT-IR spectrum of $Ar:UF_6:H_2O$ (100:1:1) sample in which the samples were mixed in a 100-cm tube prior to deposition.

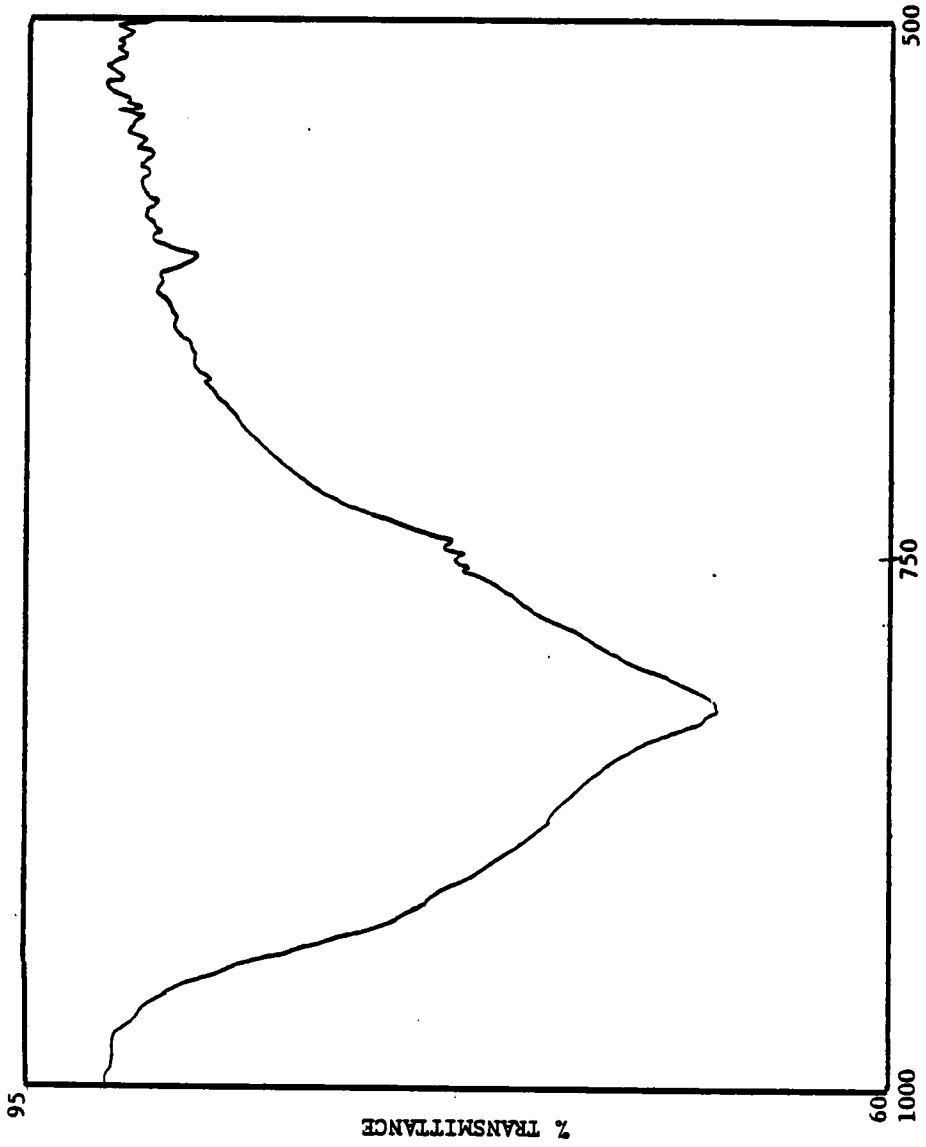


Figure 65. Spectrum recorded after sample had been annealed somewhat.

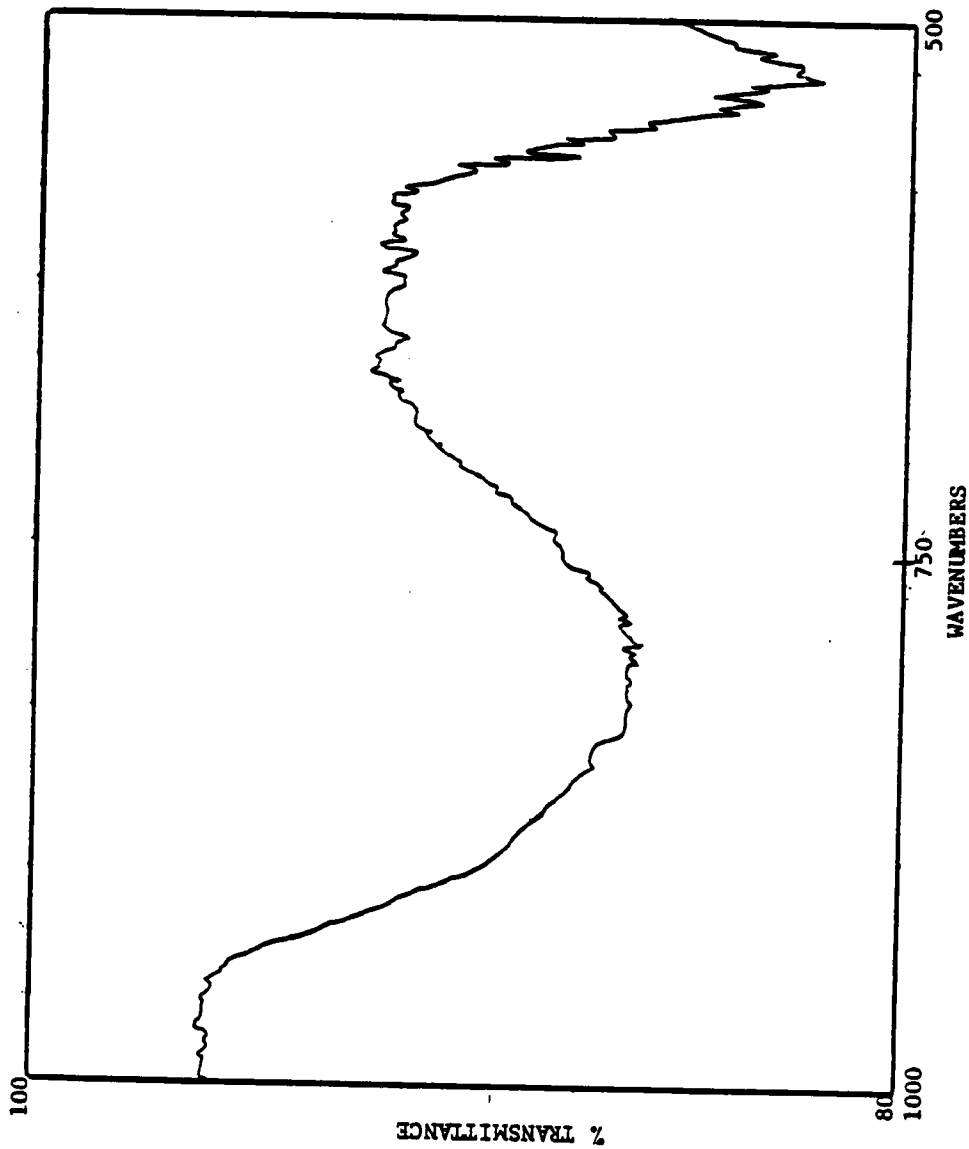


Figure 66. Matrix-isolated FT-IR spectrum of sample similar to the sample recorded in Figure 64.

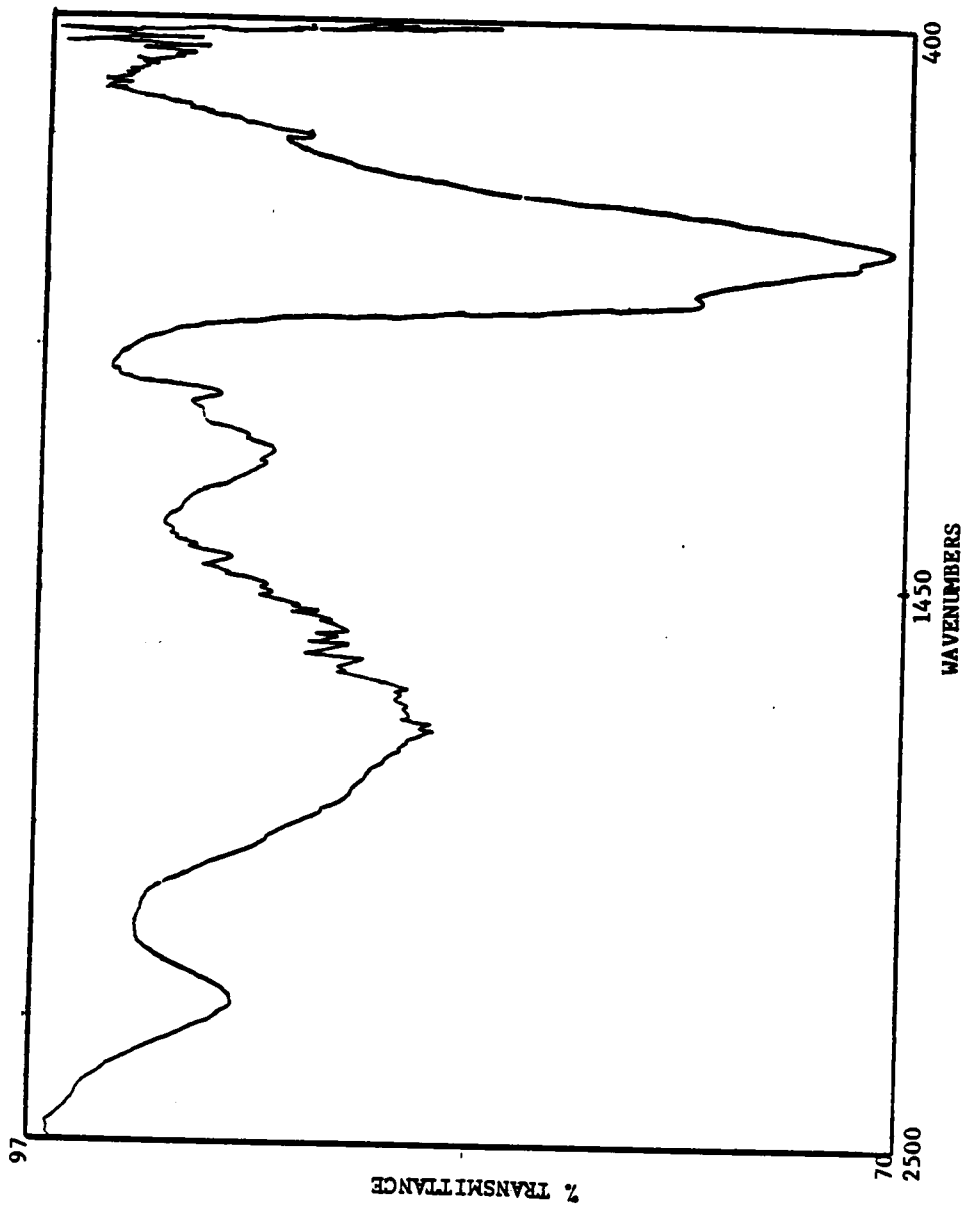


Figure 67. Spectrum recorded after sample annealed somewhat.

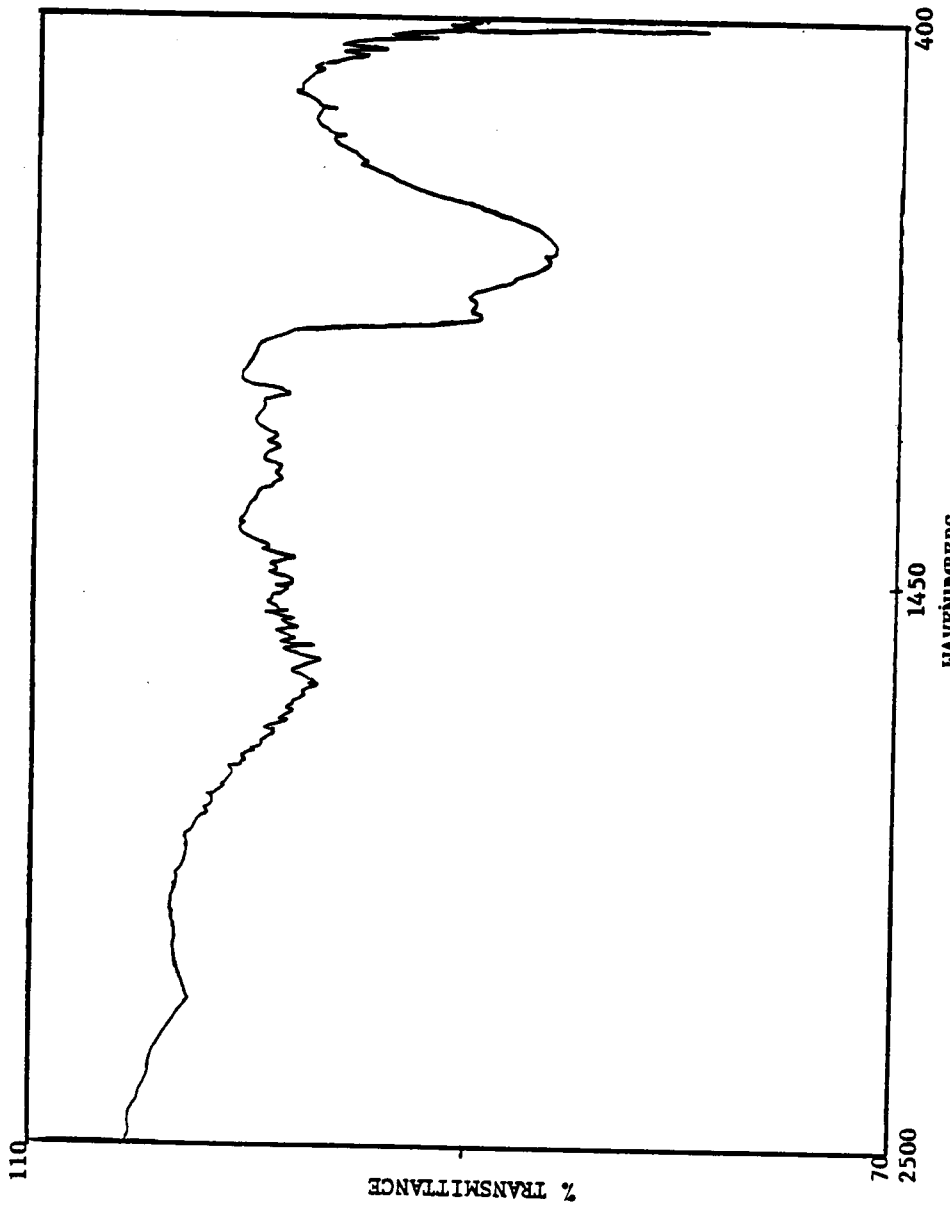


Figure 68. Spectrum recorded after sample had been annealed to about 35°K.

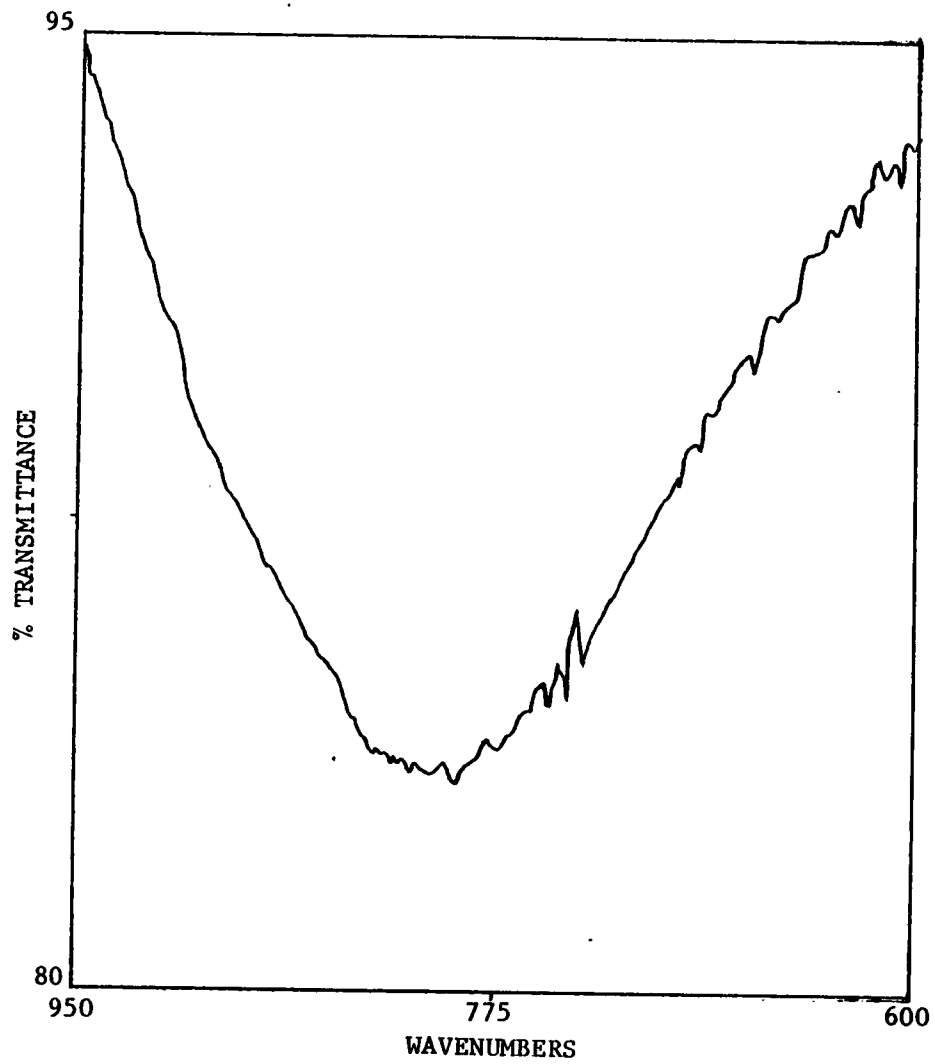


Figure 69. Enlargement of 950-600 wavenumber region of 1000:1:1 of Ar:UF_6:H_2O sample that was mixed in 100-cm tube prior to deposition.

lengthened to about 300 cm in order to allow more time for the UF_6 and H_2O samples to react. Also the tube would again be heated with heating tape during deposition. Most of the spectra recorded yielded basically the same results as the previous spectra. It was then decided to do something drastic in order to try to obtain a different result. Therefore, a 100:1 Ar:UF_6 and pure water were mixed in a 30-cm heated tube and then co-deposited. Figure 70 represents a spectrum taken of that sample being held at 16°K. And again the next spectrum, Figure 71, is also of a similar sample. Notice the broad band (950-750 cm^{-1}) has shoulders located at about 850 cm^{-1} and 940 cm^{-1}. However, subsequent annealing of this sample produced no new peaks (Figure 72), and the broad peak (950-650 cm^{-1}) receded.

What conclusions can be drawn from this set of experiments? One is that there is also a concentration factor that helps to determine the reaction of UF_6 with water. Since during the neat studies (pure UF_6 and H_2O) products were formed during the deposition, it was felt that, by lowering the concentration of the samples and allowing the samples more time to react that possibly some of the products which produced peaks at 865, 780, and 710 cm^{-1} could be isolated. However, this was not the case. What was found on the sample window was a sample whose IR spectrum showed one broad, weak peak between 950 and 650 cm^{-1} in which the apex shifted seemingly at random. However, as obtuse as this peak was, it never failed to show up. It does occur in the same region as the three peaks in the neat study. However, because of its broadness and also because of

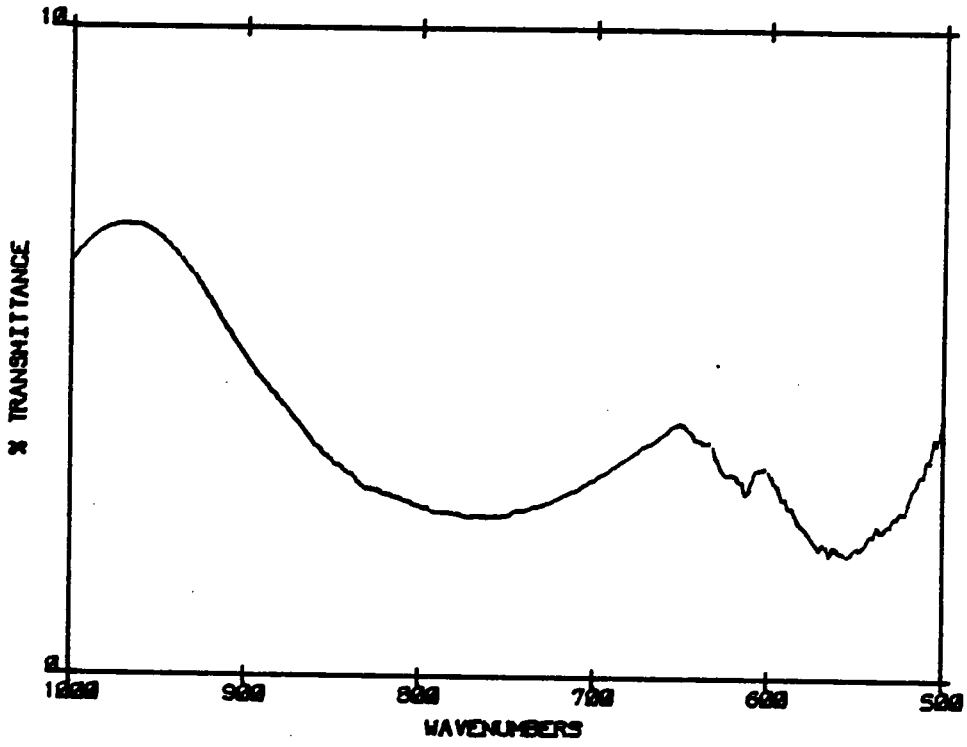


Figure 70. FT-IR spectrum of 100:1 Ar:UF_6 and pure water samples that were mixed in a heated 30-cm tube prior to deposition.

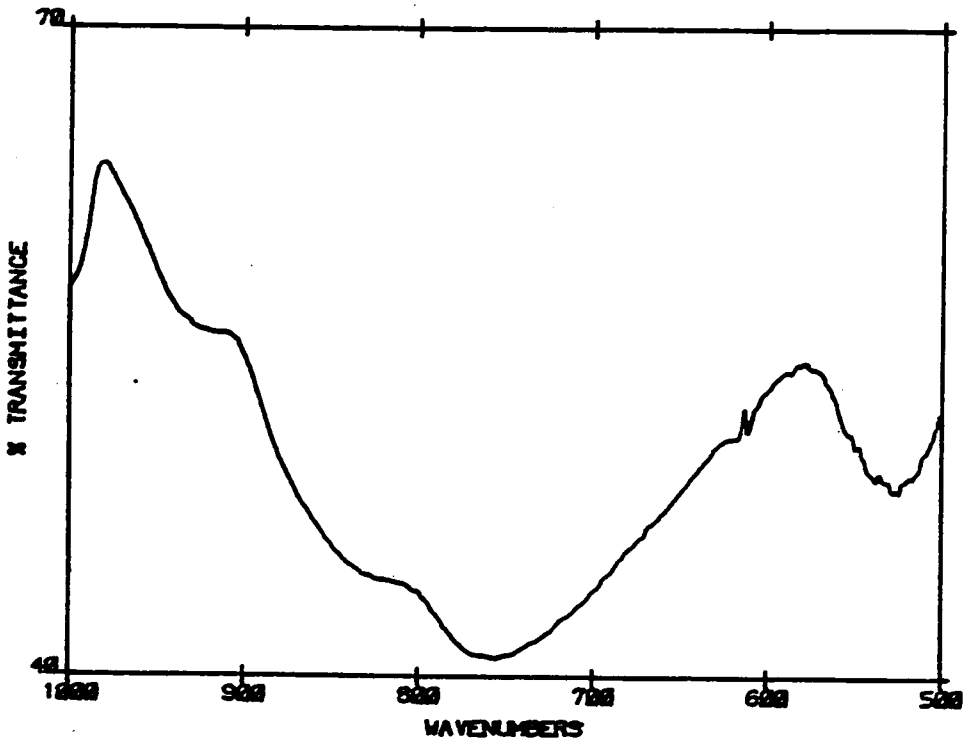


Figure 71. Spectrum of sample similar to the one recorded in Figure 70.

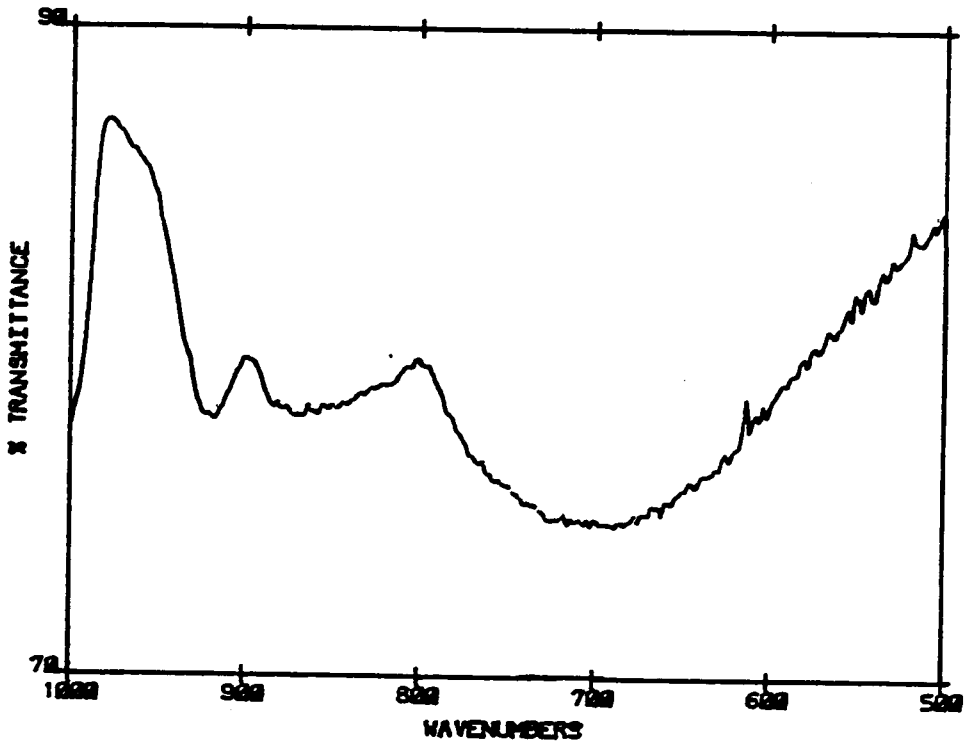


Figure 72. Spectrum of same sample after it was annealed somewhat.

the other problems (back-up and adsorption), no more conclusions can be made.

10. Low-Ratio UF_6 and H_2O Experiment

This section will detail and analyze the results obtained in the low-ratio deposits of UF_6 and H_2O in argon in which the deposition tubes inside the cryostat sample chamber were angled toward one another. The experimental procedures were those described in Chapter III, Section K. As stated earlier, the purpose of angling the tubes toward one another was an attempt to help the UF_6 and H_2O mix better since the samples would be somewhat diluted. Actually this experiment is a mixture of the neat study and the merging-stream study. Unlike the neat study, pure samples were not used. And also, unlike the merging streams study, the back-up or adsorptions problems will not be evident. It was felt that, if the proper ratios of samples were used, the IR peaks which were unveiled in the neat studies could be further detailed and analyzed.

Figure 73 is a spectrum that was taken after 5:1 $Ar:UF_6$ and 2:1 $Ar:H_2O$ samples were co-deposited on the CsI window at 16°K. There are peaks occurring at 850, 613, and 570 cm^{-1}. There are some similarities between the peak at 850 cm^{-1} and the band occurring in the same region in the merging-streams study. It is possible that the spike occurring at 613 cm^{-1} could be due to a UF_6 absorption. The broad band centering at 570 cm^{-1} is unknown.

The next spectrum (Figure 74) was taken after 5:1 $Ar:UF_6$ and a 2:1 $Ar:H_2O$ samples were co-deposited at 16°K. Notice that the peak at 850 cm^{-1} is much sharper than the one in the same region in the

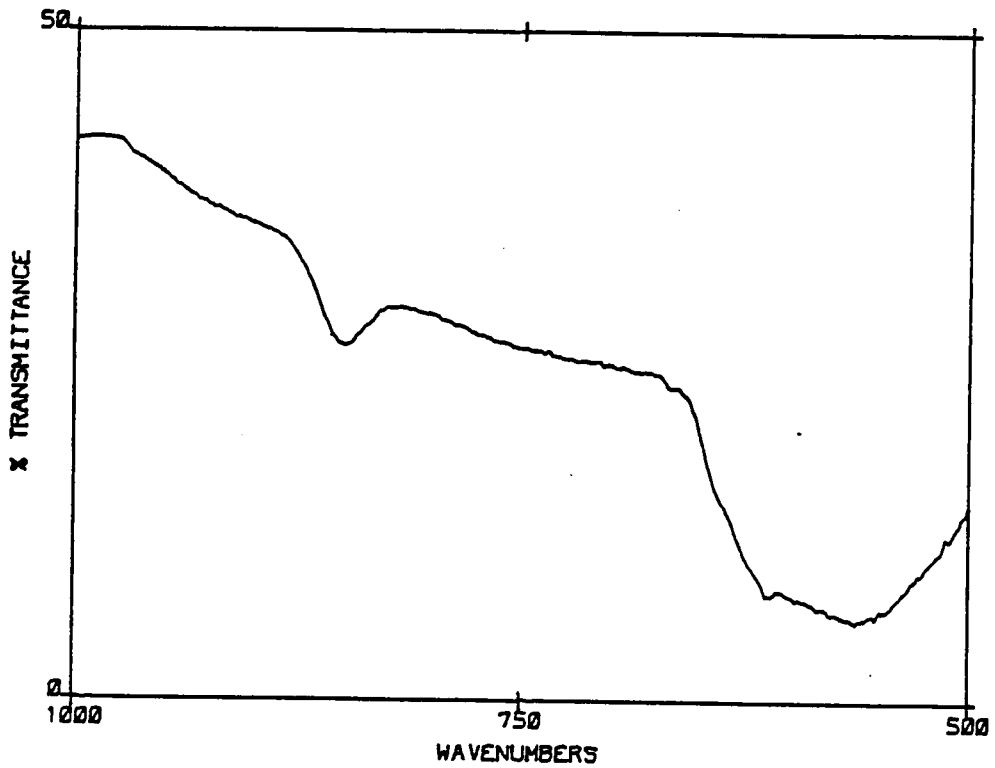


Figure 73. FT-IR spectrum of 5:1 Ar:UF_6 and a 2:1 Ar:H_2O sample that was co-deposited at 16°K.

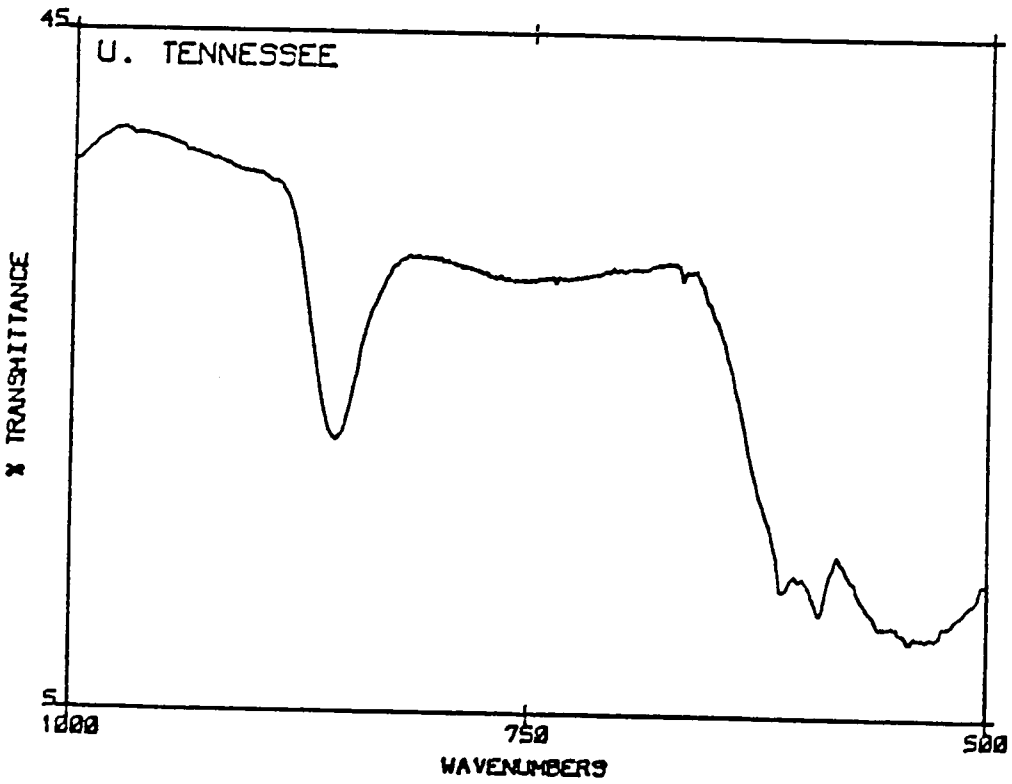


Figure 74. FT-IR spectrum of sample under same experimental conditions as in Figure 73.

previous sample. Also there appears to be a weak, broad band between 800 and 700 cm^{-1}. Other peaks occur at 610, 591, and 540 cm^{-1}. The peak at 610 cm^{-1} is near the area in which peaks were previously assigned to UF_6 absorptions. The bands at 591, and 540 cm^{-1} are unidentified.

The next three spectra (Figures 75, 76, 77) are representative of samples in which the Ar:UF_6 and Ar:H_2O ratios were both approximately 2:1. Since all three spectra are slightly different it is apparent that the apparatus that was used was not exactly designed for this type of experiment because fine tuning the deposit ratios was very difficult. It seems that a 2:1 ratio for both mixtures is the transition point between the species shown in Figure 75 and that obtained in the neat study. Figures 76 and 77 are the most similar, and bands occur at approximately 930, 860, 780, 710, 615 and 570 cm^{-1}. In Figure 75 bands occur at 865, 782, 710, 610, and 591 cm^{-1}. This spectrum is very similar to the one observed (Figure 51) after the initial deposition in the neat study. This set of spectra would appear to indicate that the bands at 930, 860, 615 (610), 591, and 570 cm^{-1} act independently, and also the bands at 780 and 710 cm^{-1} act together and independently from the others. It was apparent that an annealing study might help further solve this problem.

Figure 78 was taken after 3:1 Ar:UF_6 and 2:1 Ar:H_2O samples were co-deposited on the window at 16°K. Peaks occur at approximately 860, 605, 591, and 540 cm^{-1}. The next spectrum (Figure 79) was recorded after the sample had been warmed to approximately 130°K. Notice that a new peak has emerged at about 935 cm^{-1} and also the

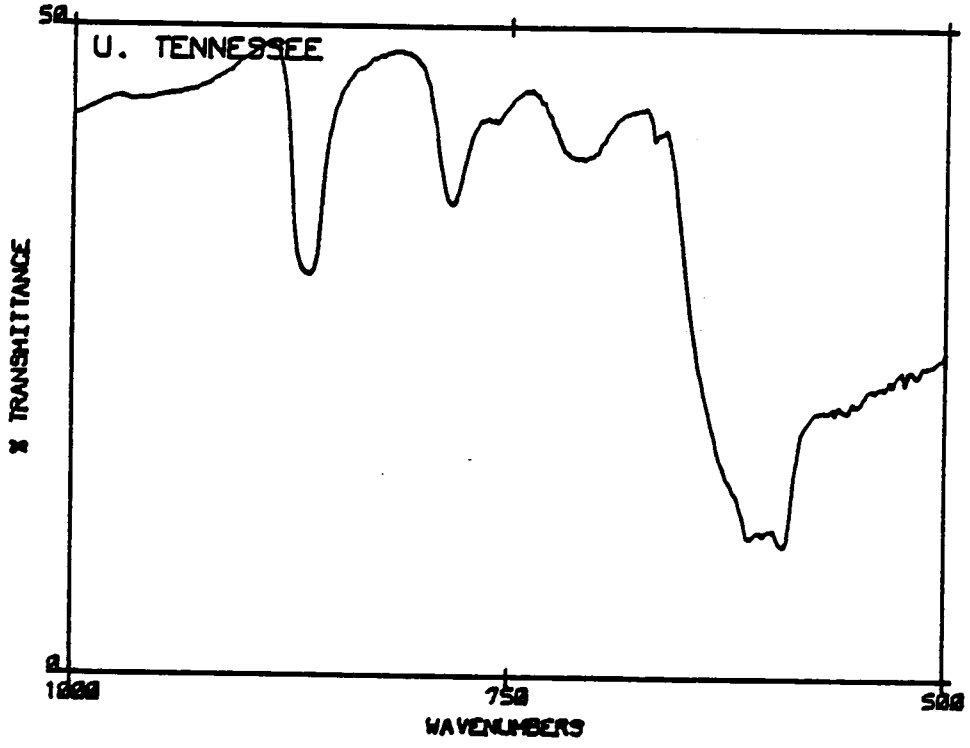


Figure 75. FT-IR spectrum of UF_6:H_2O:Ar (1:1:2) sample recorded at 16°K.

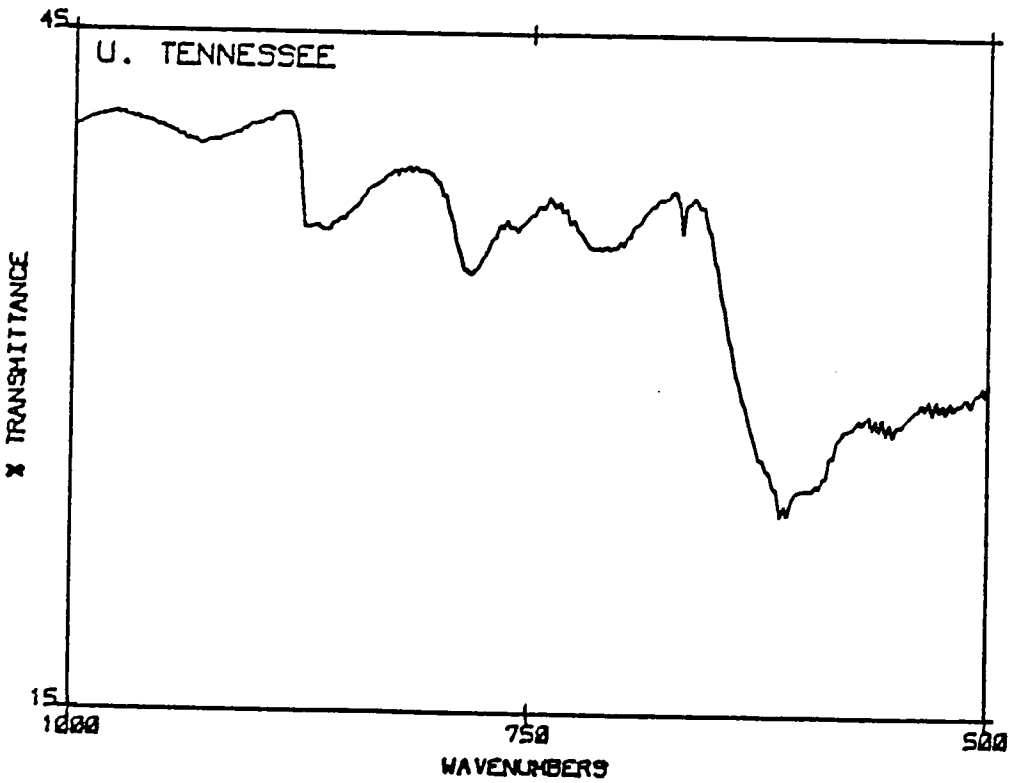


Figure 76. FT-IR spectrum of sample under same experimental conditions as in Figure 75.

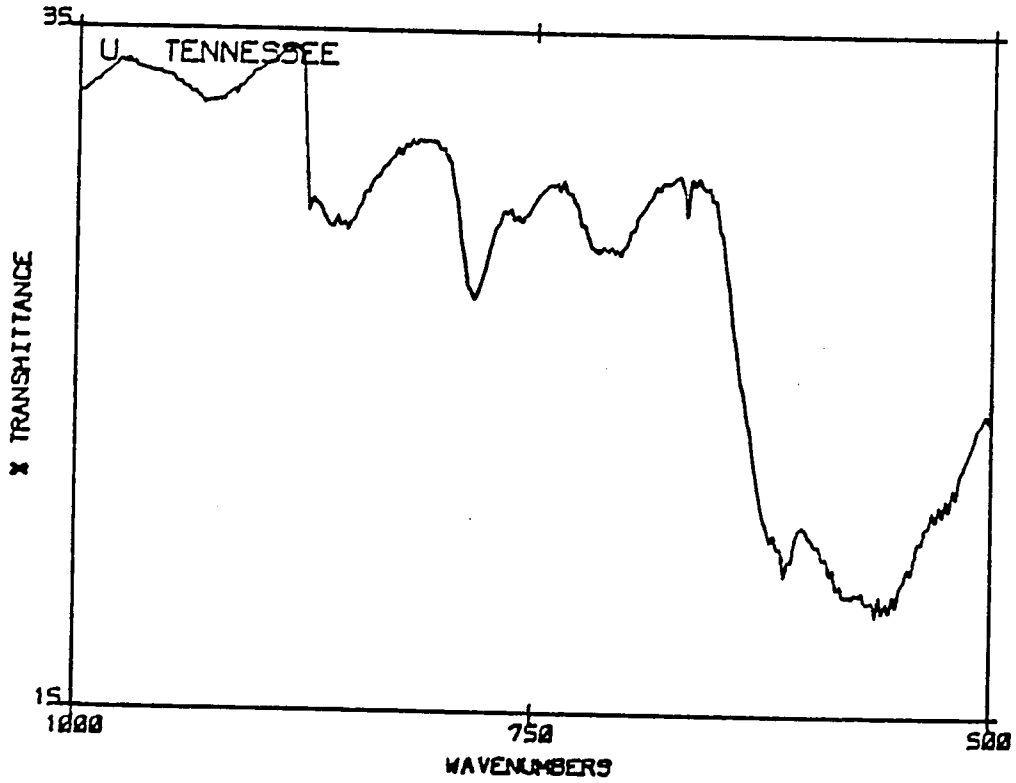


Figure 77. FT-IR spectrum of sample under same experimental conditions as in Figure 76.

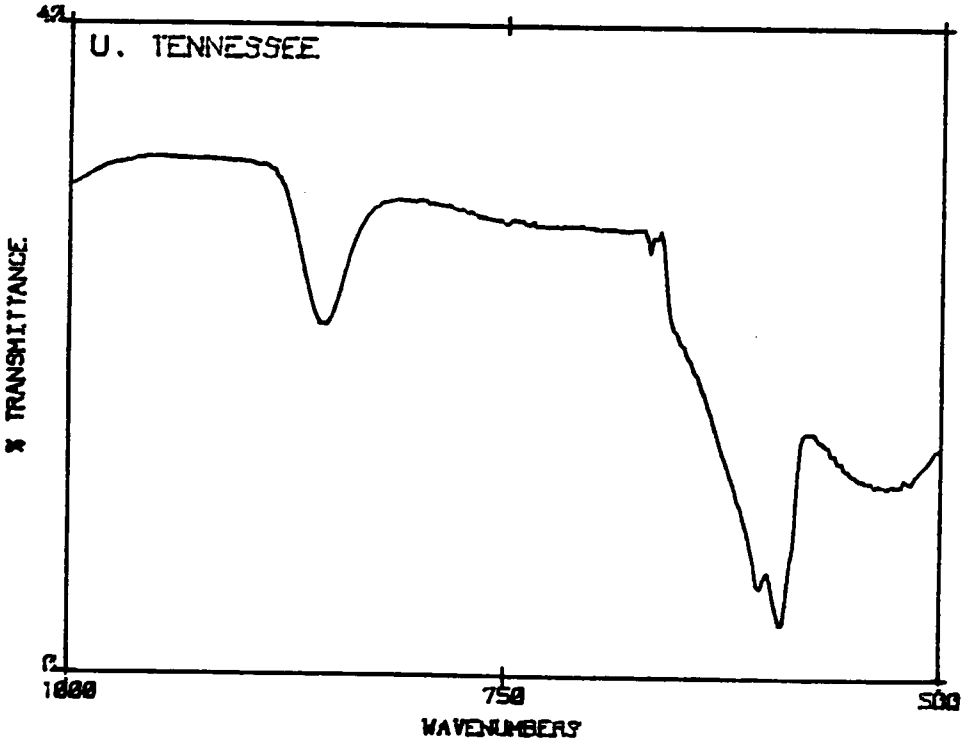


Figure 78. FT-IR spectrum of 3:1 Ar:UF_6 and 2:1 Ar:H_2O samples which were co-deposited at 16°K.

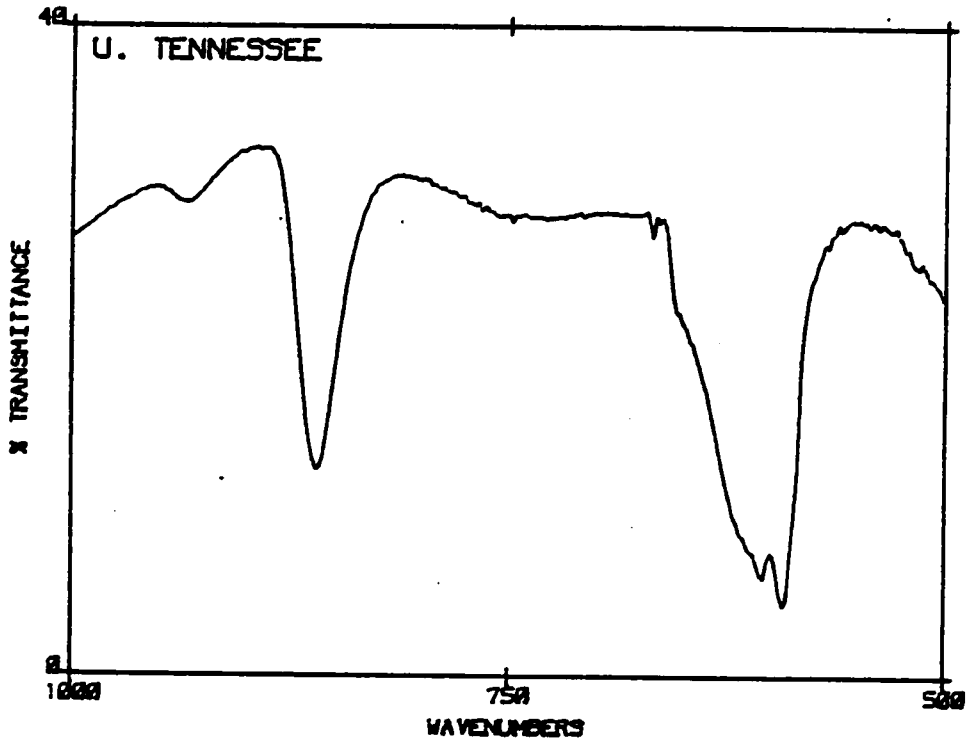


Figure 79. FT-IR spectrum of the sample after it had been warmed to approximately 130°K.

peak at 540 cm^{-1} has disappeared. The 860 cm^{-1} band has increased in intensity and a weak, broad band is appearing to emerge between 850 and 750 cm^{-1}. The next spectrum (Figure 80) was recorded after the sample had been warmed to 180°K. The 935, 860 cm^{-1} peaks have grown and two new peaks appear to be emerging at 780 and 710 cm^{-1}. Also, a new peak at about 615 cm^{-1} has appeared. It apparently was observed earlier as a shoulder on the 605 cm^{-1} peak. The 605 cm^{-1} and 591 cm^{-1} peaks have receded somewhat but are still there. The next spectrum (Figure 81) was taken after the sample had been warmed further. Notice that the 935 (now 940 cm^{-1}), 865 (860), 780, and 710 cm^{-1} peaks are growing. But, the peaks at 605 and 591 cm^{-1} have almost disappeared. Figure 82, which was recorded at about 200°K, shows that the absorptions at 865, 780, 710, and 615 cm^{-1} have decreased but that the 940 cm^{-1} has continued to grow. The final spectrum (Figure 83) in the series shows that the 780 and 710 cm^{-1} bands are gone, the 865 cm^{-1} band is very weak, and there is a slight absorption at 610 cm^{-1}. The 940 cm^{-1} band has continued to grow.

What conclusions can be drawn from these annealing experiments? The annealing experiments appear to further support the fact that there might be a number of chemical intermediates which are producing the emerging and receding bands observed in Figures 78 through 83. The bands which appear to act independently are the 940, 865, 620, 605, 591, and 570 cm^{-1}, but the 780 and 710 cm^{-1} bands act together. But, what are the possible intermediates?

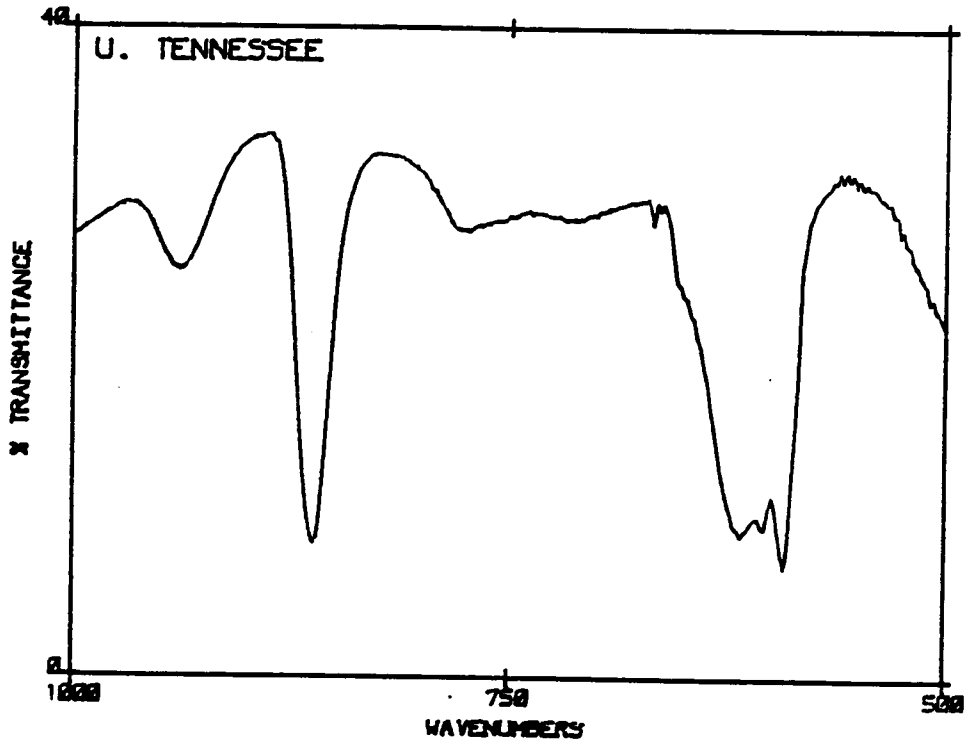


Figure 80. Spectrum recorded after sample had been warmed to about 180°K.

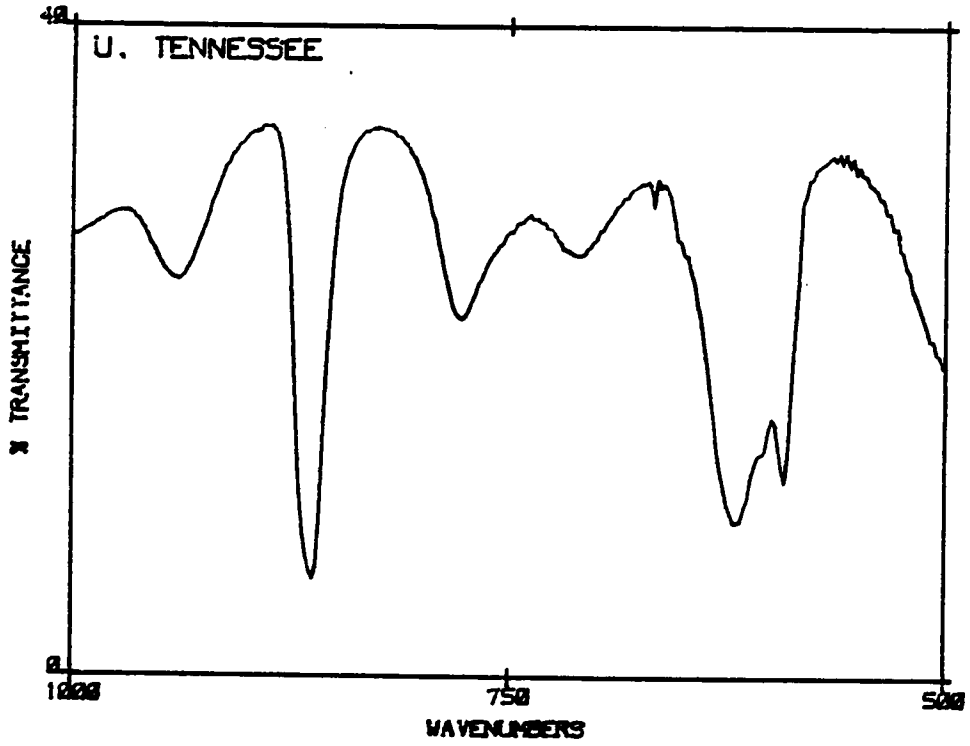


Figure 81. Spectrum recorded after sample had been warmed further.

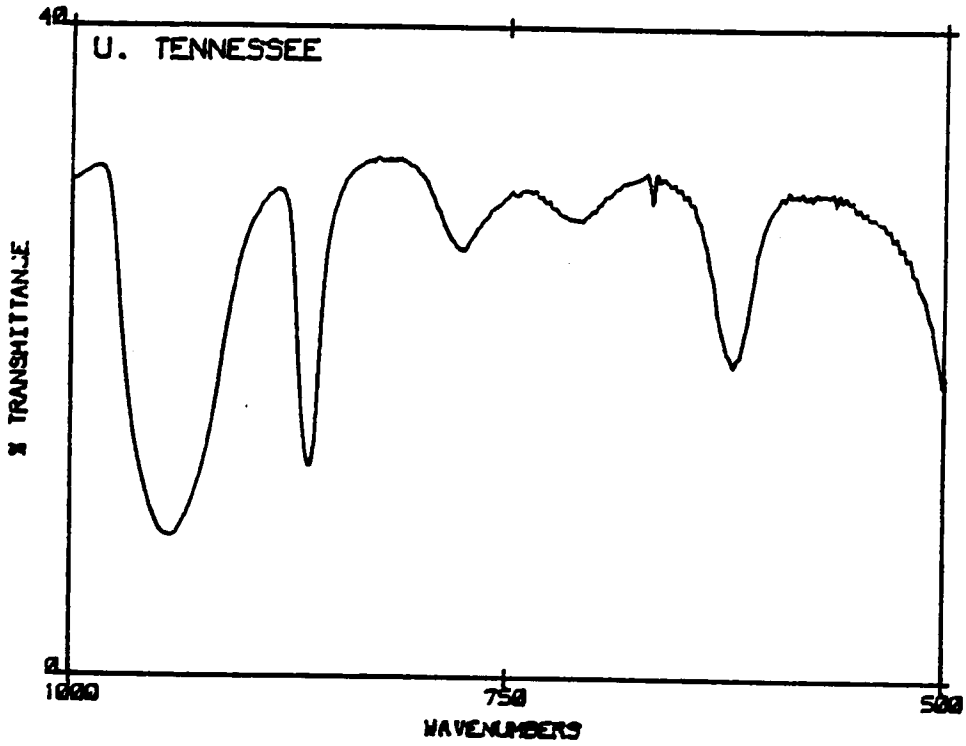


Figure 82. Spectrum recorded after sample had been warmed to about 200°K.

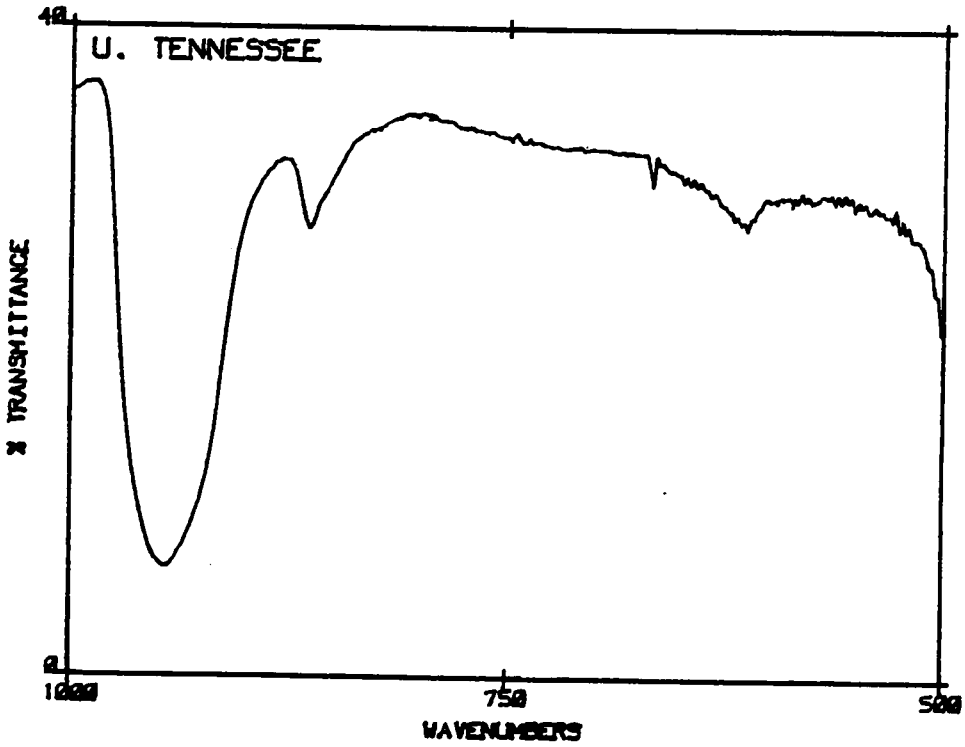


Figure 83. Spectrum recorded after sample had been warmed past 220°K.

First, it is necessary to determine the possible intermediate pathway that would be followed on going from UF_6 to UO_2F_2 via a UF_6 molecule's interaction with an H_2O molecule. First, a single water molecule might react in this fashion:

$$UF_6 + H_2O \rightarrow UF_6 \cdot H_2O.$$

Here, water forms an adduct with UF_6. Or it might react in this fashion:

$$UF_6 + H_2O \rightarrow UF_5OH \cdot HF \quad (H^+ UOF_5^- \cdot HF).$$

Another possibility is that an ionic intermediate is formed:

$$UF_6 + H_2O \rightarrow H^+UF_6OH^-.$$

And these products might then dissociate:

$$\left.\begin{array}{l} UF_6 \cdot H_2O \\ UF_5OH \cdot HF \\ H^+UF_6OH^- \end{array}\right\} \rightarrow UF_5OH + HF.$$

Then UF_5OH could react with another water molecule via:

$$UF_5OH + H_2O \rightarrow UF_5OH \cdot H_2O \quad \text{or}$$

$$UF_5OH + H_2O \rightarrow UOF_4 \cdot HF \cdot H_2O \ (H^+UOF_5^- \cdot H_2O) \quad \text{or}$$

$$UF_5OH + H_2O \rightarrow UF_4(OH)_2 \cdot HF.$$

and, then these products may dissociate:

$$\left.\begin{array}{l} UF_5OH \cdot H_2O \\ UOF_4 \cdot HF \cdot H_2O \\ UF_4(OH)_2 \cdot HF \end{array}\right\} \rightarrow UOF_4 + HF + H_2O.$$

If one uses this scheme then a possible reaction sequence might be:

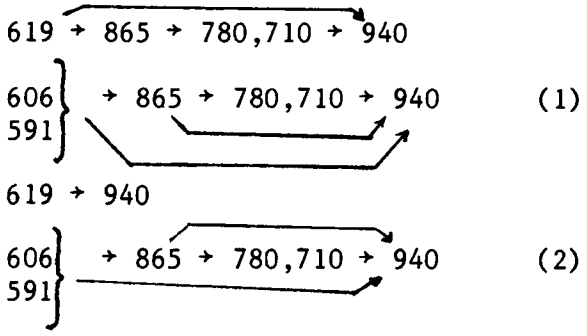
$$UF_6 \cdot X \rightarrow UF_5OH \cdot X \rightarrow \begin{array}{l} UF_4(OH)_2 \cdot X \rightarrow UF_3(OH)_3 \cdot X \\ UOF_4 \cdot H_2O \cdot X \quad UOF_3(OH) \cdot H_2O \cdot X \end{array}$$

$$\rightarrow \left.\begin{array}{l} UF_2(OH)_4 \cdot X \\ UO_2F_2 \cdot 2H_2O \cdot X \end{array}\right. \quad (X = H_2O, \text{ or } HF.)$$

If one examines this scheme one realizes that many possible intermediates might have been omitted. Ionic intermediates are a strong possibility because some oxofluoro uranium ionic compounds have been synthesized. Now, can these possible intermediates fit the bands in question in this series of spectra?

In the first few spectra several products are possibly present. UF_6 is most certainly present. Other possibilities are $UF_6 \cdot X$ $UF_5OH \cdot X$, $UF_4(OH)_2 \cdot X$, $UOF_4 \cdot H_2O \cdot X$, etc ($X=H_2O$, or HF). The band at 865 cm^{-1} is very near the 893 cm^{-1} band that has been previously assigned to a U-O stretch in solid UOF_4. It is possible that this band may be due to a U-O stretch in an isolated UOF_4 molecule or some similar adducted or non-adducted intermediate. Also, the bands at 605, and 591 cm^{-1} are very close to the U-F stretch at 619 cm^{-1} due to UF_6. Either band at 605 or 591 cm^{-1} could be due to a U-F vibrational mode caused by a UF_5X type molecule. Since the broad band at 540 cm^{-1} disappears rather quickly, it is possible that it could be due to an intermediate that is relatively unstable and perhaps partially reacted. Since it does not remain, then one must assume that it is not part of the reaction sequence; it is only formed on the initial deposit. The peaks at 606 and 591 cm^{-1} appear to be feeding the 940, 865, 780, and 710 cm^{-1} bands; as the 606 and 591 cm^{-1} bands are receding, the others are emerging. The bands at 780 and 710 cm^{-1} appear to emerge at the same time as the 940 cm^{-1} band but recede while the 940 cm^{-1} continues to grow. Also, the 865 cm^{-1} band recedes simultaneously with the 780 and 710 cm^{-1} bands and they do so only after the 606 and 591 cm^{-1} bands disappear. The

780 and 710 cm^{-1} bands could posibly be assigned to an intermediate such as $UF_3(OH)_3 \cdot X$ or $UOF_3OH \cdot H_2O \cdot X$, etc. These intermediates appear further along in the reaction sequence. The band which appears at 940 cm^{-1} is very close to the region that has been previously assigned to a UO_2 stretch in solid $UO_2F_2 \cdot 2H_2O$.[71] It is also in the same region as a similar peak that was previously assigned to UO_2F_2 impurity in a KBr pellet of UOF_4 by Paine and associates.[10] Since in Figure 82 the 619 cm^{-1} UF_6 peak is still present, one can conclude that it apparently does not feed the 606 and 591 cm^{-1} bands and it might not feed the 865, 780, and 710 cm^{-1} bands. But, it apparently does feed the 940 cm^{-1}. Here are two possible combinations. The 619 cm^{-1} band feeds the 940, 865, 780, and 710 cm^{-1} bands, and the 606 and 591 cm^{-1} bands feed them also. Or, the 606 and 591 cm^{-1} bands feed the 940, 865, 780, and 710 cm^{-1} bands, and the 615 cm^{-1} band feeds only the 940 cm^{-1} band.



Is it really possible that the second reaction sequence might be correct? Yes, because two H_2O molecules could simultaneously attack a UF_6 molecule and react to form UO_2F_2. At the higher temperatures, the appearance of the other intermediates might be less favorable. Also, one might ask why the 865 cm^{-1} peak still remained (Figure 83) after the 780, and 710 cm^{-1} peaks have

disappeared. One could only conclude that the 865 cm^{-1} peak is due to a relatively more stable molecule. Also, the 865 cm^{-1} peak could be directly feeding the 940 cm^{-1} peak. And, any of the other peaks could well have been directly feeding the 940 cm^{-1} peak. But, why then, if the 865 cm^{-1} peak was feeding the 940 cm^{-1} peak, did the 940 cm^{-1} peak not continue to grow when the 865 cm^{-1} still remained? One answer might be that there were no more H_2O molecules available at this point for any species to react with. Therefore, what one can conclude is that a fairly complex reaction sequence might be present. It is possible that it is only initiated because the proper products are formed on deposition, and that, as the temperature of the sample is increased, these products (intermediates) cannot so readily be maintained. Also, it is more than likely that neither sequence presented is correct; but that it is more complex and, in all probability, a mixture of the two, especially as the temperature increases. Every species (band) present might be feeding the 940 cm^{-1} band.

Another question one might ask is why the 865, 780, and 710 cm^{-1} bands could not be due to U-F vibrational modes. They very well could be. They could also be combination bands of UF_6 that were proposed by investigators.[72] However, it is not likely since the bands in question are fairly strong. Also, in UF_6, only the totally symmetric U-F stretch or combination bands are IR active in that region, and in a molecule such as UOF_4, only U-F bridging modes are IR active in the region under examination. Probably no U-F

bridging modes might be present because the concentrations are very low, and only small aggregates or individual molecules are forming. That is, the molecules forming might be very different from the usual crystal or lattice type molecules and possibly absorb differently in the infrared region.

Next, examine the spectrum shown in Figure 84 and compare it to Figures 78 through 83. Figure 84 represents a spectrum of a $K^+UOF_5^-$ sample recorded by W. W. Wilson and associates.[73] Notice that they are remarkably similar. What does this similarity mean? It could mean that their $K^+UOF_5^-$ sample was not pure but had a mixture of impurities. The assignments made to these bands were adopted from those previously proposed in a study by Jaubert and associates.[74] These assignments will be discussed later. It might be possible to tentatively adopt some of these assignments for the bands observed in sections 9 and 10, but they are slightly more complex and do not occur in the same positions as those found in the Wilson and Jaubert studies.

11. Low-Ratio Nozzle Studies.

The low-ratio nozzle studies added no new insights into the problem of solving the identities of the bands in question. It did, however, reveal that there was good sample mixing in the low ratio studies without the nozzle since the spectra are basically the same. It can also be seen that, in Figure 85, the spectra are somewhat sharper than those found in the annealing experiment; therefore, locations of the peaks are more clearly established.

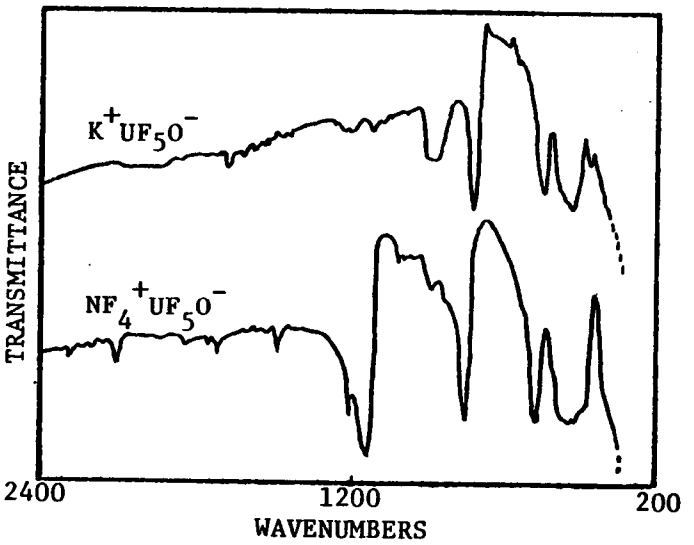


Figure 84. Infrared spectrum of $K^+UF_5O^-$ and $NF_4^+UF_5O^-$ samples recorded by Wilson and associates.[73]

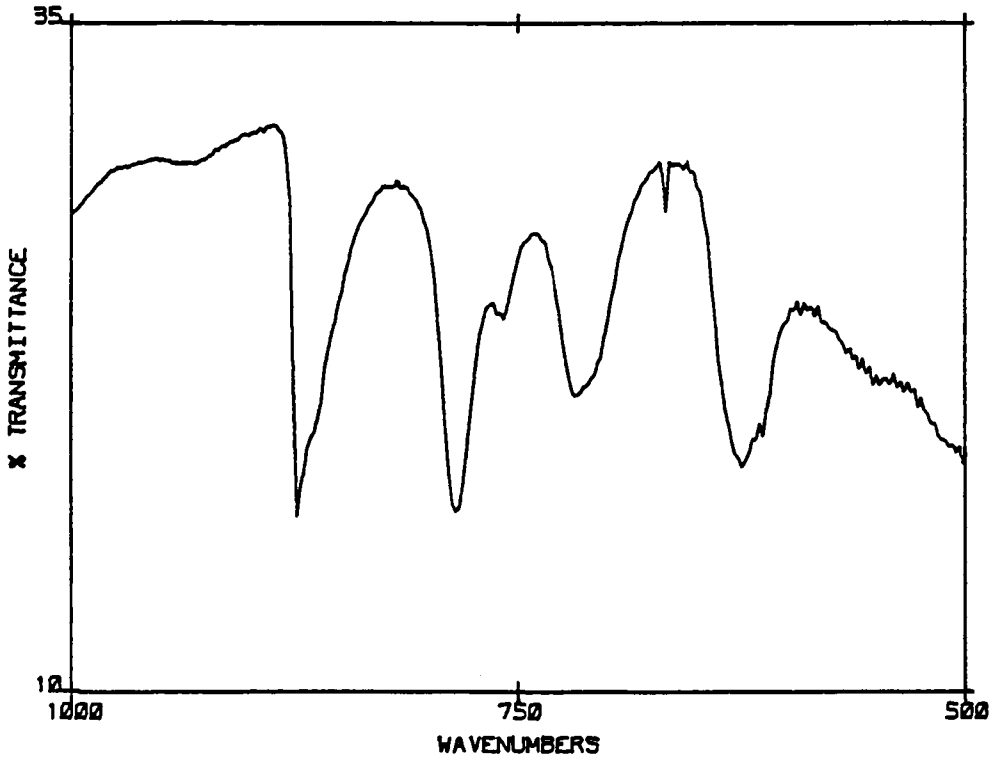


Figure 85. FT-IR spectrum of 2:1 Ar:UF_6 and 2:1 Ar:H_2O sample that was co-deposited through nozzle at 16°K.

12. UOF_4 Volatility Studies

The following is a discussion of the volatilization experiments performed on UOF_4. The experimental details were those discussed in Chapter III, Section G. Figure 86 is a spectrum which was recorded after a sample of UOF_4 was heated and volatilized, and then absorbed onto the sample window. There is a broad band with shoulders located at approximately 600 cm^{-1}. This, in all probability, could be assigned to the UF_6 stretch. Repetition of this experiment with either slow heating or fast heating yielded basically the same results. It was also observed that some debris remained on the glass sample tube, but, because of the blackening of the glass, it was difficult to discern the color of the debris. However, it can probably be concluded that the UOF_4 underwent decomposition to UF_6 and that the remaining debris was probably UO_2F_2 in accordance with the TGA trace of Paine and associates.[10]

B. Discussion

The results of the matrix-isolation and neat UF_6-H_2O studies revealed that UF_6 and H_2O would not react at cryogenic temperatures, and in fact, showed no propensity to react until temperatures above 150°K were reached. Calculations of Gibbs free energies from literature values[75,76,77] for the reaction of UF_6 with H_2O, showed the reaction to be favorable for the formation of UO_2F_2 but unfavorable for the formation of UOF_4 at 298°K. Also, calculations were done for the reaction of MoF_6 and WF_6 with H_2O. They revealed that the formation of $MoOF_4$ and WOF_4 to be favorable at 298°K, but that

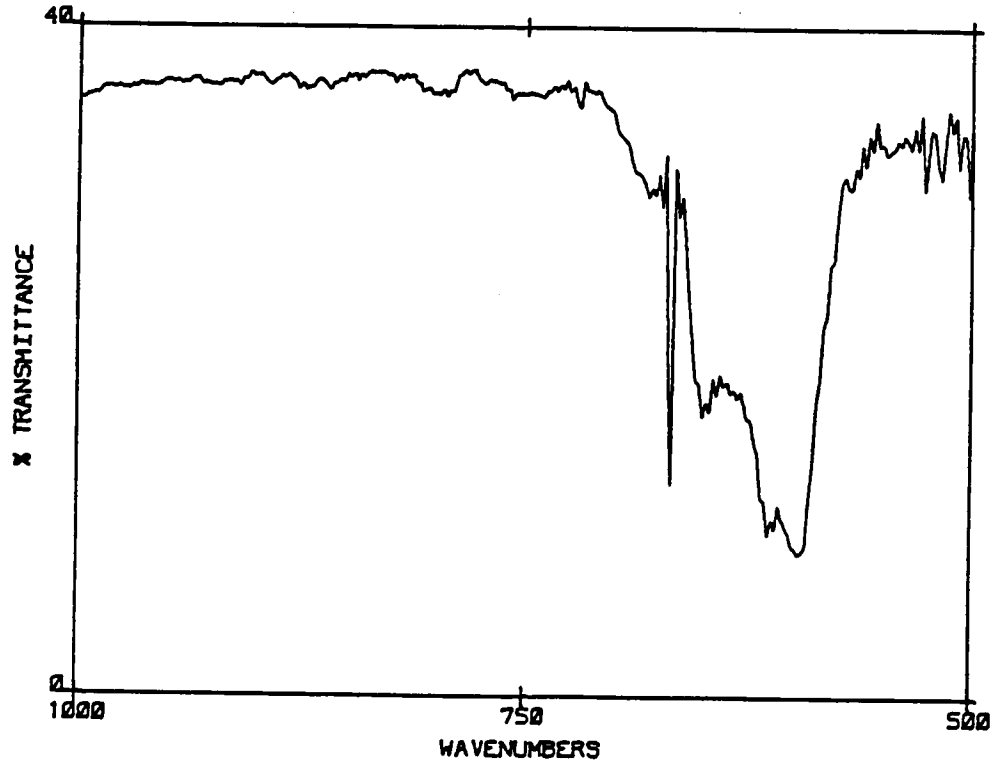


Figure 86. FT-IR spectrum of volatilized UOF_4 sample at 20°K.

this propensity decreased as the temperature decreased. Therefore, from a thermodynamic standpoint, one might expect UF_6 to act similarly. And, analogous experiments with MoF_6 or WF_6 might prove helpful.

In Table VII there are listed IR bands of UF_6, UOF_5, UOF_4, UO_3, UO_3, UO_2, and UO which were obtained in previous studies as well as IR bands which were observed in this study. During the course of this discussion, it might be helpful to refer to this table as an aid to understanding.

In the UF_6 and H_2O co-deposition matrix-isolation annealing experiments, it was seen that the samples either reacted to products that were not IR active (because no new bands appeared), reacted but then evacuated away from the window, or did not react.

Visual observation of a sample deposited on the window while it was being heated to 50°K lends evidence to the belief that the sample boiled off the window. Plus, a rise in pressure also indicated that the sample boiled off. This evidence, coupled with the fact that during the neat experiment in which pure UF_6 and pure water were co-deposited and showed no reaction at low temperatures since the respective UF_6 and H_2O IR bands remained intact, lent support to the belief that no reaction occurred in the matrix. In fact, no reaction was observed for the neat UF_6 and water co-deposition study until the sample had been warmed past 150°K. What does this evidence tell us? It tells us that the thermodynamics do not favor a reaction at these low temperatures. But, then another question one might ask, is if the thermodynamics had been favorable,

TABLE VII

IR ABSORPTIONS (cm^{-1}) OF IMPORTANT SPECIES FOUND IN PREVIOUS INVESTIGATIONS AND UF_6 HYDROLYSIS STUDY

A. Previous investigations

1. Uranium compounds
   UF_6; 1293,1160,624,186[1-3]
   UOF_4; 893,667,558,478,375[10]
   UO_2F_2; 990,260,234,146[6,21]
   $UO_2F_2 \cdot 2H_2O$; 935[71]
   UOF_5^-; 820,602,593,480[74]
   UO_3; 852,844,746,212,186,152 (matrix-isolation)[27,28,29]
   UO_2; 776,765 (matrix-isolation)[27,28,29]
   UO: 820 (matrix-isolation)[27,28,29]

2. Matrix-isolated water
   1000:1; 3733,3638,1602,1593
   100:1; 3733,3726,3709,3700,3695,3634,3574,3565, 3565,3528,3516,1626,1615,1611,1602,1593

B. UF_6 hydrolysis study

1. UF_6 vapor
   a. 10-torr
      H_2O; 3960-3540,1920-1400
      (unk); 1400-1240,980,821,480
      UF_6; 1160,619

   b. 50-torr
      H_2O; 3960-3540,1920-1400
      (unk); 1400-1240,935,855,821
      UF_6; 1292,1158,619

2. UF_6/Ar matrix-isolation
   UF_6; 619 (fine structure-627,621,619,614,609)

3. H_2O/Ar matrix-isolation
   a. 1:1000
      H_2O; 3730,3640,1612,1601,1599,1593

   b. 1:100
      H_2O; 3776,3755,3730,3724,3705,3699,3696,3633,3573,3565, 3563,3556,3552,3523,3516,1623,1614,1612,1609,1604, 1603,1601,1597,1593,1572

TABLE VII (continued)

c. 1:20
H_2O; 3697,3600-3100 (broad), 1650-1605,1602,1593

4. UF_6/H_2O/Ar matrix-isolation

Similar to 2.a and 3.a combined

5. UF_6/N_2 matrix-isolation

UF_6; 627,624,623,618,610

6. UF_6/H_2O pure

a. Before annealing
H_2O; 3800-3200,1650-1550
UF_6; 620
(unk); 865,780,710,620

b. After annealing
H_2O; 3800-3200,1650-1550
$UO_2F_2 \cdot 2H_2O$; 940
(unk); 865

7. UF_6/H_2O merging streams

UF_6; 625
(unk); 950-650,595

8. UF_6/H_2O low ratio

a. 5:1/2:1; 850,613,570
b. 5:1/2:1; 850,610,591,540
c. 2:1/2:1; 930,860,780,710,615,591
d. 3:1/2:1; (before annealing): 860,605,591,540
3:1/2:1; (intermediate): 940,860,780,710,615,591
3:1/2:1; (after annealing): 940,860

then might a reaction have occurred? That is, would the reaction have been kinetically favorable?

The answer to this question can be found by examining the results of the low-ratio deposition studies. As the concentrations of the samples were increased, more reaction occurred. That is, more peaks were observed in the 900-700 cm^{-1} region. But, no 940 cm^{-1} (uranyl) band appeared, as in the case of the neat study, until the sample had been annealed. Two conclusions can probably be drawn from these facts. First, that there is also a concentration factor as well as a thermodynamic factor which governs UF_6 hydrolysis. Second, that the hydrolysis pathway has some relatively stable intermediates and would probably be a two or more step process.

The neat study lent support to the fact that there are probably intermediates between UF_6 and UO_2F_2 in the hydrolysis reaction. But, it did not help to determine if the 865, 780, 710, bands acted together or separately. The low-ratio studies together with data from previous studies may help solve this puzzle.

In the low-ratio annealing study, bands were initially observed at 860, 605, 591, and 540 cm^{-1}. It was previously decided that the band at 865 cm^{-1} could be due to a U-O stretch in UOF_4 or to something very similar. Also, the 605 and 591 cm^{-1} bands could be due to a U-F or U-OH mode. In the previously referenced study which was conducted by Jaubert and associates[74] on UOF_5^- ion, they assigned peaks, located at 602 and 593 cm^{-1}, to a $\nu_2(a_1)$ UF_4 symmetrical elongation and a $\nu_3(a_1)$ U-F (equatorial fluorine) elongation respectively in the UOF_5^- ion. They made these assignments by

relating force-constanst calculations to experimental IR and Raman data on the $KUOF_5$, $RbUOF_5$, NH_4UOF_5, $CsUOF_5$, and $[Ph_4P]UOF_5$ molecules. Their assignments correlate very well with the present results. A UOF_5^- ion or some similar molecule is a very reasonable intermediate to assume in this reaction sequence. It is possible to go one step further and surmise that an $UOF_5^-H^+(UOF_4 \cdot HF)$ molecule might be present. An 820 cm^{-1} band in UOF_5^- was assigned to a $\nu_1(a_1)$ U-O elongation. Notice that the 865 cm^{-1} band found in this study is located between this band and the 893 cm^{-1} band assigned to the U-O stretch in UOF_4 by Paine and associates.[10] But, what happened next during the annealing experiment seems to be even more complicated.

The series of spectra upon annealing showed that the 605 and 591 cm^{-1} bands receded and that the 865 cm^{-1} band continued to grow as would be expected, but also new bands emerged at 780 and 710 cm^{-1} as well as a band at 940 cm^{-1}. The 940 cm^{-1} band has already been tentatively assigned to a UO_2 mode in $UO_2F_2 \cdot H_2O$. But, what about the 780 and 710 cm^{-1} bands? In a study by Gabelnick and associates,[27-29] they recorded FT-IR spectra of uranium oxide species vaporized from tungsten and iridium Knudsen cells and deposited in Ar and Kr matrices. They made assignments of $U^{16}O_3$, $U^{16}O_2$, and $U^{16}O$ (which are listed in Table VII), based on force-constant calculations and mass spectrometry data.[78] Notice that the 776 and 765 cm^{-1} bands for UO_2 are very close to the 780 cm^{-1} band found in this study. One would expect the UO_2 species to form after the U-O in a UF_6 hydrolysis reaction and, it therefore might correlate to this

study. The 710 cm^{-1} band cannot be correlated with any known study. It is probably due to the same species that elicits the 780 cm^{-1} band since it occurs simultaneously with it.

From the low-ratio annealing study it can probably be concluded that there are at least two relatively stable intermediates in the UF_6 hydrolysis reaction. These are the intermediates due to the 865 cm^{-1} and the 606 and 591 cm^{-1} bands. There might also be one or more intermediates of lesser stability due to the 780 and 710 cm^{-1} bands. It can also be concluded that the reaction might be more complex than just a sequential-step process. But, one might ask what can be further done to solve this problem?

One answer is to conduct this same study with similar molecules such as MoF_6 and WF_6. The IR and Raman spectra of $MoOF_4$, MoO_2F_2, and WO_2F_2 have been well-established, and it might be valuable to correlate answers found in a hydrolysis study on WF_6 and MoF_6 to this study.

Another answer is to use isotopic substitution in the same study of UF_6 hydrolysis with water. In order to do this, one could use $H_2{}^{18}O$ and D_2O to react with UF_6. If the water was of a certain percent abundance ^{18}O and a certain percent abundance ^{16}O, IR bands due to U-^{18}O stretches would be shifted from the U-^{16}O stretches. Also, a U-OD band or a $UO_2F_2 \cdot D_2O$ band would be shifted from a U-OH or $UO_2F_2 \cdot H_2O$.

Also, Raman spectroscopy might help with some of the band assignments.

LIST OF REFERENCES

LIST OF REFERENCES

1. Katz, J. J.; Rabinowitch, E. "The Chemistry of Uranium"; Dover: New York, 1951; p. 404.

2. Brown, D. "Halides of the Lanthanides and Actinides"; Wiley-Interscience: New York, 1968; p. 26.

3. Bailar, J. C.; Emeleus, H. J.; Nyholm, R.; Trotman-Dickenson, A. F. "Comprehensive Inorganic Chemistry"; Compendium: New York, 1973; p. 168.

4. Taylor, J. C.; Wilson, P. W. J. Solid State Chem. 1977, 14, 378-82.

5. Claassen, H. H.; Weinstock, B.; Malm, J. G. J. Chem Phys. 1956, 25, 426-7.

6. Bailar, J. C.; Emeleus, H. J.; Nyholm, R.; Trotman-Dickenson, A. F. "Comprehensive Inorganic Chemistry"; Compendium: New York, 1973; p. 167.

7. Seppelt, V. K.; Bartlett, N. Z. Anorg. Allg. Chem. 1977, 436, 122-6.

8. Paine, R. T.; Coleman, W. F.; Lewis, R. B.; McDowell, R. S. NBS Special Publ. 1978, 526, 253-5.

9. Wilson, P. W. J. Inorg. Nucl. Chem. 1974, 36, 303-5.

10. Paine, R. T.; Ryan, R. R.; Asprey, L. B. Inorg. Chem. 1975, 14, 1113-17.

11. Bagnall, K. W. "Lanthanides and Actinides, MTP Intl. Rev. Sci."; University Park: Baltimore, 1972; Vol. 7, p. 92.

12. Okamoto, J.; Kiyose, R. J. Nucl. Sci. Tech. (Japan) 1978, 15(6), 455-60.

13. Levy, J. H.; Taylor, J. C.; Wilson, P. W. J. Inorg. Nucl. Chem. 1977, 39, 1989-91.

14. Taylor, J. C.; Wilson, P. W. J. Chem. Soc., Chem. Commun. 1974, 232-3.

15. Jacob, E.; Polligkeit, W. Z. Naturforsch. Teil B 1973, 28(3-4), 120-4.

16. Mattson, V. L. "Kirk-Othmer Encyclopedia of Chemical Technology"; Wiley-Interscience: New York, 1970; Vol. 21, p. 34.

17. Gutmann, V. "Halogen Chemistry"; Academic: New York, 1967; Vol. 3, p. 359.

18. Brooks, L. H.; Garner; E. V.; Whitehead, E. United Kingdom Atom. Energy Auth. [Rep.] 16R-TN/CA-277 1956, 1-17.

19. Taylor, J. C. Aust. A.E.C., AAEC/E [Rep.] No. 255 1973, 1-7.

20. Bailar, J. C.; Emeleus, H. J.; Nyholm, R; Trotman-Dickenson, A. F. "Comprehensive Inorganic Chemistry"; Compendium: New York, 1973; p. 178.

21. Ohwada, K. Inorg. Chem. 1971, 33(6), 1615-23.

22. Katz, J. J.; Rabinowitch, E. "The Chemistry of Uranium"; Dover: New York, 1951; p. 569.

23. Bagnall, K. W. "Lanthanides and Actinides, MTP Intl. Rev. Sci."; University Park: Baltimore, 1972; Vol. 7, p. 92.

24. Gutmann, V. "Halogen Chemistry"; Academic: New York, 1967; Vol. 3, p. 360.

25. Katz, J. J.; Rabinowitch, E. "The Chemistry of Uranium"; Dover: New York, 1951; p. 570.

26. Siegal, S.; Hoekstra, H. R.; Sherry, E. Acta Cryst. 1966, 20, 292.

27. Gabelnick, S. D.; Reedy, G. T.; Chasanov, M. G. J. Chem. Phys. 1973, 58(10), 4468-75.

28. Gabelnick, S. D.; Reedy, G. T.; Chasanov, M. G. J. Chem. Phys. 1973, 59(12), 6397-6403.

29. Gabelnick, S. D.; Reedy, G. T.; Green, D. W. J. Chem. Phys. 1980, 73(9), 4207-12.

30. Carstens, D. H. N.; Gruen, D. M.; Kozlowski, J. F. High Temp Sci. 1972, 4, 436.

31. Bagnall, K. W. "Lanthanides and Actinides, MTP Intl. Rev. Sci."; University Park: Baltimore, 1972; Vol. 7, p. 92.

32. Gasner, E. L.; Frlec, B. J. Chem. Phys. 1968, 49(11), 5135.

33. Malm, J. G.; Weinstock, B.; Claassen J. Chem. Phys. 1968, 49(11), 5135.

34. Bagnall, K. W. "Lanthanides and Actinides, MTP Intl. Rev. Sci."; University Park: Baltimore, 1972; Vol. 7, p. 122.

35. Burns, R. C.; O'Donnell, T. A.; Waugh, A. B. J. Fluor. Chem. 1975, 12, 505-17.

36. Burns, R. C.; O'Donnell, T. A. Inorg. Nucl. Chem. Lett. 1977, 13, 657-60.

37. Barber, E. J.; Cady, G. H. J. Phys. Chem. 1956, 60, 505-6.

38. Gutmann, V. "Halogen Chemistry"; Academic: New York, 1967; Vol. 3, p. 279.

39. Bernstein, E. R.; Meredith, G. R. J. Chem. Phys. 1977, 24, 289-99.

40. Selig, H.; Sunder, W. A.; Schilling, F. C.; Falconer, W. E. J. Fluor. Chem. 1978, 11, 629-55.

41. Canterford, J. H.; Colton, R. "Halides of the Second and Third Row Trans. Metals"; Wiley-Interscience: New York, 1968, Vol. 3, p. 211.

42. Peacock, R. D.; Edelstein, N. J. Inorg. Nucl. Chem. 1976, 38, 771-2.

43. Canterford, J. H.; Colton, R. "Halides of the Second and Third Row Trans. Metals"; Wiley-Interscience: New York, 1968; Vol. 3, p. 214.

44. Winfield, J. M. "Inorganic Chemistry, MTP. Intl. Rev. Sci. Ser. 1"; University Park: Baltimore, 1972; Vol. 5, p. 279.

45. Alexander, L. E.; Beattie, I. R.; Bukovszky, A.; Jones, P. J.; Marsden, C. J.; Van Schalkwyk, G. J. J. Chem. Soc., Dalton Trans. 1974, 81-4.

46. Paine, R. T.; McDowell, R. S. Inorg. Chem. 1974, 13(10), 2366-70.

47. Robiette, A. G. J. Mol. Struct. 1977, 37, 105.

48. Iijima, K. Bull. Chem. Soc. Japan 1977, 50, 373.

49. Atherton, M. J.; Holloway, J. H. J. Chem. Soc., Chem Commun. 1978, 254.

50. Atherton, M. J.; Holloway, J. H. J. Chem. Soc., Chem. Commun. 1978, 41.

51. Brown, D. "Halides of the Lanthanides and Actinides"; Wiley-Interscience: New York, 1968; p. 31.

52. Samsanov, G. V. "The Oxide Handbook"; Plenum: New York, 1973; p. 110.

53. Elwell, W. T.; Wood, D. E. "Analytical Chemistry of Molybdenum and Tungsten"; Pergamon: New York, 1971; p. 6.

54. Samsanov, G. V. "The Oxide Handbook"; Plenum: New York, 1973; p. 112.

55. Samsanov, G. V. "The Oxide Handbook"; Plenum: New York, 1973; p. 35.

56. Samsanov, G. V. "The Oxide Handbook"; Plenum: New York, 1973; p. 32.

57. Loopstra, B. O.; Boldine, P. Acta Cryst. 1966, 21, 158.

58. Yampol'shii, V. I.; Mal'tsov, A. A. Russ. J. Inorg. Chem. 1970, 15(7), 1029.

59. Mattes, R.; Schroeder, F. Z. Naturforsch. Teil B 1969, 24(9), 1095.

60. Krasser, W. Naturwissenchaften 1969, 56(4), 213-4.

61. Weltner, W.; McLeod, D. J. Mol. Spectr. 1965, 17, 276.

62. Norman, I.; Porter, 6. Nature 1954, 174, 508.

63. Whittle, E.; Dows, D. A.; Pimentel, G. C. J. Chem. Phys. 1954, 22, 1943.

64. Downs, A. J.; Peake, S. C. "Molecular Spectroscopy"; The Chemical Society: London, 1973; Vol. 1, p. 533.

65. Daniels, F.; Alberty, R. A. "Physical Chemistry"; Wiley-Interscience: New York, 1975; p. 507.

66. Margrave, J. L.; Timms, P. L.; Jouette, M. B. Inorg. Chem. 1966, 5, 729.

67. Mason, M. G.; Von Holle, W. G.; Robinson, D. W. J. Chem. Phys. 1971, 54(8), 3491.

68. Ayers, G. P.; Pullin, A. D. E. Spectrochim. Acta 1976, 32A, 1695-1704.

69. Brentwood, R. M.; Barnes, A. J.; Orville-Thomas, W. J. J. Mol. Spectr. 1980, 84, 391-404.

70. Moskovits, M.; Ozin, G. A. "Cryochemistry"; Wiley-Interscience: New York, 1976; p. 306.

71. Hoekstra, H. R. Inorg. Chem. 1965, 2, 492.

72. McDowell, R. S.; Paine, R. T. J. Chem. Phys. 1976, 64(7), 3081.

73. Wilson, W. W.; Wilson, R. D; Christie, K. O. J. Inorg. Nucl. Chem. 1981, 43, 1551-53.

74. Jaubert, P.; Gaudreau, B. Can. J. Chem. 1977, 56, 1874-80.

75. Stull, D. R.; Prophet, H. "JANAF Thermochemical Tables"; 2nd ed., U.S. Government Printing Office: Washington, D.C., 1971; 1-1141.

76. O'Hare, P. A.; Malm, J. G. J. Chem. Thermodynamics 1982, 14, 331-6.

77. Johnson, G. K. J. Chem. Thermodynamics 1979, 11, 483-90.

78. Ackermann, R. J.; Rauh, E. G.; Chandras, M. S. J. Phys. Chem. 1969, 73, 762-9.

VITA

Stephen Paul Anderson was born at Shaw Air Force Base in Sumter, South Carolina, on March 3, 1957. He is the son of the late Joseph Anderson and of Reba Stewart Anderson of Bristol, Tennessee. He graduated from Sullivan East High School in Sullivan County, Tennessee, June, 1975 with honors. He attended The University of Tennessee, Knoxville from September 1975 until August 1980, at which time he received a Bachelor of Arts in Liberal Arts and a Bachelor of Science in Chemistry with honors.

In September of 1980 he entered graduate school at The University of Tennessee, Knoxville. He was awarded a research assistantship which was supported by a grant from the Union Carbide Nuclear Division, Oak Ridge Gaseous Diffusion Plant (K-25), Oak Ridge, Tennessee. He received the Master of Science in Chemistry in August, 1982.